Chapter 5

PLANETS AND SATELLITES OF THE OUTER SOLAR SYSTEM, ASTEROIDS, AND COMETS[1]

RAY L. NEWBURN, Jr. AND SAMUEL GULKIS

Jet Propulsion Laboratory, California Institute of Technology, Pasadena USA

OUTER SOLAR SYSTEM

The outer solar system beyond Mars, which contains more than 99% of the nonsolar mass in the solar system, is of major cosmogonic significance. Here are most of the asteroids and comets—the giant planets: Jupiter, Saturn, Uranus, and Neptune, and their 29 satellites as well as the planet Pluto which is more like a satellite than a companion planet to the giants. The giant planets and probably their satellites differ markedly from the planets and satellites of the inner solar system. In contrast to mean densities near 5 g/cm^3 for the terrestrial planets, mean densities of the major planets range from 0.7 g/cm^3 for Saturn to 1.6 g/cm^3 for Neptune. The giant planets are large with radii ranging 3.7–11.2 times that of the Earth; all rotate rapidly with periods from ca 10–ca 15 h. This rapid rotation produces a pronounced oblateness, particularly of Jupiter and Saturn. Rotational effects are also important in determining the distribution of plasma in the Jovian magnetosphere.

Earth-type planets and the giant planets differ, too, in the chemical nature of their atmospheres which are, respectively, oxidizing and reducing. The larger satellites of the giant planets also appear significantly different from the Moon, some of them, it is believed, being composed of large fractions of various ices or at least ice covered. Three satellites, Io, Ganymede, and Titan, are thought to have atmospheres, with that of Titan being quite substantial.

The major planets and their satellites are considered to be of considerable biologic interest, in addition to their importance toward understanding the formation of the solar system. Sagan [404] and other workers have shown that synthesis of complex organic compounds takes place most effectively in a reducing atmosphere. Major steps leading to the origin of life on Earth are believed to have occurred when the Earth's atmosphere was richer in hydrogen than at

[1] We wish to thank the many people who, either directly or indirectly, helped to compile quickly data used in this chapter, in particular, J. D. Anderson, T. D. Carr, O. V. Dobrovolskiy, F. P. Fanale, R. Goldstein, H. C. Graboske, A. S. Grossman, M. Janssen, T. V. Johnson, G. Null, R. J. Olness, E. Olsen, J. B. Pollack, R. Smoluchowski, V. G. Teifel, L. Trafton, D. L. Watson, and S. K. Wong for material for use prior to publication. B. Gary is thanked for assistance in compiling radio brightness temperature data used in the figures. We are especially grateful to F. Taylor who read the entire manuscript and commented critically on its contents. M. Owen and D. Mahoney are thanked for professional assistance in typing and editing the manuscript. We also thank the D. Reidel Publishing Company for permission to use historical and descriptive material from an earlier article we authored [343] which they published.

This paper presents results of one phase of research carried out at the Jet Propulsion Laboratory, California Institute of Technology, under NASA Contract No. NAS 7-100, sponsored by the National Aeronautics and Space Administration.

present. Large quantities of hydrogen would be lost from the Earth during geologic time due to the planet's inability to retain lighter gases. In contrast, major planets could retain any gas, including hydrogen. Their primitive reducing atmospheres may therefore be of major exobiologic significance [404]. The satellite Titan, for example, is a likely site of simple organic compounds, having both a reducing atmosphere and a solid surface on which complex molecules can form and accumulate.

Numerous environmental differences between inner and outer solar system objects are bases for anticipating that atmosphere and surface processes, totally different from those observable on the planets of the inner solar system, may be operative. In order to develop hypotheses about these processes, an adequate understanding of probable conditions on the planets and satellites is needed.

The purpose of this chapter is to present the best available knowledge of the outer solar system in mid-1974 to serve as a guide for studying the outer solar system. Only observational results and direct interpretation are discussed, with results of a more speculative nature limited to literature references. Emphasis is placed upon planets and larger satellites of greatest biologic interest; comets, asteroids, and the smaller satellites are also discussed but in less detail.

The principal physical and rudimentary photometric data for the five outer planets are presented in Tables 1 and 2; when using these, it is useful to remember that some data are still uncertain, especially for the outer three planets. Such uncertainties are usually indicated in the tables and, where important, are generally discussed in some detail.

Important information on planetary motions is in Table 3; many of these quantities are known to higher accuracy than those given, and additional figures can be found in the original references. Sufficient information is included for most calculations in physical planetology, but not for studies in celestial mechanics.

JUPITER

Jupiter, being the largest and nearest giant planet, is the most studied. With the flyby by

TABLE 1.—*Physical Data*

Parameter [1]	Jupiter	Saturn	Uranus	Neptune	Pluto
Reciprocal mass [2] [128]	1 047.357	3 498.1	22 759	19 332	3 000 000
Mean error in mass [3] [128]	±0.005	±0.4	±87	±27	±500 000
Mass (Earth) = 1) [2,4]	317.89	95.18	14.63	17.22	0.11
Mass, kg [2,5]	1.8989×10^{27}	5.6854×10^{26}	8.739×10^{25}	1.029×10^{26}	6.6×10^{23}
Equatorial radius (km)	71 600 [219]	60 000 [120]	25 900 [102]	24 750 [152] [6]	ca 3 200 [7]
Equatorial radius (Earth=1) [8]	11.23	9.41	4.06	3.88	ca 0.5 [7]
Oblateness [9]	1/16.7 [219]	1/9.3 [120]	1/100 [102]	1/38.6 [152]	Unknown
Mean density, g cm^{-3} [10]	1.314	0.704	1.21	1.67	ca 4.9 [7]
Equatorial surface gravity, m s^{-2} [11]	22.88	9.05	7.77	11.00	ca 4.3
Equatorial escape velocity, km s^{-1} [12]	59.5	35.6	21.22	23.6	ca 5.3

[1] Where the same source was used for all five planets, the reference number is given in this (parameter) column. In all other cases, it follows the individual datum. Additional information is given in footnotes.

[2] Includes the mass of satellite systems and atmosphere.

[3] Mean error from residuals of group means, groups being formed from results having a common method of derivation. The error for Pluto is estimated only.

[4] Calculated using 328 900.12 for the reciprocal mass of the Earth-Moon system and 81.3025 for their mass ratio [128].

[5] Calculated using data above, $G=6.673\times10^{-20}$ km^3 s^{-2} kg^{-1}, and $GM_\odot = 1.327125 \times 10^{11}$ km^3 s^{-2} [320].

[6] Improved analysis by light curve inversion [491] requires a larger scale height for Neptune's atmosphere. This would decrease the radius to optical depth unity by about 200 km. No change was made because of comparable uncertainties in several quantities.

[7] See discussion in section on PLUTO.

[8] Calculated using $R_\oplus = 6378.160$ km [320].

[9] Oblateness or optical flattening is defined as $(R_{equatorial} - R_{polar})/R_{equatorial}$.

[10] Calculated assuming all are oblate spheroids.

[11] Including centrifugal term, $g_\oplus = 9.78$ ms^{-2} at the Equator.

[12] No rotational contribution included.

Pioneer 10 on December 4, 1973, Jupiter also became the first of the giants to be studied at close range by spacecraft. In spite of this attention, knowledge of Jupiter still lags behind that of Mars or Venus, and intensive study is scheduled during the coming decade. In the pages that follow, an effort will be made to present an overview of current knowledge of Jupiter and to point out gaps in fundamental data and understanding.

Atmosphere

Background Information

The first report on dark absorption bands in the spectrum of Jupiter apparently was made by Secchi in 1863. Shortly after the turn of the century, Slipher photographed these bands in some detail. In the early 1930s, Wildt suggested, and the work of Dunham confirmed, that they were due to the presence of methane and ammonia. Pioneering measurements of temperatures of the planets were made using vacuum thermocouples, in the mid-1920s, by Menzel, Coblentz, and Lampland at Lowell Observatory and by Pettit and Nicholsen at Mt. Wilson Observatory. These showed that Jupiter was definitely a cold body, as Jeffries had argued in 1923 on theoretical grounds. Model studies analogous to the modern paper of Zapolsky and Salpeter [534] indicated that the bulk of Jupiter must be hydrogen and helium, since no other substances have sufficiently low density at low temperatures to explain the observed mean density. Baum and Code [32], in 1952, observed photoelectrically an occultation of the star σ-Arietis by Jupiter, deriving from these observations a mean molecular weight of 3.3 for the Jovian atmosphere. Although recent studies have shown that large errors are possible using Baum and Code's curve-fitting technique [504], their basic conclusion that Jupiter's atmosphere must consist mainly of hydrogen and helium remains valid. Actual spectroscopic detection of molecular hydrogen was made by Kiess et al [248] in 1960.

The classic assumption was that gases in a planetary atmosphere could be considered a uniform transparent layer, except for pure absorption at some discrete wavelengths, above a

TABLE 2.—*Photometric Data*

Parameter [1]	Jupiter	Saturn	Uranus	Neptune	Pluto
Mean opposition magnitude, V_0 [194]	−2.55	0.75	5.52	7.84	14.90 [9]
Mean surface brightness at zero phase [2] V_{mag}/(arc sec)^2	5.6	6.9	8.2	9.6	ca 18.2
Mean surface brightness at zero phase (Earth = 1)	3.98×10^{-2}	1.20×10^{-2}	3.63×10^{-3}	1.00×10^{-3}	ca 3.6×10^{-7}
Color index [3] B–V [194]	0.83	1.04	0.56	0.41	0.80
Bolometric bond albedo, A	0.45 [454]	0.61 [495]	0.33 [532] [5]	0.33 [6]	0.14? [7]
Calculated effective temperature [4] °K	105	71	57	45	42 [8]

[1] Photometric data in this table are in the widely used UBV photometric system. The broad passbands of this system were designed for stellar work, but the V-band gives a fair approximation to naked eye response. Detailed photometric properties are given in the main body of the text from modern narrow-band photometry.

[2] Calculated from V_0 and data in Tables 1 and 3.

[3] Color index of the Sun is 0.63 [194].

[4] Calculated from A, data in Tables 1 and 3, and a value for the solar constant of 1353 Wm^{-2}. This is the effective temperature each planet would have, if solar insolation were the only energy source.

[5] Original value scaled to radius in Table 1.

[6] Estimated as discussed in the subsection, *Visible Surfaces*, under URANUS AND NEPTUNE.

[7] Harris' [194] value for the visual albedo. It assumes a phase integral equal to that of Mars and a radius of 0.45 times that of the Earth.

[8] Effective temperature of a rapidly rotating body with the (very uncertain) properties listed. Pluto rotates slowly enough so that a relatively large difference between dayside and nightside temperatures can be expected. The effective temperature of a nonrotating body would be 50.5° K.

[9] Andersson and Fix [12] have shown strong evidence of long period change in this mean magnitude; they find 15.07 for 1972 at zero phase. See discussion in the section, PLUTO.

well-defined reflecting layer (clouds or solid surfaces). Abundances were determined from absorption line strengths, with allowance for mean path length through the atmosphere. The early Jovian models of Kuiper [261] were of this reflection-layer type, for indeed, with information available even 20 years ago, no other assumption was feasible. Many atmospheric abundances are still quoted as though this assumption were valid, even while recognizing that in most cases it is not.

In a dense atmosphere, especially such as that of Uranus, Rayleigh scattering begins to contribute significantly to atmospheric opacity in visible light. As long as scatterers and absorbers are homogeneously mixed, and the properties of the scatterers are constant with height, and known, the abundance and atmospheric albedo problems are still quite tractable, although in reality this is never the case. Whenever a condensable gas is a minor component in saturation equilibrium, scattering density changes independently of gas density as a function of altitude. Spectral line formation and continuum albedo values in the resulting inhomogeneous atmosphere require a major numerical effort in a large computer.

While theory is adequate for most parts of the direct problem of predicting the behavior of radiation interacting with a simple, static, one-dimensional (vertical) atmosphere of known properties, the inverse problem, requiring definition of an atmosphere from observed radiation, is far more difficult. Solution of this "atmospheric sounding" problem for Jupiter definitely requires data over a wide range of wavelengths and from point to point on the disk, which can only be obtained with adequate spatial resolution by special spacecraft experiments [456]. Up to the present, most work has consisted of solving the direct problem for families of "reasonable" models and comparing these to observations.

Further complications are of two types. One, already implied, is that Jupiter does not have a uniform atmosphere (nor does Saturn). There are obvious belts, zones, and spots (to be discussed later), and even the limited quantitative information now available indicates definite variation in many physical parameters from point to point on the Jovian disk. Attempts at temperature sounding with Earth-based spatial resolution, such as the recent work of Ohring [346], at best can give only an average over large areas of a very nonuniform planet. The second complication is that Jupiter is a dynamic body with obvious changes from month to month visible on even the poorest photographs.

Improvements in knowledge of planetary atmospheres follow a sort of iterative process, hopefully one which ultimately converges to the correct answer. The general procedure is to calculate preliminary models based upon the best estimates of atmospheric composition and temperatures. Data are then interpreted in terms

TABLE 3.—*Mechanical Data*

Parameter	Jupiter	Saturn	Uranus	Neptune	Pluto
Mean heliocentric distance, AU [341] [1]	5.203	9.539	19.182	30.058	39.439
Orbital eccentricity [341] [1]	0.0484	0.0557	0.0472	0.0086	0.2502
Orbital inclination [341] [1]	1° 18′	2° 29′	0° 46′	1° 46′	17° 10′
Sidereal period [341] [2]	11.862	29.458	84.013	164.793	247.686
Mean orbital velocity, km s^{-1} [400]	13.06	9.65	6.80	5.43	4.74
Orbital angular momentum, kg km^2 s^{-1}, calculated	1.929×10^{37}	7.813×10^{36}	1.700×10^{36}	2.514×10^{36}	ca. 1.8×10^{34}
Inclination of Equator to orbit	3.07° [369]	26.74° [369]	97.93° [369]	28.80° [369]	>50° [12]
Period of rotation	(see [4])	(see [5])	10.8 h [328] [3]	15.8 h [327] [3]	6.3874 d [342]

[1] Mean elements for the epoch 1960 January 1.5 ET.
[2] Tropical years.
[3] These periods are not accurately known. See subsection, *The Visible Surfaces*, under URANUS AND NEPTUNE.
[4] See subsection, *The Visible Surfaces*, under JUPITER.
[5] See subsection, *The Visible Surfaces*, under SATURN.

of such models. Specifically, visible and thermal (infrared) opacities, which control energy transfer, are calculated for the best available abundances, and an attempt is made to study the energy balance of the atmosphere and derive temperature and pressure profiles, perhaps for a uniform, one-dimensional atmosphere in radiative equilibrium. Trafton published details of this major step in 1967 [465] for the four giant planets. Analysis of spectroscopic data and limb-darkening curves, using improved models, confirmed the inadequacy of the reflecting-layer theory and that an inhomogeneous model was required, at least to explain the observed center to limb variations. With resulting improvements in one-dimensional models, progress is now being made toward understanding the real, three-dimensional, dynamic Jupiter and toward models of the Jovian ionosphere, but these areas constitute the research frontier and are discussed in following sections.

Composition

Molecular hydrogen is the major constitutent of the Jovian atmosphere, and theoretical understanding of its properties is the best of any neutral molecule. Since it is a homopolar molecule, H_2 has no normal dipole spectrum. A dipole moment can be induced by sufficient pressure but the resulting lines are broad, with small central intensity, and their equivalent widths are difficult to determine. Only the fundamental induced band at 2.4 μm has been seen on Jupiter by Stratoscope II [99]. Molecular hydrogen does have a small quadrupole moment, and hydrogen abundances on Jupiter result largely from studies of lines in the second and third overtone (3-0 and 4-0) quadrupole rotation-vibration bands. These lines are intrinsically very weak and appear only because the H_2 abundance on Jupiter is very large. An additional observational problem is introduced because these lines undergo observable collisional narrowing before ordinary pressure broadening sets in, making it difficult to determine accurate shapes and therefore pressures. The correct shape of such a line, narrowed by weak collisions, is believed to be given by the Galatry profile [221, 233]. Unfortunately, such lines saturate while still very weak, and the highest possible resolution is required to obtain reasonable precision in abundance. The best H_2 abundance available presently is about 65 km-amagat above a pressure near 1.7 atm [301].

Methane has a rich dipole rotation-vibration spectrum extending from 7.8 μm well into the visible. Unfortunately, easily observed high overtones in the visible and near infrared are so complex that they have yet to be theoretically analyzed. No rotational quantum number assignments exist for any overtones higher than the $3\nu_3$ band at 1.1 μm, and only the R branch of that band has been analyzed, by Margolis and Fox in 1968 [299]. Laboratory line strengths are available from Bergstralh and Margolis [46]; the Lorentz half-width from Bergstralh [45]. Abundance of methane appears to be about 45 m-amagat above a pressure level near 1.7 atm [220, 298, 301]. An independent result, using the technique of Fourier spectroscopy, which averaged over a large part of the visible disk, gave 38 ± 8 m-amagat above a pressure of about 2 atm [295].

Ammonia also has a rich dipole spectrum. Vibrational quantum numbers have been assigned to 42 bands in a recent analysis by McBride and Nicholls [314], who also carried out a rotational analysis of the $5\nu_1$ band of ammonia at 6450 Å [315]. The $5\nu_1$ band is quite complex, with many blended features, and it is not clear that accurate abundance and temperature results for Jupiter can be obtained from assignments at available laboratory and observatory resolution. An empirical curve-of-growth analysis by Mason [310] suggests an abundance of 13 ± 3 m-amagat and appears to be the best published result. This abundance should refer to the level above about 1.7–2.0 atm pressure as in methane and hydrogen, since a dense cloud deck is believed to be at that level (see section, **Atmospheric Structure**). The recent much higher abundance of Ohring [346] seems incompatible with other observations and with models assuming a solar abundance of nitrogen [506]; (see section, **Atmospheric Structure**). This result may be due to neglecting the clouds in the analysis.

Measurements of Jovian thermal disk temperatures at radio wavelengths provide data on ammonia abundance below the ammonia clouds [115, 137, 184, 525] as well as above them [183, 525]. Ammonia manifests itself through inversion-splitting of the molecule's rotational energy states. These transitions are believed to provide the principal source of radio opacity in the Jovian atmosphere. Gulkis and Poynter [184] have derived an ammonia mixing ratio of ca 1.5×10^{-4} below the clouds, based on the observed temperature spectrum (see next section, *Temperature*). This value is close to that expected for an atmosphere which contains a solar cosmic abundance of elements [278], thereby supporting the view that Jupiter's atmosphere is composed of primitive solar nebula material.

Direct spectroscopic detection of helium on a cold body is not possible from Earth's surface and is very difficult even from an Earth-orbiting satellite. The traditional assumption has been that helium is present on Jupiter in near solar abundance, but the first direct observational evidence of its presence was detection, by Pioneer 10 [239], of the 584 Å helium resonance line with a strength of 10–20 Rayleighs. Unfortunately, this measurement cannot be converted easily to a deep atmospheric abundance. Two crude abundance values for the region below the turbopause became available recently, however. Light curve inversion of multi-wavelength observations of the occultation of the star β-Scorpii by Jupiter allowed Sagan et al [406] to derive a helium fraction of $0.16^{+0.19}_{-0.16}$ by number. The solar fraction is $He/(H_2+He) \cong 0.12$ [73]. A helium fraction can also be determined from the pressure effects of helium on the H_2 rotation and translation spectrum in the far infrared [223]. The Pioneer 10 infrared radiometer experiment thus definitely indicated the presence of helium, the preliminary ratios being given as $He:H_2 = 0.6$ in the south equatorial belt and 0.8 in the south tropical zone [88]. Until more complete experimental results including an error analysis are available, continued use of the solar fraction, ca 9 km-amagat, seems reasonable.

Three new molecules have been identified recently on Jupiter by Ridgway, using a Fourier spectrometer on the 150-cm McMath solar telescope [392]. He estimates 10 cm-amagat[2] ethane (C_2H_6) and 0.2 cm-amagat acetylene (C_2H_2) as preliminary values from available data [392]. Roughly 0.9 cm-amagat phosphine (PH_3) was also detected [393]. Presence of nonequilibrium species such as C_2H_6, C_2H_2, and PH_3 in these abundances strengthens the possibility that more complex organic species are also present.

Two isotopes have been detected on Jupiter. Beer and Taylor [34] found 1.3 ± 0.3 cm-amagat CH_3D in their Fourier spectra of the 4.65 μm region. With allowance for deuterium fractionation, they derived the ratio $D:H = 4.8 \times 10^{-5}$ with error bounds of roughly $\pm 50\%$ [34]. Their results are somewhat model-dependent, that being the source of most of the probable error. Fox et al [148] reported the probable detection of $^{13}CH_4$ in Jupiter with an isotopic abundance ratio $^{12}C:^{13}C = 110 \pm 35$.

All the abundances quoted in the previous paragraphs are some form of mean in both time and space. An attempt is always made to reduce the data to a one atmosphere path. Average limb-darkening results are discussed in a section, *The Visible Surface*. However, an entire series of papers at the 1974 annual meeting of the Division of Planetary Sciences, American Astronomical Society, gave evidence of additional spatial and temporal variations in the strengths of various Jovian atmospheric components. For example, variation in the strength of the 3-0 S (1) line of H_2 by 40% in a week was reported [479]. Until such changes are clearly understood and reported, all abundance data must be treated with caution.

A number of rocket and satellite studies have been made of Jupiter at ultraviolet wavelengths. Atomic hydrogen has been detected several times by means of its Lyman-α emission at 1216 Å. In a recent rocket study by Rottman et al [399], a disk brightness of 4.4 krayleighs in this line was found, while Pioneeer 10 found 1 krayleigh [239]. The difference may be a real time fluctuation or could be due to interference in the rocket experiment from the bright hydrogen torus in Io's orbit (see section, SATELLITES

[2] Later corrected to 1 cm-amagat (*Astrophys. J.* 192:L51, 1974).

AND RINGS). Other features exist in these and other spectra (see Jenkins [235]), but resolution is still low and identification uncertain.

Spectroscopic searches have placed *upper limits* on other species in Jupiter's atmosphere. The limits depend upon the molecular band wavelength as well as its intrinsic strength, since the Jovian atmosphere is much more transparent in some regions (near 5 μm, for example) than others. More than one upper limit is given in Table 4 to provide information corresponding to different spectral regions.

Large-scale computer calculations have been carried out on the probable molecular composition of the Jovian atmosphere, assuming it is in thermodynamic chemical equilibrium. The most extensive work has been undertaken by Lewis and coworkers. Beginning with cosmic abundances, Lewis [278] showed that at temperatures from the freezing point of water to above 1000° K, virtually all oxygen is contained in H_2O molecules, all carbon in CH_4, all nitrogen in NH_3, and all sulfur in H_2S. At lower temperatures, H_2O freezes out and H_2S is removed through the formation of NH_4SH clouds [506].

TABLE 4.—*Upper Limits on Undetected Gases in the Jovian Atmosphere*

Gas	Wavelength, μm	Upper abundance, limit cm atm	Reference
C_2H_4(ethylene)	10.5	0.5	[163]
	5.3	5	[163]
	0.8715	200	[354]
CH_3NH_2 (methylamine)	12.8	0.05	[163]
	1.52	2	[98]
	1.0325	300	[354]
HCN (hydrogen cyanide)	14	1	[163]
	4.75	70	[163]
	1.53	5	[98]
	1.0385	200	[354]
C_2N_2 (cyanogen)	4.7	2	[163]
H_2S (hydrogen sulfide)	8.0	300	[163]
	1.58	25	[98]
	0.22	0.08	[9]
SiH_4 (silane)	10.5	1	[163]
	0.9738	2000	[354]

Molecules such as PH_3, C_2H_2, and C_2H_6 are distinctly nonequilibrium species, however, and indicate the occurrence of dynamic processes to some extent.

Temperature

Fundamental improvements in detectors of middle- and far-infrared radiation became available in the early 1960s; during this same period, the sensitivity of radio telescopes to millimeter waves was also improved, making studies of Jupiter practical at these wavelengths. Temperatures at wavelengths shorter than 1 mm are given in Table 5 in two groups: disk brightness temperatures and subsolar-point blackbody temperatures from thermal maps.

Thermal radio radiation from Jupiter was first detected at 3.15 cm wavelength in 1956 and 1957 [313]. These early observations gave a temperature of $145° \pm 26°$ K which was reasonably consistent with the estimated equilibrium temperature of Jupiter and with infrared measurements. Subsequent observations of Jupiter at longer wavelengths revealed rapid increase in temperature with increasing wavelength. It was suggested by Drake [125] and later confirmed by observations that the longer wavelength radiation from Jupiter is generated by high energy electrons trapped in the magnetic field of Jupiter in regions similar to those of the Van Allen belt around Earth.

Thermal emission from Jupiter's atmosphere and radiation belt (synchrotron) emission are now known to contribute equally to Jupiter's total emission near 7-cm wavelength. Presence of the synchrotron emission component makes it difficult to measure accurately the planet's thermal disk spectrum. Attempts have been made to separate disk from nonthermal emissions by using radio interferometric techniques and by making certain assumptions about the polarization properties of synchrotron emission. The interferometric method of separation is the most reliable of the two methods although there are few measurements using this technique. Berge [39, 40], Branson [63], and Olsen have used the interferometric technique to derive atmospheric emission at wavelengths from 2–21 cm. Dickel [115] combined his polarimetric observations of

Jupiter with interferometric results and atmospheric modeling to derive the thermal spectrum from short millimeter wavelengths to 21 cm. The resultant disk spectrum of Jupiter is shown in Figure 1. (For data used in this figure see [179, 343, 483]). The observed spectrum (after removal of synchrotron emission) rises from a value near 140° K at 1.25 cm to over 350° K at 21 cm. The generally accepted interpretation of this spectrum is that it is due to a deep convective atmosphere, in which ammonia exists as a trace constituent and is the principal source of radio-opacity.

A large number of rotational temperatures have been derived for Jupiter. Since the atmosphere is not isothermal, temperatures so derived are obviously a form of weighted mean over the absorbing region. The Curtis-Godson approximation is frequently employed to determine the appropriate weighting factor in a vertically inhomogeneous model atmosphere, so that the model can be compared directly to observations. This is a valid procedure, even for the collision-narrowed lines in the quadrupole spectrum of H_2 [301]. In applying it to Jupiter, however, proper allowance must be made for the effects of absorption and scattering in the cloud layers, which requires that these be modeled also.

Margolis [298] showed that a simple reflecting layer model could be used for temperature, pressure, and abundance determinations as long as observations were strictly limited to the center of the disk. Apparently, this is because the upper cloud deck is strongly forward scattering and of moderate optical depth in the infrared, while the second cloud layer is very dense and behaves like a reflecting layer [301]. Explanation of center-to-limb variations requires a full inhomogenous atmosphere treatment, however. Therefore, most of the rotational temperatures reported are of little quantitative value, since they combine data taken all over the disk. It can be stated, however, that temperature at the second (main) cloud deck must be higher than any of the measured rotational temperatures, and several of these are $\geq$ 180° K [300, 358].

The width of the pressure-induced fundamental band of H_2 required a temperature of 200°–

TABLE 5.—*Jovian Brightness Temperatures to 1 mm*

Wavelength, μm	Disk brightness temperature, °K	Reference	Remarks
7.5–8.2	140	[163]	In ν_4 band of CH_4; covered 65% of disk
9.2–12.0	127	[163]	In ν_2 band of NH_3; covered 65% of disk
30–45	136 ± 1	[16]	Calibration assumes Mars is a 235°K blackbody
45–80	150 ± 5	[16]	Do.
65–110	153 ± 7	[16]	Do.
30–300	133 ± 1	[16]	Do.
1.5–350	134 ± 4	[23]	Stellar calibration

Wavelength, μm	Subsolar point temp., °K	Reference	Remarks
5	See remarks	[241, 357, 508]	Radiation primarily from discrete sources with temperature perhaps ca 300° K
7.9	See remarks	[165]	Limb-brightening curve only, normalized to disk center $\Delta\lambda/\lambda$ ca 0.015
8.4	See remarks	[165]	Limb-darkening curve only, normalized to disk center $\Delta\lambda/\lambda$ ca 0.015
8.2–9.2	130–135	[507]	Correlated with surface features; higher values in belts than in zones
8–14	129	[516]	Temperature shown is average of 5 nights; individual nights shown in reference
17.5–25	150?	[163, 285]	Low reports variation in time and over disk, but complete details unpublished
14–25	126	[88]	Pioneer 10 result for the South Equatorial Belt
28–40	123	[288]	Calibrated with α Boo and α Her but Jupiter observations made at large air mass
30–55	145	[88]	Pioneer 10 result for the South Tropical Zone

225° K, according to Danielson [99]. Since absorption in such bands varies as the square of the density, this temperature presumably would refer to a better defined level near the main cloud deck. The meaning of all temperature measurements is understood much more plainly in terms of the models discussed later in this section.

The Visible Surface

Clouds. The surface of Jupiter is shown to consist of alternating bright "zones" and dark "belts," even through a small telescope, with the zones generally whitish or yellowish and the belts more often brownish or reddish. The better photographs taken from Earth and those of Pioneer 10 show an intricate structure of spots, festoons, plumes, and waves [146]. Grays, blues, and blacks show up locally. The overall impression is one of pastels, although local areas can have considerable saturation.

The clouds of Jupiter have been "known" for many years to be of ammonia cirrus, i.e., clouds of small frozen ammonia particles. It will be indicated in the discussion of atmospheric structure that indeed, there must be a layer of ammonia cirrus clouds, but recent work indicates that this layer must be rather tenuous. At longer wavelengths, one apparently sees through these clouds, at least near the center of the planetary disk, and through a clear region below them to a second, more substantial cloud deck that is perhaps made up of ammonium hydrosulfide particles.

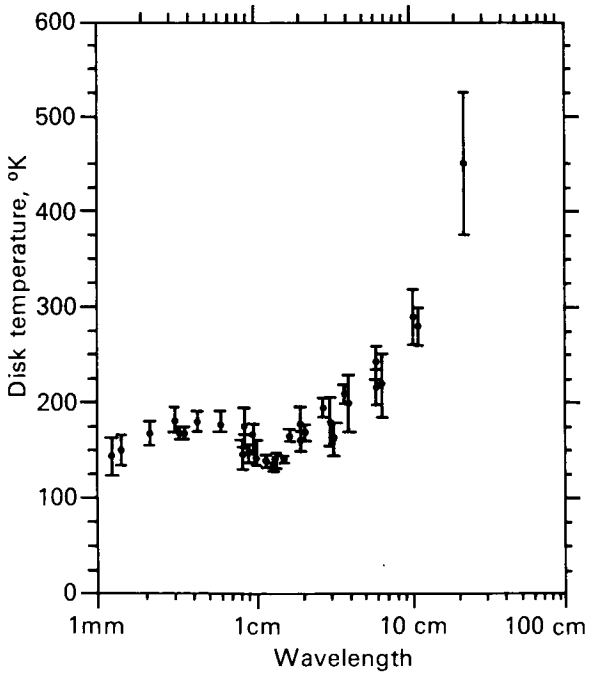

FIGURE 1.—Microwave spectrum of Jupiter's disk radiation.

The source of colors and cause of the banded appearance of Jupiter are not known in detail, although there are a number of hypotheses about the former. For example, Owen and Mason [356] suggest that the dominant yellowish color might be caused by a dilute mixture of $(NH_4)_2S$ in the NH_4SH cloud deck. Lewis and Prinn [282] added the suggestion of $(NH_4)_2S_x$, or elemental sulfur. A detailed study by Prinn of ultraviolet ($\lambda \leq 2700$ Å) radiation transfer and photolysis in the Jovian atmosphere [374] indicates that some radiation of wavelength greater than 1600 Å should penetrate through the atmosphere to the clouds and may result in photolysis of NH_3 and H_2S. He suggests that these begin chain reactions which may result in a freezing out of such colored material.

Sagan and Khare [246, 405] reported on laboratory experiments in which various mixtures of CH_4, C_2H_6, NH_3, H_2S, and liquid H_20 were irradiated by mercury emission at 2537 or 2537 and 1849 Å. Reaction products included a high molecular weight reddish-brown polymer and various amino acids. Another nonequilibrium process, electrical discharge, may result in complex organic molecules. Ponnamperuma and coworkers [81, 325, 523] studied the products of electrical discharges in mixtures of CH_4 and NH_3. Hydrogen and nitrogen were liberated, and HCN and various nitriles were found among the volatile products, which was of considerable biological interest because nitriles hydrolyze to amino acids. A reddish nonvolatile reactant was also formed which yielded, upon acid hydrolysis, a number of amino and imino acids.

If the Jovian atmosphere is convective to great depths, as suggested by radio data, then the high temperatures will tend to destroy any complex organic molecules. Whether a steady state is possible, with sufficiently rapid production by photolysis and/or discharge to maintain visible

amounts of them, depends on a number of completely unknown factors. The prominent ideas of a decade ago, that colors are caused by free radicals or solutions of sodium in ammonia, have fallen into disfavor as the atmospheric structure of Jupiter has become better known.

The detailed structure and motions of the Jovian clouds are direct evidence of extremely complex dynamic behavior. Although they remain in alternating dark belts and light zones parallel to the Equator of the planet, complex phenomena occur, particularly at the edges of the belts. A tremendous amount of data on the visible appearance of Jupiter over a long period has been collected and described by Peek [361]; his book should also be consulted for standard nomenclature for the visible surface.

Information on the rotation period within individual belts and zones has been gathered by Chapman [83], Reese [383], and Inge [224]. For example, these data show that since 1917, the north temperate current at the south edge of the north temperate belt has rotated even more rapidly than the equatorial belt. Over the years, there have been many attempts to correlate solar activity with activity in Jovian cloud belts or the Great Red Spot, as variously defined. A sampling of recent papers seems to say yes [25], no [144], and maybe [26, 376, 377].

It is not absolutely certain which phenomenon, if either, belts or zones, lies higher in the atmosphere. There is agreement that the upper cloud deck is nonuniform; but Teifel [460] finds more absorption in the λ-6190 methane band above dark belts, and Owen and Westphal [357] find less absorption in the even stronger λ-8940 methane band above the belts. The hottest spots on the planet are in belts, localized blue to black areas showing temperatures of 300° K or greater [508], although these may be holes where radiation from deeper regions easily penetrates. Temperature maps indicate that belts have higher temperatures than zones, however, even where there are no hot spots, which may indicate they are lower than the light-colored zones. The origin of belts is a complex hydrodynamic problem [for example, see 159, 207, 447, 477], and even an empirical description of them still lacks physical detail.

Rotation. One of the interesting problems of Jovian meteorology is that clouds making up the visible surface rotate as two rather distinct systems. Points within about 10° of the Equator constitute System I, whose standard meridian rotates with a period of 9 h 50 min 30.003 s. Points lying more than 10° from the Equator in either hemisphere constitute System II, whose standard meridian rotates with a period of 9 h 55 min 40.632 s [361]. Cloud motions relative to standard meridians make a choice of period completely arbitrary; however, some exact standard is needed for reference, and the numbers used have historical significance. The so-called equatorial jet which constitutes System I has been a particularly vexing meteorologic problem. It rotates more rapidly than any other visible surface part (except for the small north temperate current), and apparently more rapidly than the body of Jupiter (System III).

A true rotation period is difficult to define unless a body has a solid surface for reference, and Jupiter may not have such a surface (see section, **Body Structure**). The most likely true period seems to be that in which the magnetosphere rotates. This rate has been measured by radio astronomers at both decameter and decimeter wavelengths, and it is generally referred to as System III. A modern value of the System III period, based upon both decimeter and decameter studies, is 9 h 55 min 29.75 s ± 0.04 s [78]. If Jupiter should be fluid throughout, the concept of average or body rotational period will be difficult to define and of little use.

Great Red Spot. The most permanent feature of Jupiter's visible surface is the famous red spot. An elongated area of some 38 500 km in length by 13 800 km in width when at its largest in the 1880s [382], the Great Red Spot was probably seen 300 years ago and definitely noted in observations made more than 120 years ago [361]. The spot became most famous during the period 1879–1882, when its color was quite intense. Since that time, its visibility and color have waxed and waned, and even though the color has disappeared entirely at times, the location of the spot, the so-called red-spot hollow, has always been obvious. The red spot was very

prominent during 1962 and 1963, and remained quite "healthy" through 1965. It started to fade in 1966, and by February 1968 was extremely weak. Then, it suddenly began to strengthen and soon was back to its old prominence of 4 years earlier [382, 384, 388, 435, 436, 437]. This can be seen from the isodensitometry of Banos and Alissandrakis [27]. During 1969, its size averaged about 28 200 by 13 700 km [382].

The remarkable feature of the spot is that it does not seem to be solidly attached to any fixed surface but has wandered through 1200° of longitude during the past century (movement with respect to a mean motion of Jupiter which minimizes the red spot motion). There have been numerous short-period oscillations in regard to the steadier motion. Solberg [436] found a 3-month periodicity in these smaller excursions, and data for 7 consecutive years now give the oscillation a mean amplitude of 0.8° and a period of 89.89 ± 0.11 d [382]. The circulating current has had a rotational period of 90 d with respect to System II during this time and may be driving the red spot in this oscillation. Meanwhile, the spot's center latitude remained nearly fixed, as always. During 1968–69, it had a mean value of $-22.25° \pm 0.03°$ and always remained between $-22.0°$ and $-22.5°$ [382]. New data for 1969–71 have been given by Reese [384, 386].

It is interesting that at 5 μm and at 8–14 μm, the red spot is cooler than its surroundings [241, 515]. This is compatible with several observations showing less absorption above it [53, 329, 356] and suggests the feature penetrates to a high atmospheric level.

In January 1966, a small dark spot moving along the north edge of the south temperate belt approached the red spot, started around its south side, and circled it almost 1.5 turns before it disappeared [387]. Its period of circulation was 9 d. During the following year, four other dark spots, at least two from the south equatorial belt, showed similar behavior, though seen through only part of a turn around the red spot. These four spots had a circulation period of 12 d. Reese and Smith [387], reporting these fascinating observations, suggest that perhaps different atmospheric levels were involved.

Older hypotheses on the nature of the red spot were variations of a solid island floating in dense atmosphere [361], but increased knowledge of physical conditions in the Jovian atmosphere has made such theories highly improbable [402]. No known substance can be both solid and have a lower density than the Jovian atmosphere at temperatures and pressures thought to exist there. If the floating object is supposed to have sufficient vertical extent to reach a depth where phase changes offer a level in which to float, then it would almost certainly be disrupted by the stresses at pressure levels of 0.1–10 Mbar [208]. Furthermore, an object floating in a density discontinuity would tend to be moved in latitude (toward the Equator) by the Eötvös force [402].

It was proposed by Hide in 1961 that the red spot might be the upper end of a Taylor column, a stagnant column of fluid caused by a two-dimensional atmospheric flow unable to surmount a topographic feature [202, 203]. The gross longitudinal motion is attributed to actual change in the rotation period of Jupiter's mantle caused by hydrodynamic motions in the core [202]. Of course, if Jupiter has no solid surface, then additional hypotheses must be invoked to save the Taylor column, such as the topographic feature being a magnetic loop or the upper end of an internal convection cell. Smoluchowski [431] has suggested that the topographic feature, causing the Taylor column, could be nearly pure solid hydrogen floating in helium-rich liquid hydrogen. However, there would still be the problem of explaining the latitude constraint. There have also been fluid-dynamic objections to the Taylor column hypothesis. The "original" Taylor column was considered as an application of the Taylor-Proudman theorem for a homogeneous fluid. Such columns, which have been produced in the laboratory [208], are completely stagnant with no vorticity or exchange with their surroundings. The question arises whether a similar structure can exist in a real baroclinic atmosphere and perhaps have some exchange with its surroundings. Hide [206] considers it likely, while Stone and Baker [448] consider it unlikely, as do Sagan [403] and Kuiper [265, 266]. In part, this becomes a question of semantics: Should the resulting structure be called a Taylor

column even if it exists? Hide [204, 206] continues to study the problem while viewing his hypothesis cautiously.

Golitsyn [170] suggests that the characteristic period for major changes in Jovian circulation may be 3×10^5 yr or more, and, therefore, the red spot may simply be "a large long-lived eddy." Streett et al [450] have been studying the so-called Cartesian diver hypothesis in which a mass of hydrogen-rich solid floats in neutral buoyancy in a stratified fluid mixture of hydrogen and helium deep in the atmosphere and changes the surface appearance, perhaps through its effect on atmospheric convection or even creation of a Taylor column. Kuiper [266] studied a model of "organized cumulus convection" for the red spot and made persuasive arguments in its behalf, although Maxworthy [312] found considerable fault with the dynamics of his description.

The Great Red Spot of Jupiter is, at present, a fascinating, mysterious object, unique in its size and stability among atmospheric phenomena in the solar system. Until some hard, quantitative knowledge of Jovian atmospheric dynamics is obtained, it will remain one of the solar system's intriguing puzzles.

Photometric properties. Acquisition of photometric data on Jupiter is not an easy task. Complex atmospheric absorption and scattering cause rapid changes in photometric properties with wavelength. Rapid rotation limits the time available for detailed study and secular changes in the visible surface alter even disk-integrated properties as well as detailed properties. Finally, the phase angle of Jupiter, as observed from Earth, never exceeds 12°, so it is not possible to measure the phase function, phase integral, or complete photometric function. Jupiter's mean opposition magnitude has ranged over 0.45 magnitude at various oppositions since 1862 [194]. The value in Table 1 is the mean of these, although during 1963–65 [529] the actual value was $V_0 = -2.70$, 0.15 magnitude brighter. Harris [194] suggests that a phase coefficient of 0.005 magnitude/degree is appropriate at small phase angles for visual data. This implies that current observations will always be needed whenever the best possible photometric data are required.

A group associated with Harvard College Observatory carried out extensive photometry of Jupiter and Saturn from 1962 through 1965 in southern France and South Africa [230, 231], using 10 narrowband filters as well as UBV. Their detailed response curves are given by Young and Irvine [529]. The effective wavelengths and geometric albedos which resulted for the 10 narrow passbands are given in Table 6, having been corrected to agree with data in Table 1 and a visual solar magnitude of −26.8. The magnitudes given are an average of South African [231] and French [230] data. When tabulated chronologically, these data show a change in Jovian color from 1963 to 1965 [210].

TABLE 6.—*Jovian Geometric Albedos*

Passband	Effective wavelength, Å	Geometric albedo
v	3147	0.261
u	3590	0.305
s	3926	0.350
p	4155	0.404
m	4573	0.449
l	5012	0.483
k	6264	0.547
h	7297	0.415
g	8595	0.305
e	10635	0.295

Good reflected light, integrated photometry of Jupiter at wavelengths beyond 1.1 μm does not exist, one reason being that the extensive absorptions by CH_4 and NH_3 beyond that wavelength leave only a few windows through to the continuum. Spectra at longer wavelengths have been taken [35, 98, 99, 163, 236], but none give absolute integrated results (although Danielson's [99] wide-slit measurements come close).

Satellite and sounding rocket studies of the Jovian ultraviolet spectrum have been made, in addition to the Pioneer 10 experiment, but calibration has been a difficult problem; many of the early results are not mutually compatible. Recent photometry, benefiting from improved measurements of the solar ultraviolet, has been obtained by Wallace et al [496]. Their Orbiting Astronomical Observatory (OAO–2) results covered the wavelength region from 2100 to

3600 Å at a resolution of 20 Å and showed a radiance factor of 0.25 at 3000 Å and 10° phase, rising to 0.31 at 2500 Å, and dropping back to 0.25 between 2000 and 2100 Å. True geometric albedos would perhaps be 5% larger, while corrections to the solar absolute magnitude and Jovian radius used in this document would decrease the final result by about 7%. Fluctuations in ultraviolet flux within about 0.05 magnitudes occur in one 10-h rotation of Jupiter, the planet being faintest when the red spot is on the central meridian [408]. There are no accurate albedos below about 2000 Å because the solar continuum is falling rapidly to nearly zero below 1800 Å. Rocket spectra show some faint emission, due possibly to H_2, throughout the region from 1250 Å to about 1600 Å [399].

Since the phase angle of Jupiter never exceeds 12°, the phase integral q cannot be measured from Earth. Limb-darkening curves have been used to derive approximate values for q: $q(U) = 1.55$, $q(B) = 1.60$, and $q(V) = 1.65$, but there is no unique relation between limb darkening and phase integral, and these values could be grossly in error [194]. Taylor assumed a phase integral of 1.6 at all wavelengths, to derive a bolometric Bond albedo of 0.45 [454]. The uncertainty in the latter was considered to be about ± 0.07.

Limb-darkening curves have been derived by a number of observers both in and out of specific molecular bands [24, 201, 329, 337, 354, 459, 460]. Infrared equatorial and meridional limb-darkening curves have been taken from 0.6 to 2.0 μm [56]. Detailed photoelectric photometry has been carried out in 24 bands from 0.30 to 1.10 μm [364], in which the north and south tropical zones have been compared with the combined north equatorial belt and equatorial zone, with sizable differences found. Even more detailed work has been done [53], using 8 bands from 1.4 to 1.63 μm, taking data at 41 points on the Jovian disk and at three phase angles, from which an NH_3 absorption map of Jupiter, limb-darkening coefficients, and some CH_4 distributional data have been derived.

Polarimetry is a rather neglected technique for atmospheric study. Morozhenko and Yanovitskiy studied the entire disk of Jupiter as well as the disk center in seven passbands [330, 331]. They derived a refractive index for atmospheric aerosols (1.36), which is that of ammonia, and particle diameters ca 0.4 μm. In detailed polarimetry, much stronger polarization was found at Jupiter's poles than near the equator, for example [187], and even considerable asymmetry is found between the two poles [154, 156]. At short wavelengths near the Equator, the polarization is typical of molecular scattering, while at longer wavelengths, there is evidence for aerosols. Much larger optical depths appear to be reached near the poles, perhaps indicating fewer ammonia particles there. With careful interpretation and improved models of the Jovian atmosphere, polarization measurements should offer fairly direct, local information on cloud heights and atmospheric aerosol content at the time of observation; this is information difficult to obtain in any other way.

The recent report of circularly polarized visible (6800 Å) light from Jupiter [243, 244, 245] was unexpected. At first, polarization was positive in the south polar region, and twice as large and negative in the north polar region, with fractional values a few times 10^{-5}. Then, as Jupiter approached opposition, magnitude decreased to zero; after opposition, it increased but with opposite sign, indicating atmospheric multiple scattering to be responsible for the effect.

Energy Balance

An apparent discrepancy between solar energy absorbed by Jupiter and energy emitted by the planet was emphasized by Opik [349]. A bolometric albedo for Jupiter of 0.45 implies that the effective temperature should be 105° K [454]. Brightness temperatures have been measured at virtually every wavelength in the infrared, and an effective temperature as low as 105° K seems impossible. The very broadband measurement covering 1.5–350 μm yielded a temperature of 134° K [23] which is revealing, since more than 99% of the energy of a 105° K blackbody is emitted in this wavelength range. It can be argued that the bolometric Bond albedo for Jupiter could be seriously in error (see subsection *Photometric properties*), but even if Jupiter were a blackbody

(with zero bolometric albedo), which it clearly is not, its effective temperature would only be 121° K. Only 15% (or 0.45 ± 0.07) total uncertainty in the bolometric Bond albedo is estimated [454]. An albedo of 0.38 would raise the effective temperature to 109° K.

Jupiter rotates in less than 10 h. If the thermal relaxation time of the radiating "surface" of Jupiter is long compared with 5 h, it must radiate effectively from the total surface of the planet. If it relaxed to a very low temperature in much less than 5 h, then it would effectively radiate only from the lighted hemisphere, whose radiation balance temperature could be a factor of as much as $2^{0.25}$ greater than 105° K (or 124° K). In fact Pioneer 10 showed that there is no difference between day and night side temperatures [88], as was expected from theoretical calculations and from thermal limb-darkening curves.

An effective temperature of even 125° K implies contribution from an internal energy source of 7×10^{-4} W cm^{-2}, an amount of power equal to that absorbed from the Sun (assuming the Bond bolometric albedo of 0.45 is correct). An effective temperature of 134° K corresponds to an internal source of 1.2×10^{-3} W cm^{-2}. This internal source has large effects upon both models of the Jovian interior and model atmospheres.

Atmospheric Structure

Models

Pressure-temperature-altitude profiles for the Jupiter atmosphere have been calculated by a number of authors. These models are based on many simplifying assumptions, meant to be representative of average conditions. Local variations of atmospheric parameters (weather) are ignored. Dynamics are included in calculations only insofar as they determine the average static structure.

Standard model atmospheres generally consist of a tropospheric region in which the deep atmosphere is in convective equilibrium with an upper troposphere in radiative equilibrium. An accurate model of the thermal opacity of the upper atmosphere is required to compute models of the radiative region. The dominant source of thermal opacity in this region has been shown to be pressure-induced translational and rotational absorption by molecular hydrogen [465]. Ammonia furnishes some additional opacity, the greatest amount coming from the ν_2 rotation-vibration band at 10 μm [160, 467]. Other sources of atmospheric opacity are the ν_4 methane band at 7.5 μm, cloud layers, and any aerosols present in the atmosphere. The methane band provides complete absorption of more than 100 cm^{-1} of spectrum even above the effective temperature level of 134° K in the Jovian atmosphere [455], but this is a very small fraction of total opacity. Polarization measurements of Morozhenko and Yanovitskiy [331] noted only small concentrations of aerosols but may have referred to strictly high atmospheric levels. Stratoscope II observations of the 3.0 μm bands of NH_3 require many larger solid particles for satisfactory explanation of the observed band strengths [409].

Almost two-thirds of the energy enters the Jupiter troposphere by convection, driven by the internal energy source. About 45% of incident solar energy is reflected, more than 10% is absorbed fairly high in the atmosphere in strong methane bands [476], a very small amount is absorbed in gaseous ammonia and molecular hydrogen, and the remainder—slightly more than 40%—must be absorbed by clouds at various levels.

A model atmosphere for Jupiter was published recently which includes thermal opacity of molecular hydrogen and ammonia and takes proper account of dynamic effects [477]. This model is reproduced as Table 7. It assumes an effective temperature of 135° K, $He:H_2 = 0.1$; $CH_4:H_2 = 3 \times 10^{-3}$; maximum $NH_3:H_2 = 1.7 \times 10^{-4}$; and surface gravity 2500 cm s^{-2}. Omission of cloud layers is the model's most obvious deficiency. Methane was also not included; hence, there is no atmospheric heating or opacity and no modeling of the temperature inversion region of the atmosphere above the tropopause. Also, there is still some disagreement as to best values for the pressure-induced opacity of H_2 [426], and changes could result.

It is necessary to mention at this point that

temperature and pressure profiles were obtained from the S-band (2.3 GHz) occultation experiment [250] on Pioneer 10, which produced measurements deep into the neutral atmosphere, reaching a level of 2.8 atm for daytime entry and about 2.4 atm for nighttime exit. Assuming a composition of 85% H_2 and 15% He, atmospheric temperature at these pressures was found to exceed 700° K, considerably higher than convective equilibrium models and ground-based infrared and radio observations had predicted. This result now appears to be incorrect; the discrepancy is believed to be due to an incorrect inversion procedure which resulted from neglecting the oblateness of the planet. For example, the Trafton-Stone model has a temperature of 180° K near 1 atm whereas the occultation result gives a temperature near 500° K at this same pressure level. Most infrared and radio measurements from Earth have indicated a temperature about 130°–150° K at pressure levels about 0.3–1 atm, whereas the Pioneer 10 occultation result yielded temperatures between 300°–450° K over this pressure range.

Another important difference between the models and occultation data is the temperature lapse rate. Pioneer 10 measured a temperature lapse rate of about 2.5° K/km which is substantially greater than adiabatic for the assumed composition. It is not currently understood how these discrepancies can be reconciled. Kliore et al [250] suggest that the presence of cloud or dust particles in the 1–30 mbar pressure altitude range could confuse interpretation of infrared data. However, they correctly point out, this would not explain observations at microwave frequencies.

TABLE 7.—*Radiative Dynamical Model Atmosphere for Jupiter*[1]

Depth, km	Temperature, °K	Pressure, log dynes cm^{-2}	Density, g cm^{-3}	H_2 abundance, km-amagat	Optical depth at 520 cm^{-1}
0.0	105.6	3.843	1.694(−6)	0.26	0.000
14.4	105.6	4.231	4.263(−6)	0.63	0.003
22.3	106.1	4.444	6.927(−6)	1.03	0.008
29.7	106.8	4.643	1.088(−5)	1.63	0.020
34.2	107.5	4.764	1.430(−5)	2.16	0.035
41.0	109.4	4.945	2.129(−5)	3.27	0.080
46.3	111.8	5.083	2.862(−5)	4.49	0.15
53.1	115.7	5.270	4.215(−5)	6.91	0.30
57.0	119.9	5.349	4.933(−5)	8.30	0.50
60.2	123.3	5.425	5.707(−5)	9.87	0.70
63.7	127.6	5.505	6.636(−5)	11.9	1.00
67.2	132.4	5.582	7.624(−5)	14.2	1.40
69.9	136.9	5.639	8.422(−5)	16.2	1.80
71.1	139.0	5.664	8.768(−5)	17.1	2.00
73.8	144.8	5.717	9.521(−5)	19.3	2.61
76.7	150.9	5.773	1.039(−4)	22.0	3.37
79.2	156.2	5.819	1.116(−4)	24.5	4.16
81.5	160.9	5.859	1.188(−4)	26.8	4.95
85.7	169.7	5.930	1.362(−4)	31.6	6.88
89.0	176.5	5.984	1.444(−4)	35.8	8.65
95.2	189.1	6.079	1.677(−4)	44.5	13.3
100.4	199.5	6.153	1.885(−4)	52.8	18.2
109.1	216.6	6.269	2.268(−4)	69.0	30.1
116.1	230.3	6.356	2.606(−4)	84.3	42.6
122.1	241.9	6.427	2.922(−4)	99.2	55.8
127.3	252.1	6.486	3.212(−4)	113.7	69.7
131.9	261.1	6.537	3.487(−4)	127.8	84.3

[1] From Trafton and Stone [477].

A two-cloud layer model for that part of the Jovian atmosphere accessible to optical astronomy is now almost unanimously accepted. Although suggested at least as early as 1966 by Savage and Danielson [409], the theoretical studies of Lewis [277, 278] gave a firm physical basis for two distinct cloud layers. The Lewis models have strongly influenced interpretations. All current models show the upper cloud layer as ammonia cirrus in saturation equilibrium with its base near 150° K (the exact value a function of ammonia abundance) and extending upward with rapidly decreasing density to the tropopause (ca 106° K). In simple one-dimensional models, such as we are considering here, the optical depth of this upper cloud layer in visible light is 1.5–3.0 [220]. Therefore, much of Jupiter seen through a telescope is this upper layer, and the obvious two-dimensional structure of belts, zones, and so forth, implies the strong possibility of considerable variation in its thickness over the disk. The lower layer is usually assumed to be a classic reflecting layer of great density, probably NH_4SH as suggested by Lewis with a base near 225° K [277]. The latest results of Weidenschilling and Lewis [506] for the Trafton and Stone model [477] suggest that the base may be near 200° K and the clouds no thicker than the upper deck of NH_3 clouds. Thus, it may be possible to see to even deeper levels in the Jovian atmosphere in areas where NH_3 clouds may be very thin, perhaps to water ice clouds with a base near 270° K. The 5 μm radiation in dark belts may, in large part, come from these lower levels. Abundances, base pressures, and even crude rotational temperatures given in the composition section are in general agreement with the Trafton-Stone model. The greatest uncertainties remain the lack of aerosol data and poor spatial resolution of most observations over an obviously inhomogeneous planet, although continued improvement in all optical parameters for atmospheric gases also can be expected.

Above the tropopause, there is a minimum of observational data at present. There is a temperature inversion caused by methane band absorption, especially at 3.3 μm, heating the upper atmosphere. Clearest observational evidence is in the 7.9 μm limb *brightening* observed by Gillett and Westphal [165]. The light curve inversion of data from β-Scorpii occultation by Jupiter [406] indicates a temperature near 180° K at 10^{15} molecules cm^{-3} density and rising to 220° K near 5×10^{13} molecules cm^{-3}. Theoretical models by Wallace et al [497] tie onto the Trafton-Stone model nicely at the 30 mbar level and show a rise to 140° K at 3×10^{-2} atm and 155° K above 10^{-3} atm. There are a number of theoretical studies on the ionosphere above the 10^{13} molecule cm^{-3} level [76, 319, 420, 451].

The radio brightness temperature disk spectrum of Jupiter (Fig. 1) provides data on the thermal structure and composition of Jupiter's atmosphere beneath the clouds in the region inaccessible to optical and infrared observations. Although interpretation of radio data is model-dependent, these observations provide important constraints on possible models. For example, an atmosphere with a temperature profile which is isothermal immediately beneath the clouds is inconsistent with the observed spectrum. Gulkis and Poynter [184] have shown that the observed spectrum is consistent with a H_2-He convective model atmosphere in which temperature rises to at least 400° K and in which ammonia is present in solar cosmic abundance. Gulkis et al [183] analyzed pressure-broadened ammonia absorption in the Jovian microwave spectrum and derived a pressure of 0.48 atm at 130° K.

Dynamics

The banded structure of Jupiter is clear evidence that dynamic forces play an important role in its atmospheric structure. Evaluation of the problem by Stone [446] has shown that the mean temperature structure (previously indicated) is very near radiative-convective equilibrium. He finds static stability very low, advection a very weak, large-scale effect because of the internal heat source and size of the planet, and departures from equilibrium damping out with a time constant of decades [446]. The nature of the instability which causes Jupiter to take on its observed zonal flow pattern is still unknown. Trafton and Stone [477] have discussed various dynamic modes, suggesting three not ruled out by observation, which singly or in

combination may be responsible for Jupiter's behavior: "an inertial instability regime," considered by Stone [445]; a "radiation-condensation instability regime," discussed by Gierasch [159]; and "a forced convection regime" which appears not to have been studied. Thus, even the cause of the basic zonal structure of Jupiter remains unknown in detail, while the causes of such features as the equatorial jet and Great Red Spot are totally speculative. Dynamics is a frontier of Jovian research.

Body Structure Interior Models

For two major reasons, in a few decades the interior of Jupiter may be better understood than any planet except, possibly, Earth. Jupiter must be composed almost entirely of hydrogen and helium, since only these gases can make up a structure of sufficiently low density at nonstellar temperatures. These are the simple species most likely soon to be described quantitatively in the difficult range of pressure and temperature immediately beyond easy laboratory attainment. Further, Jupiter has a large internal energy source. The explanation of this source and the means by which its energy is transported to mean optical depth unity in the atmosphere provide additional strong boundary conditions not present in most planets. As the equation of state and transport properties of hydrogen and helium mixtures improve and are coupled with accurate boundary conditions of energy flux, atmospheric composition and state, magnetic field, and gravitational potential obtained from future space missions, a unique structure is likely to result.

There are two basic types of Jupiter models, both linked closely with two basic ideas about the planet's origin. The gravitational instability hypothesis assumes fluctuations in the primordial nebula occurred which were of sufficient magnitude that self-gravitation became comparable to disruptive solar tidal forces in some areas and materials in the nebula began to collapse [75]. The process of collapse is essentially that of stellar formation, except that bodies with 0.07 solar masses or less never start nuclear fusion, and just continue to collapse and cool [175]. Initial evolutionary studies of a homogeneous body of Jovian mass showed that, after reaching an early maximum temperature of 40 000° K, the body would rapidly cool and collapse, reaching the present Jupiter's state of radius and luminosity (energy production) in just under 2×10^9 years [172, 173]. A more realistic calculation, including Smoluchowski's [433], recommended changes to include stratification and heating effects caused by hydrogen and helium immiscibility, is expected to stretch this time out to ca 4×10^9 years.[3]

Static models of Hubbard [215] which fit into this logical framework, are homogeneous, completely convective (adiabatic) models for current Jovian boundary conditions. Temperature, pressure, and hydrogen to helium ratio at any point completely specify the model [216]. The hydrogen to helium ratio required is about 2 (by mass), however, which is considerably smaller than solar abundance (of more than 3), though not obviously in conflict with present crude observations of atmospheric ratio.

The second origin hypothesis assumes gravitational capture of gas by a high-density core [75]. Such theories commonly assume a solar ratio of hydrogen to helium, since it is difficult to understand how these could have been fractionated in the outer planets [75]. Models, such as Hubbard's, can be applied equally here, simply by terminating the convective calculation at the core surface, which gives more freedom for change in the hydrogen-to-helium ratio by picking a proper core size.

All homogeneous models can be subject to the criticism that they ignore complex details of the phase diagram of the H_2-He system which are now becoming available. Hydrogen and helium have very limited mutual solubility in the liquid and metallic states [432, 449]. Smoluchowski [432] expects stable boundaries to exist between phases, with heat flow across the boundaries by conduction and within each phase by convection. If the central temperature is a "cool" 7500° K, he then expects the sequence of phases shown in Figure 2 [432]. A "hot" model with a 10 000° K central temperature would be fluid throughout but would consist of a helium rich core (containing

[3] H. C. Graboske, Jr., private communication.

dissolved hydrogen) topped by a metallic hydrogen mantle (containing dissolved helium), and finally a supercritical molecular hydrogen atmosphere (containing helium, perhaps with separation of hydrogen and helium phases) [432, 433]. To either of these, a heavy element core could also be added. Thus, the question remains open of Jupiter having a solid surface anywhere. The complex hydrogen-helium phase diagram, which remains quantitatively uncertain, is today's major source of uncertainty in Jovian models.

The ultimate source of the internal energy radiated from Jupiter may be largely gravitational. Several authors have pointed out that straight gravitational contraction of ca 1 mm yr^{-1} with a current central temperature ca 10 000° K could supply the observed luminosity [143, 215, 430]. If gravitational unmixing occurs, perhaps resulting in formation of a core, then the present luminosity is possible with a lower central temperature, but the core must grow each year by about 2×10^{-11} of Jupiter's total mass [143]. Separation of the hydrogen-rich and helium-rich layers is considered a likely contributor to luminosity [407, 432], although its importance relative to straight contraction cannot be assessed quantitatively. Any actual phase changes are also contributing to the overall energy balance in some manner. At present, simple cooling may well be the major contributor to the energy production [218]. Yet the high interior temperatures, which probably exist today to make this true, ultimately are themselves most likely gravitational in origin. The primordial nebula itself was probably very cool at Jupiter's distance from the Sun [280].

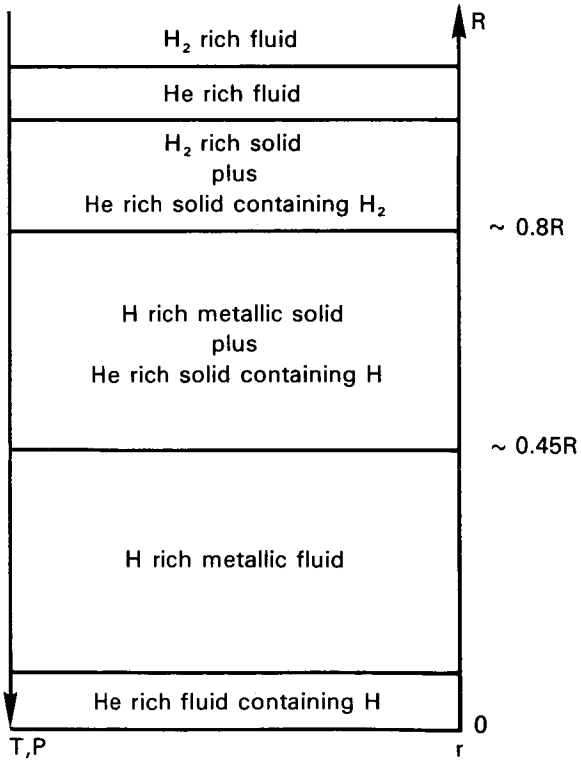

FIGURE 2.—Schematic ordering of H and He phases in the interior of a cool model of Jupiter. (After [432])

Detailed physics of model building is complex, largely because the equation-of-state and transport properties of the material involved are not well-understood and rely almost entirely on theoretical derivations. A comprehensive outline of most of the theoretical methods has been given by Hubbard and Smoluchowski [218], and details of the theory behind evolutionary calculations have been provided by Graboske et al [173]. A typical Jupiter model [218] is in Table 8; it fits no particular set of boundary conditions, and does not include the complex hydrogen-helium phase details. It does show the general trend of pressure and density in the interior of Jupiter.

Magnetosphere

The existence of a Jovian magnetosphere, first inferred from Earth-based radio observations [79], was confirmed by the first in situ measurements [186] of Pioneer 10. The Jovian magnetosphere, as inferred from Pioneer 10 magnetic field and particle measurements, is substantially different from the Earth's. In particular, the magnetic field exhibits a large outward extension, approaching a disk-shaped configuration, at distances greater than 20 R_j. Figure 3 is a schematic diagram of the disk model of Jupiter's magnetosphere [486]. Highly energetic electrons and protons exist throughout the magnetosphere, concentrated in a thin disklike configuration at radial distances greater than 20 R_j. Inside 20 R_j, the magnetic field becomes more dipolar in form and energetic particle-trapping appears to be similar to Earth's Van Allen belt.

In the following sections, nonthermal radio

emissions from Jupier are described, followed by discussions of magnetic field, energetic particles, and plasma contained within the magnetosphere.

Nonthermal Radio Emission

Radio emission from Jupiter has been observed over the wavelength range from 1 mm to ca 650 m. A representative flux density spectrum of the observed emission is shown in Figure 4. The observed spectrum at wavelengths greater than 7 cm is dominated by nonthermal radiation; at shorter wavelengths the emission is dominated by atmospheric thermal radiation. Details of the thermal portion of the spectrum are shown in Figure 1 and discussed in the sections on Composition and Temperature. The nonthermal portion of the spectrum has at least two clearly distinguishable components, a centimeter and decimeter component, extending from ca 0.1 to ca 1 m, and a decametric and hectometric component, important at wavelengths longer than 7.5 m.

The centimetric/decimetric component is due to synchrotron emission from high-energy electrons trapped in Jupiter's magnetic field. The origin of the hectometric/decametric component is not yet well-understood. Current knowledge of Jovian nonthermal radiation has been summarized [79, 444, 502, 503]. Dickel et al [115] summarized all available brightness temperature observations of Jupiter's microwave spectrum.

TABLE 8.—*"Typical" Model of Jupiter*[1]

Radius, 10^4km	Fractional mass	Pressure, Mbars	Density, g cm^{-3}
6.9	0.99	0.004	0.03
6.5	0.97	0.24	0.4
6.0	0.90	1.1	0.7
5.5[2]	0.80	2.5	1.1
5.0	0.70	4.5	1.6
4.5	0.60	7.6	1.9
4.0	0.40	11	2.3
3.5	0.30	15	2.6
3.0	0.20	20	3.0
2.5	0.10	24	3.4
2.0	0.06	28	3.7
1.5	0.03	32	3.9
1.0	0.01	35	4.1
0.5	0.001	36	4.2
0.0	0.0	37	4.2[3]

[1] From [218].

[2] Approximate radius at which the molecular hydrogen-metallic hydrogen transition is assumed to occur in most models.

[3] Not including a possible dense core.

Decametric and Hectometric Radiation

The behavior of decametric radiation has become quite clear in the 20 years since its discovery, although understanding of its mechanism generation is still vague. Decametric activity has been detected at ground-based observatories at frequencies between 3.5 [533] and 39.5 MHz [501], with possible detection at 43 MHz [255]. Recent observations of Jupiter with Earth-orbiting radio-telescopes tuned to frequencies well below the ionospheric critical frequency have extended the range of frequencies at which Jupiter has been detected from 3.5 MHz downward to 450 kHz [114]. Unlike synchrotron emission which is continuous, the decametric component is emitted sporadically, with intense bursts lasting short intervals. The flux density spectrum of the bursts shows rapid increase in flux density with decreasing frequency over the range from 40–10 MHz (7.5–60 m), peaks near 10 MHz, and then decreases at still lower frequencies.

On Earth reception, decametric radiation usually consists of noise which is intensity-modulated to form randomly occurring bursts characterized by a hierarchy of time structure. An entire activity period containing many bursts is known as a Jovian noise storm, which ordinarily lasts from several minutes to several hours. Quiescent periods between storms may last for hours, days, or weeks. Bursts generally have durations of 0.5 to 5 s, but occasionally bursts are much shorter or much longer. The bandwidths of individual bursts are usually between 0.05 and 2 MHz. Bursts with durations of 0.5 to 5 s are known as "L" bursts, while those of shorter duration are called "S" bursts. The L-burst waveform is believed to be due to diffraction effects in the interplanetary medium [124]. The S-burst waveform, on the other hand, is presumably of Jovian origin.

Measurements of all four polarization param-

eters have been made by Sherrill [419], and Barrow and Morrow [29]. Sherrill concluded that the degree of polarization is usually at least 0.8 above 15 MHz and is practically 1.0 above 20 MHz. Polarization is always right-handed at 22.2 MHz and higher frequencies. The left-handed circular component becomes relatively more prominent as frequency is reduced, but the right-handed component is still predominant down to 10 MHz. The average axial ratio of individual bursts is approximately $|0.5|$, but occasionally bursts appear to be purely circular, with an axial ratio of unity. The true meaning of polarization data is not known at this time, although a likely interpretation is that radiation is being emitted into some characteristic mode of polarization at the point of origin and is modified substantially as it propagates out through the Jovian magnetosphere on its trip to Earth. Thus, polarization measured on Earth probably reflects both initial conditions of polarization at its point of origin and superposed propagation effects.

A characteristic feature of Jovian bursts is their tendency to recur at nearly the same central meridian longitude (CML), measured in System II. Characteristic histograms of occurrence probability as a function of CML are shown in Figure 5 for two different frequencies. In the vicinity of 18 MHz, emission appears to originate from at least three longitude zones, generally referred to as sources A, B, and C (as indicated in Figure 5), or as the main source, the early source, and the late or third source. The characteristic structure of histograms allows definition of a rotation period for Jupiter. In 1962, the International Astronomical Union [225] adopted the rotational period of 9 h 55 min 29.37 s as the "best-fit" period to histogram data. This period has been named System III (1957.0). It has become clear more recently that this period is incorrect [78, 80, 180, 443]. The mean value of Jupiter's decametric rotation period is estimated [78] to be 9 h 55 min 29.75 s $\pm$0.04. This period is

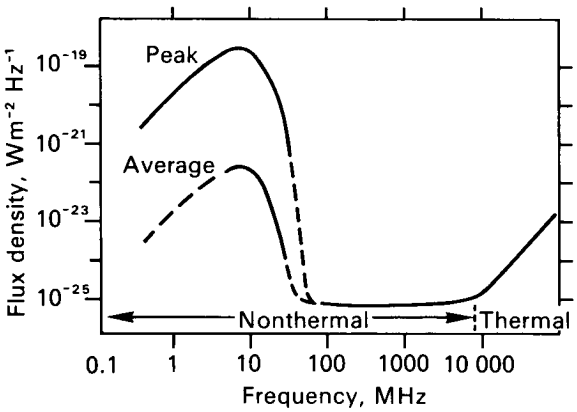

FIGURE 4. – Schematic appearance of Jupiter's observed radio spectrum.

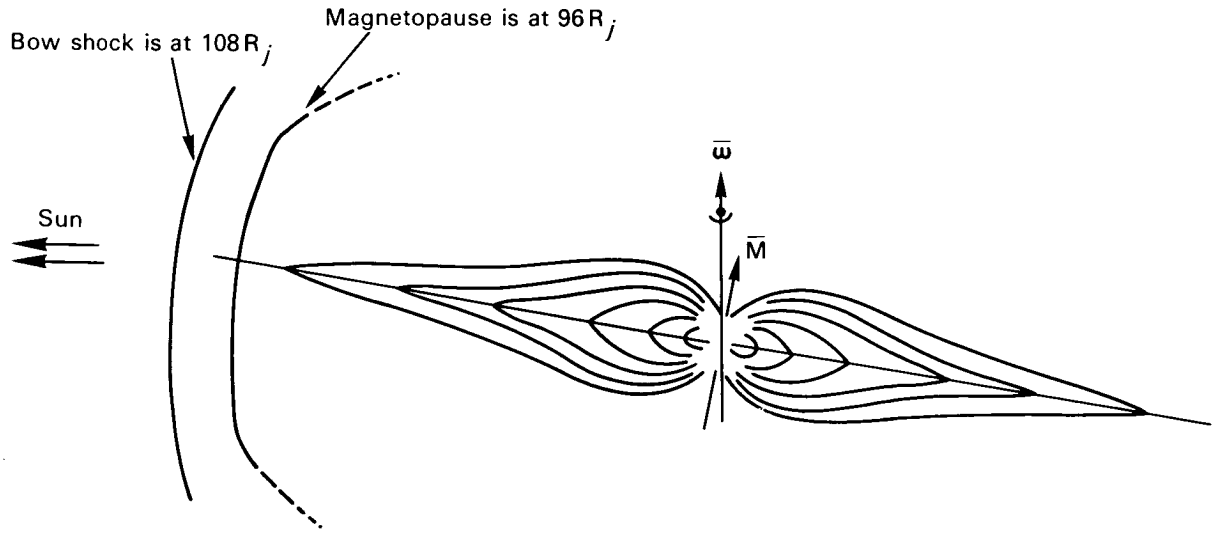

FIGURE 3. – Magnetodisk model of Jupiter's magnetosphere. (Adapted from [486])

0.4 s longer than System III (1957.0). Such correction implies that features on Jupiter in the System III (1957.0) longitude system will drift to higher longitudes at a rate of ca 3.6°/yr.

Upper limits on source sizes of individual Jovian emission events have been determined with long baseline interferometers. Dulk [126], using baselines up to 487 000 λ, obtained an upper limit to the size of an incoherent source of 0.1″ (400 km at Jupiter) at 34 MHz. Carr et al [80] observed individual S-bursts at 18 MHz with interferometers having baselines up to 450 000 λ. Their preliminary results indicate that if S-burst sources are incoherent, at least some of them must be smaller than 0.1″. Despite the high angular resolution achieved, the positional uncertainties of the source of emission are still very great.

An unusual property of decametric emission discovered by Bigg [52] is the modulating effect of the satellite Io. Recently Desch and Carr [114] reported a similar modulating effect of the satellite Europa, which shows up at frequencies less than 1.3 MHz. Bigg found that the majority

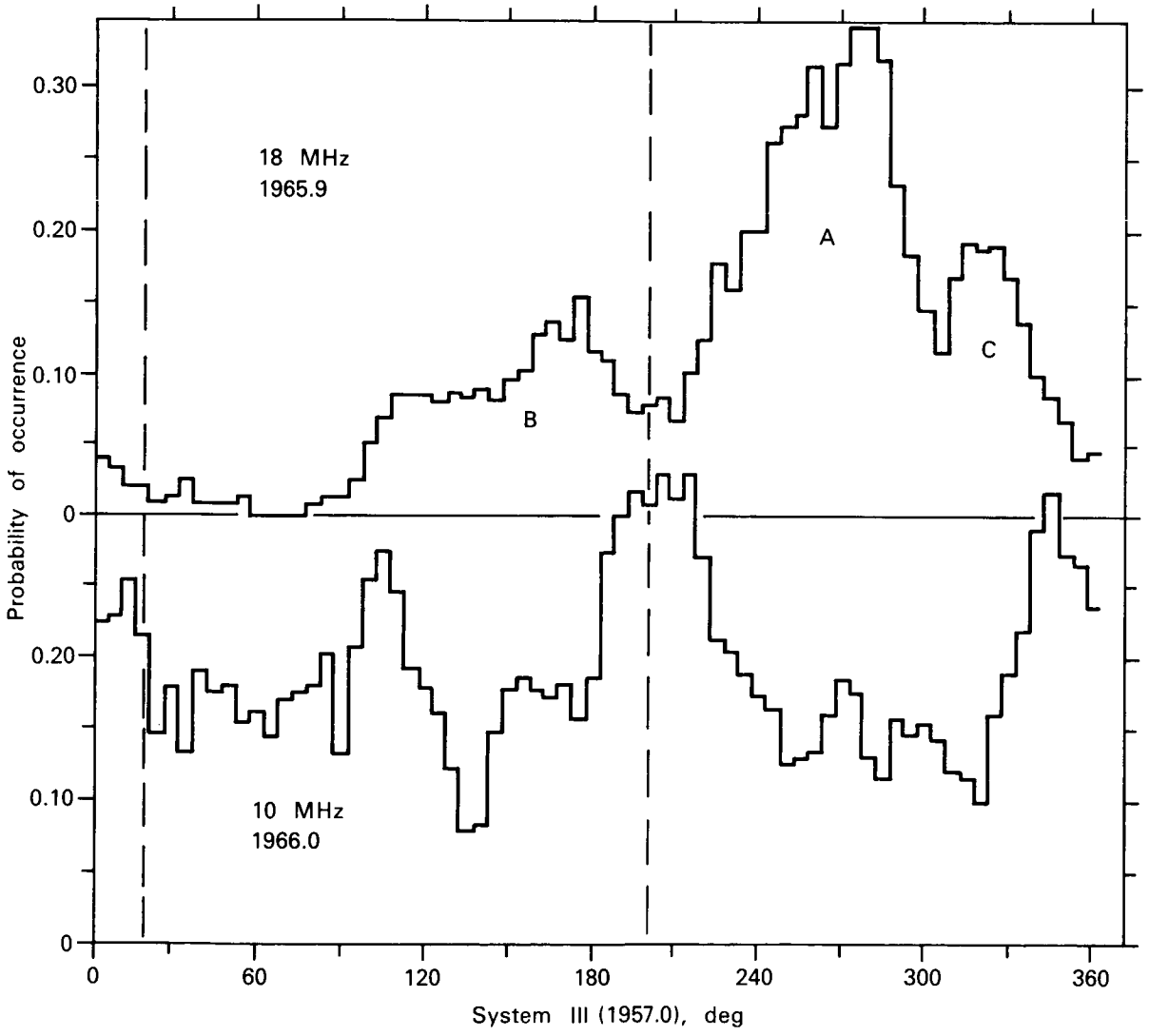

FIGURE 5. – Histograms of occurrence probability as a function of central meridian longitude (CML); CML values of magnetic poles are indicated by vertical dashed lines [79]. (See text)

of the stronger source B emission events occur when the orbital position of Io is within a few degrees of 93° from superior geocentric conjunction, and that most source A events occur when Io is near 246°. This effect has been well-verified [79, 502]; however, it is now apparent that while many source A events depend on Io's position, many do not.

Conseil et al [91] have recently shown a close relationship between solar wind velocity and the phase of Io during radio bursts from Jupiter. Most source B emission is Io-dependent. The Io effect is apparently much less pronounced at 10 MHz [127, 389] than at higher frequencies. There is no widely accepted theory which explains how Io modulates emission, although a number of ideas have been advanced [71, 132, 140, 167, 168, 308, 410, 502]. Gurnett [185] has recently suggested that photoelectrons are emitted from Io's surface and accelerated in a sheath surrounding Io. This suggestion is interesting in light of the Io ionosphere detected by Pioneer 10.

Understanding of the complete mechanism of creation of decametric radiation is still highly speculative. Two phenomena probably occur: (1) generation of an anisotropic distribution of particles or waves; and (2) generation of decametric radiation by them. Measurements of true source positions relative to Jupiter's disk would help to eliminate a number of the many conflicting theories.

Centimetric and Decimetric Radiation

Jupiter emits a nearly constant flux density of about $6.0 \pm 1.0 \times 10^{-26}$ W m^{-2} Hz^{-2} (4.04 AU) at wavelengths from about 5 to 300 cm. Interferometric observations at wavelengths of 10 to 20 cm indicate that radiation is coming from an area much larger than that of the planetary disk.

Figure 6 shows Berge's [39] suggested brightness contours of the 10-cm radiation. An interesting result of this study is that the disk temperature for the thermal component at 2880 MHz appears to be ca 260° K, nearly twice the effective temperature of Jupiter. Branson [63] obtained brightness temperature maps of emitting regions at 1407 MHz at each of three values of CML spaced 120° apart. They illustrate strikingly the large emitting region, and its rocking as the planet rotates. At wavelengths above 21 cm, the belt structure has not been measured accurately, and there is considerable disagreement in available experimental data as to whether or not the overall extent of emission increases with increasing wavelength [178].

Throughout most of the decimetric spectrum, radiation is linearly polarized, the degree of linear polarization reaching a maximum of ca 25% at 21 cm and decreasing toward longer and shorter wavelengths [115]. The direction of the electric vector rocks back and forth ± 10° relative to the rotational Equator as the planet rotates. Radiation also shows a small degree of circular polarization [38, 252, 413]. Observations of circular polarization provided information about polarity of the dipole and magnetic field strength within the Jovian magnetosphere. Circular polarization measurements of Komesaroff et al [252] have been used to derive a field strength in the radiation belts between 0.4 and 1.9 G. These measurements agree well with the magnetic field model based on Pioneer 10 measurements, predicting a field strength of 0.7 G at 1.8 R_j. The results also confirm that Jupiter's magnetic dipole is antiparallel to that of the Earth, which was first pointed out by Warwick [500] and corroborated by Berge [38].

Accurate position measurements of decimetric centroid emission relative to the optical disk have been made [40, 317, 394, 443] which indicate that the Jovian magnetic field is well-centered

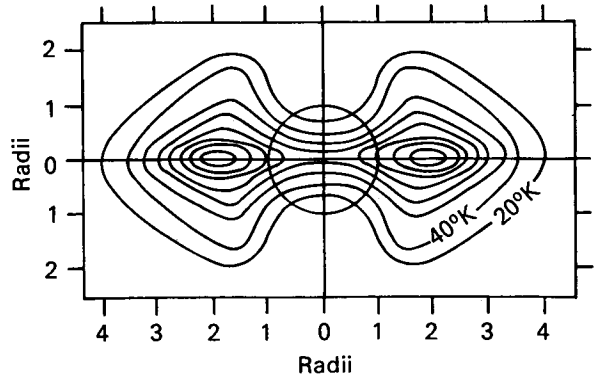

FIGURE 6.—Brightness temperature model of Berge [39]; contour interval is 20° K; CML (System III) is 20°.

and reasonably symmetric. Results rule out displacements greater than several tenths of a diameter.

The possible dependence of decimetric flux density on solar activity has been discussed by many authors (e.g., [79]). Investigation of the possible dependence of total flux density on solar activity was carried out by Gerard [158] from December 1967 to August 1968; he found evidence for positive correlation between the 11.13 cm Jovian total flux and solar activity as measured by the 10.7 cm solar flux. Measurements made in 1971 at 12.7 cm wavelength showed that Jupiter's flux density had varied by ca 20% over a period of 8 years [249], although this change could not be correlated with solar activity.

A mean rotation period of Jupiter can be determined at decimetric wavelengths by comparing longitudinal distribution, of either polarization angle or total intensity, with similar distribution obtained several years later. More precise decimetric results are given in Table 9. The weighted mean of decimetric measurements is estimated to be 9 h 55 min 29.71 s ± 0.07 s [78], which is not notably different from the period obtained at decametric wavelengths, but is a significant departure from System III (1957.0). There is no indication that the period has changed over the interval for which observations have been made. Decimetric determinations of the rotation period are as shown in Table 9.

TABLE 9.—*Decimetric Determinations of Jupiter's Rotation Period*

Reference	Rotation period
Bash, Drake, Gundermann, and Heiles [31]	09 h 55 min 29.70 s ± 0.04 s
Davies and Williams [105]	09 h 55 min 29.50 s ± 0.29 s
Komesaroff and McCulloch [251]	09 h 55 min 29.83 s ± 0.16 s
Whiteoak, Gardner, and Morris [514]	09 h 55 min 29.69 s ± 0.05 s
Gulkis, Gary, Klein, and Stelzried [181]	09 h 55 min 29.74 s ± 0.05 s
Stannard [443]	09 h 55 min 29.74 s ± 0.03 s

In summary, the distinguishing characteristics of this component are its flat nonthermal spectrum, the large, distinctive shape of the emitting region, relatively high degree of linear polarization, very small degree of circular polarization, and variations of all of these with rotation. Shortly after discovery of this component, it was suggested [125] that synchrotron radiation from relativistic electrons was the source of this radiation. A number of authors can be credited for having laid the groundwork which proved conclusively that the synchrotron mechanism was indeed responsible for this radiation [82, 137, 138, 139, 463]. In 1974, previous models were reviewed and a new model developed for electron and proton fluxes in radiation belts [444], based on knowledge of Jupiter prior to the Pioneer 10 encounter with Jupiter.

Magnetic Field

A single bow shock crossing was observed with the Pioneer 10 magnetometer [428] at 108 R_j during the inward passage of the spacecraft. Magnetic field strength increased from 0.5 to 1.5 γ (1 $\gamma = 10^{-5}$ G) at the bow shock. The magnetopause was first observed at 96 R_j as a well-defined boundary, with the magnetic field strength increasing to 5 γ. Magnetic field strength remained near 5 γ from 90 to 50 R_j but was very irregular, frequently dipping to 1 γ. As evidence for the large variability of the outer magnetosphere, the magnetopause boundary first encountered near 96 R_j appeared to move in past the spacecraft as it neared 50 R_j. Similar multiple encounters with the magnetopause boundary were seen on both the inbound and outbound spacecraft passage.

The field strength rises monotonically beginning at about 25 R_j and going inward, and the direction becomes more dipolar. Data acquired between 2.84 and 6.0 R_j, enabled Smith et al [429] to fit an eccentric dipole model to the data. The dipole has a moment of 4.0 G R_j^3 and a tilt angle with respect to Jupiter's rotation axis of 11°. The System III (1957.0) longitudes of the magnetic pole in the northern hemisphere are 222°. The field is directed in the opposite sense to that of Earth. The dipole is displaced from the center of Jupiter by 0.11 R_j in the direction of latitude 16° North and System III (1957.0) longi-

tude 176°. The dipole tilt and longitude of the pole are in reasonable agreement with values inferred from radio astronomy measurements.

The large outward extension of the magnetic field is evident by comparing measured field strength between 50 and 90 R_j with the 4 G surface dipole field measured inside 6 R_j. The latter would yield a field which varied as the inverse cube of the radial distance from the dipole with a strength of 3.2 γ at 50 R_j, whereas the measured field was ca 5 γ throughout the region, which suggests that the magnetic field is inflated or being pulled out away from the planet. The inflation is probably due to stress produced by a corotating plasma in a magnetosphere dominated by centrifugal forces. The view that additional pressure must dominate magnetic pressure is supported by the observation that magnetic energy density just inside the magnetosphere (10^{-10} erg/cm^3) is less than the estimated solar wind energy density (5×10^{-10} erg/cm^3).

Energetic Particles

Prior to the first detection of the Jovian bow shock by Pioneer 10, energetic particles were detected by the spacecraft when it was about 360 R_j from the planet [421]; the particles appeared in the form of sudden increases in electron fluxes, with energies ranging from about 1 to 30 MeV. Peak intensities were $\geq$ 100 times interplanetary quiet time levels and events lasted about 2 d. These particles, it is believed, escaped into the interplanetary medium from the bow shock or magnetosphere of Jupiter.

Within the magnetosphere at Jovicentric distances from ca 20 to 100 R_j, high-energy electrons and protons, like the magnetic field, are concentrated in a disklike region near the magnetic equatorial plane. Stable trapping of particles in this region is doubtful, so that some authors refer to this region as the quasi-trapping region. Inside ca 20 R_j, where the magnetic field becomes more dipolar, energetic electrons and protons appear to be stably trapped. Particles are not tightly confined near the magnetic Equator in this region. Detailed spectra of electrons and protons in the trapped particle region are not available at this time, although individual experimenters have given preliminary values. Simpson et al [422] find that the peak omnidirection electron flux greater than 3 MeV is ca 2.5×10^8 electrons cm^{-2} sec^{-1} (at $L=3.1$). Peak omnidirection flux of protons greater than 35 MeV is 6×10^6 protons cm^{-2} sec^{-1} at $L=3.4$. Van Allen et al [485] give the following provisional expression for omnidirectional intensity J_0 of electrons with energy $\geq$ 21 MeV within the region $3.5 < L < 12$ R_j

$$J(E_c > 21 \text{ MeV}) = 3\times10^8 \exp\left[-\frac{L}{1.45}\right] \left(\frac{\cos^6\Lambda}{\sqrt{4-3\cos^2\Lambda}}\right)^{m/2} \quad (1)$$

In this expression, J is in electrons/cm^2 s, L is the magnetic shell parameter in units of R_j, Λ is the magnetic latitude, and $m=3.5+\left(\frac{3.86}{L}\right)^8$ is the pitch angle parameter.

Plasma Density

A "thermal plasma" must also exist in addition to energetic particles contained with the magnetosphere. Plasma density is an important parameter in theories of satellite-magnetosphere interactions, decametric and decimetric radiation, and configuration of the magnetosphere itself. The Pioneer 10 payload was not able to provide direct unambiguous data on this plasma distribution; hence it is necessary to rely almost solely on theoretical considerations to determine this quantity [64, 167, 226, 321, 322]. These theories have recently been reviewed by Mendis and Axford [322], who reached the general conclusions:

- the thermal plasma should corotate with the planet,
- thermal plasma should be concentrated toward the equatorial plane,
- centrifugal forces due to rotation of the planet are important in determining distribution of plasma,
- a nonthermal component of plasma in the ionosphere is responsible for populating the magnetosphere,
- recombination sets the limit of maximum plasma density.

Both Ioannidis and Brice [226], and Mendis and Axford [322] derived models in which maximum plasma density is ca 30 cm^{-3}. This occurs around $L=10$ (10 R_j in the equatorial plane).

SATURN

Saturn appears similar to Jupiter in many ways, with the obvious exception of its ring system. A magnetic field has not yet been detected on Saturn but this could have escaped detection thus far. With mean density of only 0.70 g cm^{-3}, the bulk of this planet once again must be dominated by hydrogen and helium as, presumably, is its atmosphere, although no measurement of its mean molecular weight exists. Theoretically, the problems of atmosphere and interior are essentially the same as those discussed for Jupiter, and will not be repeated.

Ground-based observation of Saturn is much more difficult; Saturn has only one-third the surface brightness of Jupiter, and all means of detection relying upon surface brightness require at least three times the exposure or integration time. The planet is nearly twice as far from the Sun as Jupiter and twice as far from Earth, so that the total flux received from Saturn on Earth is down by a factor of roughly 16 from that received from Jupiter. Also, geometric resolution of Saturn's surface seen from Earth is only half as great as that for Jupiter. It is not surprising that knowledge of Saturn is less extensive.

Atmosphere

Composition

Molecular hydrogen was first positively identified in the Saturn atmosphere through detection of two lines of the 4-0 overtone in its quadrupole spectrum by Münch and Spinrad in 1962 [336]. Lines in both the 3-0 and 4-0 overtones have since been used to derive abundances, temperatures, and pressures in the usual way. The most recently published work suggests an abundance of 76 ± 20 km-amagat of H_2 at an effective pressure[4] of between 0.4 and 1.0 atm [133]. A study of 14 plates [47], each containing the S(0) and S(1) lines of the 3-0 band, taken over a 3-month period suggests that the apparent abundance is variable between perhaps 75 and 140 km-amagat or more.

Detection of methane on Saturn followed the same historical sequence as on Jupiter. There have been three recent high-dispersion studies of the R branch of the $3\nu_3$ methane band at 1.1 μm: photographically recorded slit spectroscopy [44], photoelectrically scanned slit spectroscopy [471], and Fourier spectroscopy of most of the disk [106]. Each took reasonable care to exclude the ring. Trafton's result is larger by a factor of 3 than Bergstralh's for the same half-width, while the result of de Bergh et al falls in between. There is some indication of temporal variation, as in the H_2 lines. Part of the variation is probably due to differences in techniques used to locate the continuum. The best choice at present appears to be using the result of de Bergh et al [106], 42 ± 11 m-amagat above a reflecting layer base pressure of 2.8 ± 0.6 atm, recognizing that this is a planetwide average and that the reflecting layer model is very questionable for Saturn. All results are much smaller than the early estimate, 350 m-amagat (of Kuiper [261]) made empirically using shorter wavelength bands. The difference is certainly caused in part by comparison of Kuiper's spectra with laboratory results originating at far higher temperatures, but it may also be, in part, an indication of a complex inhomogeneous atmosphere.

The abundance of NH_3, on Saturn remains a matter of considerable debate. Dunbar reported its presence in an amount "probably not more than 2 m at atmospheric pressure" [130]. Later, when ammonia could not be detected [351, 440], it was suggested that there had been confusion with weak methane lines. Ammonia was again reported [166] in 1966, the lines being about 0.15 ± 0.06 the strength of the corresponding band (6450 Å) in Jupiter. Small temperature changes on Saturn would cause considerable change in the amount of gaseous ammonia in the atmosphere "above the clouds." There is "fairly impressive evidence for short-period changes (occurring in a few years) in the atmosphere of Saturn" [166]. Spectra at 6450 Å taken in

[4] The effective pressure is half the base pressure in a reflecting layer model atmosphere.

December 1970 [97] showed no ammonia, and an upper limit of 7 m-atm was derived.

Cruikshank [97] also reported that observations of the strong 1.5 μm ammonia band in 1969 by Kuiper, Cruikshank, and Fink failed to detect ammonia, and allowed an upper limit in abundance of only 20 cm-atm above optical depth unity to be set at that wavelength. An upper limit of about 2 cm-amagat was reported from studies [309] in the 4150-cm^{-1} region during 1973–74, while in the λ6450 band, an amount was detected "an order of magnitude less than on Jupiter"[5] (ca 1 m amagat?). These observations are not as different as they might seem, since apparent abundance on Jupiter in the former band is 50–100 times less than in the latter, and none of these measurements is precise.

There is a hint of the strong ν_2 band of ammonia at 10.5 μm in the spectrum of Gillett and Forrest [161]. Measurements of the thermal disk temperature of Saturn at radio wavelengths provide strong support for the presence of ammonia in its atmosphere. Interpretation of radio data implies a relative concentration of ammonia beneath the clouds of 3×10^{-5} [269] to 1.5×10^{-4} [184].

There is no observational evidence for helium on Saturn, but with proof of its presence on Jupiter, confirming earlier theoretical expectations, there is little doubt that it will be found eventually on Saturn as well.

The medium resolution spectrum ($\Delta\lambda/\lambda \approx 0.015$) of Saturn in the 7.5–13.5 region [161] gives a hint of two other species found on Jupiter, perhaps 2 cm-amagat of phosphine (PH_3) and a small amount of ethane (C_2H_6). High-resolution spectra will be required for definite proof that these gases are present.

Temperature

Modern temperature measurements on Saturn, in the infrared and microwave regions of the spectrum, were first made at about the same time as those on Jupiter. A compilation of infrared results is given in Table 10. Radio emission from Saturn has been observed over the wavelength range from ca 1 mm longward to ca 94 cm. Figure 7 shows disk brightness temperatures at radio wavelengths [343, 483, 528]. A distinct feature of Saturn's spectrum is the wavelength dependence of the measured temperature. The temperature increases from near 130° K at millimeter wavelengths to close to 540° K at 94 cm; this behavior is qualitatively similar to the thermal radio spectrum of Jupiter.

Suggestions have been advanced to explain the marked increase in temperature with wavelength. Excess radiation may be due to (1) nonthermal emission from a trapped radiation belt, (2) thermal radiation from Saturn's rings, (3) free-free emission from Saturn's ionosphere, or (4) emission from Saturn's atmosphere. There is little experimental evidence so far to support the first three mechanisms. Interferometric measurements have been made [41, 43, 66] over the wavelength range 3.7 to 21 cm which rule out strong emission from either a radiation belt or the rings. It is estimated [41] that at 21-cm wavelength no more than 6% of

TABLE 10.—*Saturn Brightness Temperatures to 1 mm*

Wavelength, μm	Brightness temperature,[1] °K	Reference	Remarks
5	ca. 120	[286]	
7.7–7.9	129	[161]	15% of disk obscured by rings
8.5–11.5	ca. 103	[161]	Do.
10–14	100 ± 3	[5]	
10–14	c 99 ± 3	[5]	Measures actually refer to + 17° latitude
17–25	c 97.3 ± 2	[338]	Limb was $95.5° \pm 2°$ K
30–45	89 ± 4	[16]	All of rings as well as disk
45–80	94 ± 2	[16]	Do.
65–110	97 ± 5	[16]	Do.
125–300	93 ± 4	[16]	Do.
30–300	88 ± 1	[16]	Do.
45–300	91 ± 1	[16]	Do.
1.5–350	97 ± 4	[23]	Do.

[1] Values preceded by a "c" are center of disk temperatures. Others refer to averages over most or all of the disk. Possible ring contributions are noted in the remarks column.

[5] E. Barker, D.P.S. Meeting, Palo Alto, 1974.

the total radiation can come from visible rings, nor more than 5% from a radiation belt.

In order to explain the spectrum on the basis of free-free emission from Saturn's ionosphere, an emission measure many orders of magnitude larger than expected for Jupiter would be required [182]. Since solar ionizing flux is less at Saturn than at Jupiter, and their compositions are similar, it is expected that the emission measure of Saturn's ionosphere is less than Jupiter's. Therefore, it is unlikely that free-free emission from a hot ionosphere can explain the observed spectrum. A number of authors [182, 269, 524] have shown that the gross features of Saturn's centimeter wavelength spectrum can be explained in terms of thermal emission by an atmosphere whose opacity is wavelength-dependent and in which ammonia is assumed to be the principal source of opacity at radio wavelengths. A deep convective atmosphere is required to explain the observations. Saturn's spectrum was also measured [524] in the vicinity of the 1.25-cm inversion band of ammonia; evidence was found of ammonia as a constituent gas in the upper atmosphere.

Three studies of the $3\nu_3$ methane band on Saturn [44, 106, 471] resulted in rotational temperatures between 130° and 140° K in spite of diverse abundances. A rotational temperature ca 80° K from hydrogen quadrupole lines was found [133], and departures from equilibrium by hydrogen at these temperatures were noted. This problem is probably even more acute on Uranus. Any apparent hydrogen rotational temperature in a region where kinetic temperature is under 100° K likely cannot be given the usual interpretation as an equilibrium thermodynamic temperature.

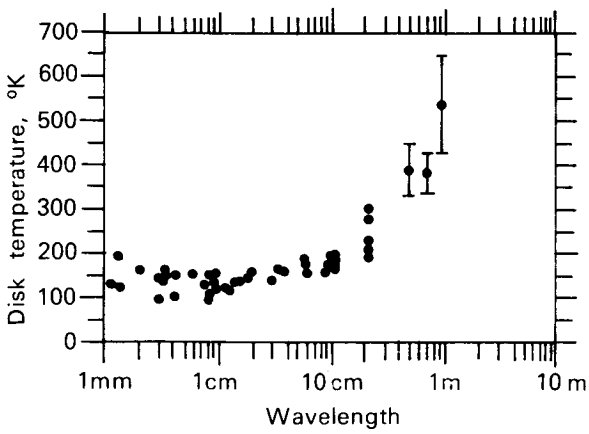

FIGURE 7.—Microwave spectrum of Saturn. Error bars are only shown for longest wavelengths where there are few measurements.

The Visible Surface

The clouds on Saturn appear to be in a state of differential rotation, the period increasing from 10 h 2 min (±4 min) at the Equator to 6% greater at 27° latitude, 8% greater at 42° latitude, and 11% greater at 57° latitude, as determined from Doppler spectroscopy [326]. Saturn has a so-called equatorial band, which is dark in blue light and bright in red light, six named cloud belts in each hemisphere, and light zones between these, for a total of at least 25 distinct degrees of shading under optimum observing conditions [385].

White spots appear on Saturn on rare occasions, persisting for a few days or weeks, never achieving the prominence or lifetime of the sporadic spots on Jupiter [1]. A recent spot at latitude −57.3° set a record for both persistence and high south latitude. Its motion during a 490-d period from October 1969 to February 1971 appeared to be a damped 169-d sinusoid about a mean rotation period of 10 h 36min 27.9 s ± 0.2 s [385]. The spot measured 8000 km north and south by 6000 km east and west.

Data were collected [117] on motions of eight earlier, well-observed spots which showed that three high-latitude objects (+57°, +36°, and −36°) had rotation periods around 10 h 38 min, while four spots within 8° of the Equator had periods between 10 h 12 min and 10 h 15 min. A spot at −12.3° had a period of 10 h 21 min. Thus, spot motions are not in good agreement with the spectroscopic rotation period. Moore recognized possible sizable errors in his work. Also, it is known that typically a spot may be driven at a distinctly atypical rotation rate (or at least such is true on Jupiter), so perhaps the results are not surprising. Nine spots and one spectroscopic study are not sufficient data to

suggest a firm hypothesis. Hide [205] suggests that better observations will show a discrete equatorial jet similar to the one on Jupiter.

Shades of orange, blue, and so forth have been reported on Saturn by experienced observers, but all colors are extremely subtle, except for predominating variations from white to pale yellow to brownish yellow [1]. Their origin is unknown, but speculation is similar to that about Jupiter. Visible clouds are probably ammonia cirrus but somewhat more dense than on Jupiter (see section, **Atmospheric Structure**).

It is extremely difficult to obtain good integrated (full disk) photometry of Saturn because of the rings. Utilizing the 3 years of Harvard photometry [230, 231] obtained with the ring inclination varying relative to Earth, Irvine and Lane [228] reduced it to "no-ring" data. The resulting geometric albedos are in Table 11. These authors also derived approximate no-ring phase coefficients of 0.013 ± 0.007 mag deg^{-1} for $\lambda\lambda 3500-5000$ and 0.035 ± 0.010 mag deg^{-1} for $\lambda\lambda 6200-10\,600$. In the infrared from 2–3.2 μm, Saturn has a higher reflectivity than Jupiter, while from 3.2–4.2 μm the reflectivity of both planets is very low [236]. The combined reflectivity of planet and ring is about 30% higher at 2500 than at 3500 Å and seems to decline at still shorter wavelengths [496].

Much of the detailed photometry for Saturn is in the form of polar or equatorial scans. Binder and McCarthy, [56] in particular, have furnished both equatorial and meridional limb-darkening curves in nine passbands from 0.6–1.55 μm. Normal albedos (or close approximations) as a function of wavelength for the center of the disk, at a resolution of about 500, were obtained by Teifel in 1968 [461]. Selected values from this work are in Table 12. In yellow and red light, the equatorial band is the brightest region on Saturn, and the north polar region, the darkest [461]. In blue to violet light, the polar region becomes quite bright and the equatorial band fades [461]. Both weak and strong methane bands show decreasing absorption from center to limb along the Equator and increasing absorption from center to pole along the central meridian [354, 461]. Methane absorption at $-20°$ latitude is 25–28% greater than at the Equator, much more than a straight air mass (secant) effect [461]. These effects can be interpreted in terms of varying density of ammonia aerosols with latitude.

Energy Balance

Photometry of Saturn is far more difficult than for Jupiter, because of the rings. No near-infrared, integrated photometry has been published beyond 1.06 μm; many energy balance studies have simply used the bolometric Bond albedo of Jupiter, although existing data tend to indicate a somewhat higher value for Saturn.

Calculations in this chapter are based upon Walker's [495] unpublished value of 0.61, resulting in a calculated effective temperature of 71° K. A rapidly rotating body of zero albedo at Saturn's distance from the Sun would have an effective temperature of 90° K. The broadband measurement of Aumann et al [23] is 97° K. Thus, it appears that Saturn, like Jupiter, is radiating more energy than it receives from the Sun—three and a half times as much, accepting the 0.61 bolometric albedo and the 97° K temperature. It

TABLE 11.—*Integrated Photometry of Saturn* [1]

Passband	Geometric albedo	Passband	Geometric albedo
U	0.169	4573 Å	0.318
B	0.302	5012 Å	0.377
V	0.436	6264 Å	0.498
3590 Å	0.184	7297 Å	0.376
3926 Å	0.199	8595 Å	0.297
4155 Å	0.240	10 635 Å	0.417

[1] Data from [228].

TABLE 12.—*Detailed Photometry of Saturn* [1]

Wavelength, Å	Normal albedo	Wavelength, Å	Normal albedo
4100	0.26	6050	0.67
4400	0.31	6200	0.50
4800	0.42	6400	0.72
5200	0.48	6600	0.71
5600	0.52	6800	0.67
5850	0.67		

[1] Center of disk data from [461].

has been pointed out that the rings are not as cold as was once thought, and that the measurement of Aumann et al undoubtedly includes a ring contribution. However, at the time of that measurement (Dec. 2, 1968) the rings were inclined only 13.2° to the Sun and not intercepting as much energy as in recent years.

Also, Murphy's recent work [338] indicates a temperature for the disk center at 17–25 μm of 97.3° K, with little decrease toward the limb. Thermal opacity in this passband is less than immediately on either side of it, but it does not appear that the 17–25 μm brightness temperature could be sufficiently higher than the true effective temperature of Saturn to otherwise explain the apparent energy imbalance.

Atmospheric Structure (Models)

Thermal opacity in Saturn is dominated by pressure-induced H_2 absorption, as for Jupiter [476]. Thermal structure is more uncertain because the magnitude of the internal energy source is less well-determined, the hydrogen to helium ratio is unknown, and the temperature lower (making the relative amounts of ortho- and parahydrogen a factor). The NH_3 abundance is also uncertain and has not been included as an opacity source in the existing radiative equilibrium calculations of Trafton and Münch [476]. There is evidence of methane absorption in the high atmosphere of Saturn as for Jupiter, the 7.7–7.9 μm temperature rising to 129° K [161].

A nominal radiative-convective model constructed for Saturn [359] is given as Table 13. A major difference between the structure of Saturn's and Jupiter's atmospheres is caused by much smaller local gravity, which greatly increases scale height. Palluconi assumed a wet adiabatic gradient wherever it exceeded the radiative gradient, a good approximation to the effects of dynamics [359], especially when other uncertainties are so much greater. His assumed composition (footnote in Table 13) did not include H_2S, so no NH_4SH clouds are shown. Actually, such a layer might be expected at the very top of the solid H_2O cloud layer, which is shown. The effective pressure of H_2 and CH_4 line formation has been given as ca 0.5–1.5 atm. This is the region within the ammonia cloud layer and matches the 130–140° K methane rotational temperature in Palluconi's model. A 5-μm temperature of ca 120° K [286] fits well enough as the temperature of the cloud tops. Microwave studies in the NH_3 inversion line at 1.25 cm indicate optical depth unity is reached at a temperature

TABLE 13.—*A Nominal Saturn Model Atmosphere* [1]

Pressure, atm	°K	Density, g cm^{-3}	Altitude,[2] km	H_p, km	H_ρ, km	w, mg l^{-1}	Comments
0.100	77.0	3.59×10^{-5}	81.1	26.9	26.9		
0.168	77.0	6.04×10^{-5}	67.1	26.9	26.9		Tropopause
0.300	95.0	8.37×10^{-5}	49.8	33.1	51.7		
0.727	130.0	1.55×10^{-4}	15.3	45.4	69.7	0.003377	
1.00	145.2	1.91×10^{-4}	0.0	50.7	77.3	0.0762	Zero altitude [2]
1.12	151.0	2.05×10^{-4}	−5.9	52.7	80.2	0.205	NH_3 cloud base
3.00	210.0	3.95×10^{-4}	−67.5	73.4	109.5		
3.94	230.0	4.74×10^{-4}	−88.4	80.3	119.1	0.0743	
5.10	250.0	5.64×10^{-4}	−109.9	87.2	128.0	0.574	Solid H_2O
6.92	275.9	6.94×10^{-4}	−138.1	96.3	141.3	4.82	Solution H_2O-NH_3 cloud base
10.0	309.9	8.93×10^{-4}	−175.5	108.1	157.6		
30.0	434.1	1.91×10^{-3}	−317.0	151.5	216.4		
100.0	617.8	4.48×10^{-3}	−536.0	215.6	302.1		
300.0	841.3	9.99×10^{-3}	−813.7	293.6	405.5		
1000.0	1166.2	2.37×10^{-2}	−1232.1	406.9	554.9		

[1] From Palluconi [359]. The composition used is H_2, 88.572%, He, 11.213%, H_2O, 0.105%, CH_4, 0.063%, Ne, 0.013%, NH_3, 0.015%, and others, 0.019% by number; H_p is the pressure scale height, H_ρ is the density scale height, and w is the mass of cloud per unit volume of gas.

[2] The zero altitude is arbitrarily selected at 1 atm pressure.

near 135° K and a pressure of about 2/3 atm [524]. All of this fits together as well as can be expected, given the present limited number of observations upon which to base model calculations.

No optical observations show any evidence of penetration of radiation from below the top cloud deck, such as was true for Jupiter. Nor is this any surprise, given the greater cloud density expected. The previously discussed limb-darkening curves for the equatorial belt would indicate that a simple reflecting layer model for spectral line formation is inappropriate, because they show decreasing rather than increasing absorption from center to limb. It may well be that a reflecting layer model can be used for relative abundances at the center of the disk, while scattering must be included to explain limb darkening, as for Jupiter. Finally, it must be remembered that there is considerable spatial variation over the disk of Saturn [56] and probably temporal variations as well. A single static atmospheric model can hardly be expected to explain such changes.

Body Structure (Model Interiors)

The contemporary philosophy behind model interiors of Saturn is the same as for Jupiter. In practice, however, it is difficult to derive a completely convective Saturn model. Even though its mean density is much lower than Jupiter's, Saturn's mass, and therefore its gravitational compression, are sufficiently smaller that models of Saturn have always required a much larger helium-to-hydrogen ratio than Jupiter and often a high molecular weight core as well [218]. Hubbard's completely convective models [214] required a mass fraction of only 27% hydrogen and a very high central temperature. If the internal energy source is somewhat smaller than previously thought, because of confusion with flux from the rings (see section, *Energy Balance*), and a core is included, then a perfectly satisfactory hydrogen-to-helium ratio can presumably be accommodated, whatever the ratio may be.

A typical Saturn model interior by Hubbard and Smoluchowski [218], in Table 14, is only meant to show the general trend of probable physical conditions inside Saturn. (Refer to the original literature for specific models.)

TABLE 14.—*A typical Saturn Model* [1]

Radius, 10^4 km	Fractional mass	Pressure, Mbar	Density, g cm^{-3}
5.7	0.98	0.001	0.01
5.5	0.95	0.01	0.06
5.0	0.84	0.1	0.3
4.5	0.8	0.4	0.6
4.0	0.7	0.9	0.9
3.5	0.6	1.9	1.1
3.0 [2]	0.5	2.5	1.4
2.5	0.4	4	1.7
2.0	0.3	5	1.9
1.5	0.25	6	2.0
1.0	0.2	7	ca 3
0.5	0.05	ca 10	ca 3
0.0	0.0	ca 10	ca 3 [3]

[1] From Hubbard and Smoluchowski [218].

[2] Approximate radius at which the molecular hydrogen-metallic hydrogen transition is assumed to occur in most models.

[3] Not including a possible dense core.

URANUS AND NEPTUNE

Uranus and Neptune have proven rather intractable bodies, for obvious reasons. Uranus has a visual surface brightness less than 1/10 Jupiter's. Its total visual flux at opposition is less by a factor of more than 1000, while Neptune's visual flux is less by an even larger factor. Infrared and microwave flux densities are also less than for Jupiter. Nevertheless, steady improvement in optical and microwave instruments has made possible significant progress in understanding these unique bodies, especially during the past 5 years.

Atmospheres

Composition

The existence of hydrogen on Uranus and Neptune was first inferred observationally by Herzberg [200] in 1952 by comparing a planetary feature seen by Kuiper [261] in Uranus and Neptune with laboratory spectra showing the λ8270 pressure-induced dipole $S_3(0)$ line of H_2. In 1963, Spinrad [439] reported observation of the first H_2 quadrupole line in Uranus, S(0) of the 4-0 band, and finally in 1973 the quadrupole lines in Neptune were detected by Trafton [473].

There are now several sets of observations at present of the Uranian quadrupole lines, and these do not agree particularly well. It is not now clear whether these differences could be caused by real variations, as for Jupiter and Saturn, or whether they reflect observational difficulty, since it is particularly hard even to locate the continuum accurately on Uranus and Neptune. Because attempts to derive actual abundances are strongly model-dependent, only equivalent widths are given in Table 15, and the abundance problem is considered in the section, *Atmospheric Structure (Models)*. The pressure-induced dipole lines of H_2 are all very broad, shallow features, and particularly difficult to measure accurately in a spectrum with strong CH_4 absorption everywhere. Approximate equivalent widths for three of these lines in each planet have been given by Belton and Spinrad [36].

The first to report absorption bands in the spectrum of Uranus was Secchi, in 1869. Wildt suggested in 1932 that these might be caused by CH_4; in 1933, Dunham proved this for an infrared band on Jupiter; and by 1934, Adel and Slipher showed it to be true for Uranus. Slipher's work in the first decade of the 20th century confirmed earlier conjectures that Neptune's spectrum was very like that of Uranus, except that absorptions seemed even stronger. The work of Wildt, Dunham, Slipher, and Adel therefore confirmed the presence of methane on Neptune.

Each laboratory study of CH_4 at increased path-length and resolution seems to result in identification of previously unexplained features in the spectra of Uranus and Neptune. Owen's 1967 study [353] of the λ7500 (Kuiper) CH_4 bands at path-lengths of 5.15 km-amagat suggested the presence of 3.5 km-amagat of methane on Uranus and 6 km-amagat on Neptune. These numbers were necessarily crude because of unknown effects, on the line equivalent widths, of temperature differences between laboratory and planet. Laboratory spectra of methane at 8.45 km-amagat and new spectra of Uranus in the λ7500 band by Lutz and Ramsay [290] gave line strengths and improved wavelengths, suggesting even greater methane abundance on Uranus.

It has been shown very recently [355] that the λ6420 feature usually attributed to an induced dipole transition in H_2 was at least largely caused by methane. Even a 10.1 km-amagat laboratory column of CH_4 was inadequate to match this and other Uranian features. Assuming spectra result from a mean atmospheric path in the Uranian atmosphere of three times a vertical column again suggests even more than 3.5 km-amagat of methane. The actual abundance is both temperature- and model-dependent but is certainly very large. Many very high overtone bands show considerable strength even below 5000 Å, which can be seen in the spectra of Galkin et al [153]. Photometry by Wamsteker [499] suggests that methane abundance on Neptune may be smaller than on Uranus, rather than larger as is usually assumed. Additional observations of both planets are acutely needed.

TABLE 15.—*Equivalent Widths* (m Å) *of H_2 Quadrupole Lines in Uranus and Neptune*

Planet	Uranus						Neptune
Observer and reference	Giver & Spinrad [166]		Lutz [289]	Price [373]	Trafton [472] [1]	Encrenaz & Owen [133]	Trafton [473]
Dateline	Dec. 1964	Mar. 1965	May–July 1971	May 1972	3–0 1972 4–0 1972–73	Feb. 1973	May–July 1973
S(0), 4–0 λ6435	26 ± 10	37 ± 12		62 ± 19	30 ± 3	30^{+4}_{-3}	28 ± 4
S(1), 4–0 λ6368	37^{+25}_{-10}	49 ± 15		58 ± 13	29 ± 3	29^{+6}_{-3}	31 ± 4
S(0), 3–0 λ8273			95 ± 25		170 ± 18		
S(1), 3–0 λ8151			114 ± 15		167 ± 20		

[1] Also private communication.

Ammonia has not been identified in optical spectra of Uranus or Neptune. Its presence is expected theoretically, but only deep in their atmospheres [280]. There is some observational evidence of its presence in the rather uniform brightness temperatures of all the major planets near the ammonia inversion band at 1.25 cm [184].

There is no direct observational evidence of helium on Uranus and Neptune. The thermospheric temperature of Neptune (discussed in the next section) suggests that helium abundance can be *no higher than* 50% by number.

Trafton [475] has found a number of strong unidentified lines in the spectrum of Uranus between 1.04 and 1.07 μm. It is suggested that these might be caused by a methane isotope or one of the simple hydrocarbons produced from methane, although they may equally be caused by some other new atmospheric gas.

Temperatures

Low [284] made the first thermal infrared measurements of Uranus in 1966, reporting a temperature of 55°±3° K in the 17.5–25 μm window. Harper et al [193] found a value of 45° K for the 350 μm region and Low et al [288] measured 49°±3° K between 28 and 40 μm. Recently working at the high altitude (4200 m) Mauna Kea Observatory, Morrison and Cruikshank were able to measure the flux from both Uranus and Neptune between 17 and 28 μm. They report 54.7°±1.8° K for Uranus and 57.2°±1.6° K for Neptune [333]. These temperatures are all based upon slightly different planetary radii, but a one percent change in radius causes a temperature change of only about 0.1° K at these temperatures and wavelengths.

Radio emissions from Uranus and Neptune have been observed over the wavelength range 1.4 mm to 11 cm. The representative disk brightness temperature spectra for these planets are given in Figures 8 and 9. Most of the data used to compile these figures are in references [179, 343, 483]. Similar to Jupiter and Saturn, brightness temperatures of these planets are near 130° K near 1 cm wavelength, and increase at longer wavelengths. Based on solar heating alone, these planets would have a temperature near 50° K. A simple explanation for these planets being so warm at radio wavelengths is that radio emission originates deep in the atmosphere where it is warmer and denser than in the infrared radiation level. Trace amounts of ammonia are believed to provide atmospheric opacity [179]. While a great number of molecules absorb near 1-cm wavelength and become progressively more transparent at longer wavelengths, only two, NH_3 and H_2O, have very strong absorption lines in this wavelength region and are likely constituents of the major planet atmospheres. Hydrogen (H_2) and helium may also contribute to the opacity through their induced dipole moments.

The only spectral lines observed on Uranus

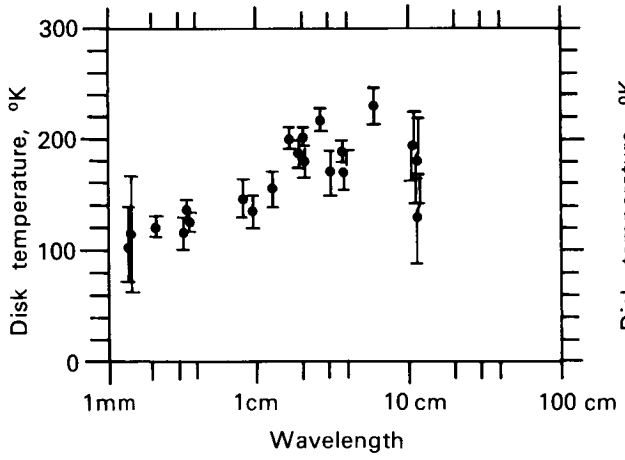

FIGURE 8.—Microwave spectrum of Uranus.

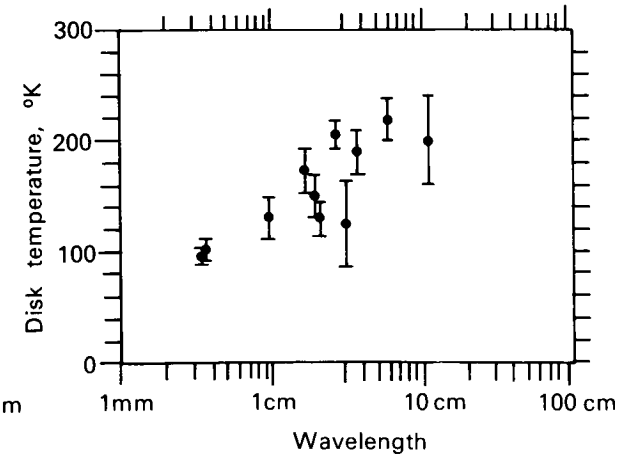

FIGURE 9.—Microwave spectrum of Neptune.

or Neptune with definitely known quantum numbers are the molecular hydrogen lines. Rotational temperature can be derived for each pair of lines in a given band (listed in Table 15) if H_2 is assumed to be equilibrium hydrogen rather than normal hydrogen. These temperatures generally fall in the 110–120° K range. Scatter in measurements and the peculiar behavior (already discussed) of the more extensive Saturn data suggest cautious interpretation.

Tentative quantum number assignments by Owen in the λ6800 band of methane suggest a rotational temperature of 60° ± 15° K [352]. Since this is some 25° K lower than the temperature to be expected for the observed amount of methane in saturation equilibrium, its meaning is quite uncertain.

The star BD−17° 4388 was occulted by Neptune in 1968, observations being made in Australia and Japan. The original results from Australia were reported by Freeman and Lynga [152], from Japan by Kovalevsky and Link [254]. A complete analysis of the Australian observations by means of light curve inversion, recently published [491], indicates an upper atmospheric scale height of 55–58 km. This implies a temperature of 150 ° K for a pure H_2 atmosphere and higher yet in direct proportion for larger values of molecular weight. Veverka et al [491] suggest that the large methane abundance on Neptune should assure effective radiative cooling of the thermosphere, implying that the H:He ratio can be no greater than 50% by number density.

Uranus is unique in the solar system in its axial inclination of 98°. The axis of Uranus was practically in the plane normal to the solar radius vector in 1966, all parts of the planet exposed to the Sun during one 10.8-h rotation. In 1985, the north pole of Uranus (assuming north is defined by the angular velocity vector) will face the Sun continuously, and temperatures in this visible hemisphere might rise as much as 20%, assuming no effective heat exchange between northern and southern hemispheres. Stone [447] suggests the radiative relaxation time for Uranus is so long that substantial seasonal effects are unlikely. He predicts that the polar regions, receiving more heat from the Sun per orbit, will be hotter than the Equator.

The Visible Surfaces

Uranus normally appears as a small bluish-green disk, even through a large telescope, and is featureless except for a reasonable amount of limb-darkening. The Stratoscope II balloon telescope during its flight of March 26–27, 1970, found no surface features, i.e., an upper limit of 5% contrast on any beltlike feature at wavelengths λλ3800–5800 [102]. Yet the best of the classic visual observers, using large refracting telescopes (aperture > 50 cm) at times of superior "seeing" [2], usually reported two faint equatorial belts on either side of a bright equatorial zone and darker poles. Almost all observers found these belts inclined somewhat to the plane of the satellites [2]. Perhaps the belts vary in contrast.

Neptune is almost always described as a small, featureless bluish-green disk when seen through a moderate to large telescope. Dollfus described it as showing pronounced limb darkening and very weak spots of irregular shape, but no band structure [116].

In determining rotation periods, astronomers turned to spectroscopic and photometric techniques, since there were no obvious surface features to use. In spectroscopy, rotational velocity is measured from the Doppler shift of spectral lines. In 1930, Moore and Menzel [328] published a spectroscopic rotation period for Uranus of 10.8 h (the period generally quoted today). They noted it could be in error by as much as a half hour, although it was in substantial agreement with the 1912 spectroscopic result of Lowell and Slipher. Similarly, Moore and Menzel [327] published in 1928 the rotational period still quoted for Neptune, 15.8 ± 1.0 h.

Campbell [2][6] reported that in 1916 the light from Uranus fluctuated by 0.15 magnitudes in a period of 10 h 49 min 26.4 s, although the variation seemed to disappear later.

A long list [194] gives positive and negative reports on light fluctuations from Uranus since that time. Whether any of these variations were real, perhaps related to belt activity, or the product of inadequate early photometry is still not

[6]This is a secondary reference.

certain, but variations using a modern photoelectric photometer have not been reported. The situation for Neptune is similar.

The large amount of methane in the atmospheres of Uranus and Neptune causes tremendous absorption in the red and near-infrared and is at least partially responsible for the bluish-green colors of these planets. It appears that some hydrogen pressure-induced absorption is also required to match the geometric albedo of each [499]. Matching the geometric albedo data is the most important constraint available in constructing model atmospheres.

There are three important sets of albedo data: Wamsteker [499] covers completely 0.3–1.1 μm at a resolving power $\lambda/\Delta\lambda$ ca 30 on both planets; Appleby and Irvine [15] and Appleby [14] cover 10 wavelengths on Uranus and seven on Neptune at slightly higher resolution; and Younkin [530] covers completely 0.33–1.11 μm at 50 Å ($\lambda < 0.7$ μm) and 100 Å ($\lambda > 0.7$ μm) resolution for Uranus only. Scaled to the same planetary radii, the three sets of results agree reasonably well.

Younkin's data have the highest peaks and troughs in the red and infrared, of course, since it has the highest resolution in this region of strong methane bands. His geometric albedo curve for Uranus scaled to the radius of Table 1 is shown in Figure 10. Neptune is shown to be nearly identical to Uranus at wavelengths shorter than 0.54 μm but with lower peaks and shallower troughs in the region of methane absorption, perhaps indicating broader methane bands [499]. The albedo of Uranus was measured at wavelengths of 1.26, 1.62, 1.74, 2.17, and 2.27 μm with 0.098 to 0.062 μm passbands, resulting in values of 0.02 or less at each wavelength [55]. Ultraviolet albedos have become available from the orbiting astronomical observatory. The albedos for Uranus and Neptune were found to be about the same at λ2590 as at λ4000, while Uranus appears to have a still hegher albedo (ca 0.7) at λ2110 [408].

The bolometric geometric albedo for Uranus has a value of 0.32 [530, 532]. When scaled to the radius of Table 1, this becomes 0.27. Adopting Younkin's suggested value of 1.25 for the phase integral at all wavelengths, a bolometric Bond albedo for Uranus of 0.33 can be derived. The existing photometry of Neptune is sufficiently similar to that of Uranus to adopt the same value. Since the maximum phase angle achieved by Uranus is only 3.1°, as viewed from Earth, and that of Neptune only 1.9°, it is obvious that accurate radiation balance studies can only be carried out from space probes.

The limb-darkening curve is one final important type of data which furnishes an important boundary condition on atmospheric models. Difficulties in obtaining meaningful results on bodies only 4 and 2.5 arc seconds in angular diameter are obvious, and, in fact, no data exist for Neptune. Danielson et al [102] obtained excellent curves for $\lambda\lambda$3800–5800 from their Stratoscope II photographs of Uranus. Sinton has shown there is come limb-brightening at 8870 Å in the middle of a strong methane band where the albedo is only 1%–2% [424].

Atmospheric Structure (Models)

The thermal atmospheric opacities of Uranus and Neptune are dominated by molecular hydrogen, as are Jupiter and Saturn [465, 468]. Additional opacity induced by methane, as suggested by Fox and Ozier [147], would become important only if either planet proved to have a large internal energy source. The measured infrared temperatures discussed above for Uranus all seem compatible with expected effective temperature calculated from purely solar heating except for the 300–500 μm result, which is anomalously low. The 17–28 μm value for Neptune seems high, however, and Trafton [474] suggests an internal heat source which may be tidal dissipation caused by Triton, Neptune's very large, close satellite.

Definite sources of visible opacity in the Uranus and Neptune atmospheres include Rayleigh and Raman scattering of H_2, very weak quadrupole and stronger induced dipole absorption of H_2, and very strong methane absorption. A pure molecular atmosphere containing only these opacities cannot match measured geometric albedos and H_2 and CH_4 line equivalent widths on either planet [36, 499]. A dense cloud layer of solid NH_3 particles must form at about 170° K and 8 bars on Uranus, if that gas is present, as expected [375], and if Trafton's temperature profile from his thermal opacity work is a rea-

sonable first approximation [465]. There should also be a thin CH_4 haze with a base at about 60° K and 0.4 bar. Such a model is consistent with the Stratoscope II limb-darkening curves [102], and the amount of H_2 above the NH_3 cloud tops ($\gtrsim 370$ km-amagat) is reasonably consistent with measured equivalent widths of H_2 quadrupole lines [36] and with observed geometric albedos [499]. Recent work indicates the mixing ratio of CH_4 cannot be above about 10^{-2}, or too thick a CH_4 cloud layer will result [100]. The case for Neptune is less clear because few observations are available. With higher surface gravity, pressure at the NH_3 cloud deck would be higher, the amount of H_2 above this deck larger, and any reflection from the deck less important than on Uranus. There may be thin argon clouds high in Neptune's atmosphere [475].

Detailed inversion of the light curve obtained when Neptune occulted the star BD−17° 4388 in 1968 furnishes the only quantitative observational data on the upper atmosphere of Neptune. Veverka et al [491] found the "quasi-linear" scale height to be 55–58 km, although there is localized structure showing swings between about 30 and 80 km. At a number density of 10^{15} cm^{-3}, the temperature would be about 130° K in a pure H_2 atmosphere, with a small positive temperature gradient reaching to higher elevations. Any mixture of heavier gases raises this temperature in direct proportion to the mean molecular weight. No analysis of the complex details of the refractivity profile has been made because too much data is missing. The ionosphere of Neptune is expected to be somewhat cooler than that of Jupiter [491] because of the greater amounts of methane and its photoproducts, which are efficient radiators, and the lower effective temperature of Neptune. No observational data exist for the upper atmosphere of Uranus.

Body Structures

Real models, analogous to those for Jupiter and Saturn, do not exist for the interiors of Uranus and Neptune. Calculation of the unique mass-radius relationship for homogeneous, cold bodies [534] indicates that these planets probably contain large amounts of lighter elements but are not so hydrogen-rich as Jupiter and Saturn [217]. A number of models containing large amounts of metallic ammonium (NH_4) or a mixture of CH_4, NH_4, H_2O, and Ne in solar abundances were constructed during the 1960s [370, 380, 390], but recent radical changes (ca 10%) in the best values for the radii of Uranus and Neptune have rendered them obsolete, even as crude models.

Makalkin [296] has reintegrated the cold (equation of state at 0° K) Neptune models of Reynolds and Summers [390] using the new radius. The resulting best fit occurs in a model with a larger fluid envelope and smaller solid core of higher central density, although it actually does not fit observed data well. Makalkin [296] suggests a hot model as the best possibility to improve the fit, although he notes that the composition could also be juggled. Zharkov and Trubitsyn [537] have run hot models for Uranus and Neptune with adiabatic temperature gradients. In such models, heavy element cores must be liquid, starting with atmospheric temperature even as low as 50° K at 1 bar pressure level.

It is not possible to state at present if Uranus and Neptune have solid surfaces, however, if they do, the surfaces are probably at depths of at least 5000 km. Improved values for radius, oblateness and higher order gravitational terms, rotation period, and atmospheric composition and structure are all needed as boundary conditions before interior model-building can produce convincing results.

PLUTO

General Background and Physical Data

Pluto was discovered by Tombaugh on February 18, 1930, after 25 years of deliberate, intense search [464]. Its orbit is the most eccentric and most highly inclined of any planet. Near perihelion, which it reaches next in 1989, it is nearer the Sun than Neptune can ever come, and midway between its nodes, it lies a billion and a quarter km above the ecliptic plane. Because of that inclination, there is no chance at present of a catastrophic encounter with Neptune.

A special perturbation study covering 120 000 years was presented in 1965 by Cohen and

Hubbard [90]; it uncovered an apparently stable libration in the Pluto-Neptune couple over 19 670 years. The study indicated that Neptune and Pluto never approach nearer than about 18 astronomical units (AU) to each other, and that the closest approach always occurs when Pluto is near aphelion. More recent studies have reinforced this conclusion. Williams and Benson [520] carried out a 4.5×10^6 yr integration which confirms the 20 000-yr oscillation over the longer period, and which has uncovered other resonances, in particular, an important one with a period of 3 955 000 years. The total effect of these terms is to increase the minimum Pluto-Neptune distance and the apparent stability of the outer solar system. Wilkins and Sinclair [517] have noted the minimum distance (16.7 AU) between Pluto and Neptune is much greater than the minimum distance (10.6 AU) between the planets Pluto and Uranus.

The supposition that Pluto might be an escaped satellite of Neptune was originated by Lyttleton [291]. The escape hypothesis was later championed by Kuiper [264] and Rabe [378, 379] as a likely outcome of Kuiper's protoplanet theory of the origin of the solar system. The two escape mechanisms proposed are completely different, however. Pluto seems physically more like a satellite of a giant planet than one of the planets themselves. On the other hand, resonance studies noted in the previous paragraph seem to indicate extreme stability of Pluto's orbit. It has been suggested as unlikely that the 20 000-yr libration began more recently than the time at which planetary masses stabilized at their present values [520]. The current stability and earlier escape from Neptune are not necessarily incompatible, but these studies inevitably make the escape hypothesis seem less attractive than previously. Only detailed study and comparison of Pluto and Triton seem likely to indicate if they might have had a common origin.

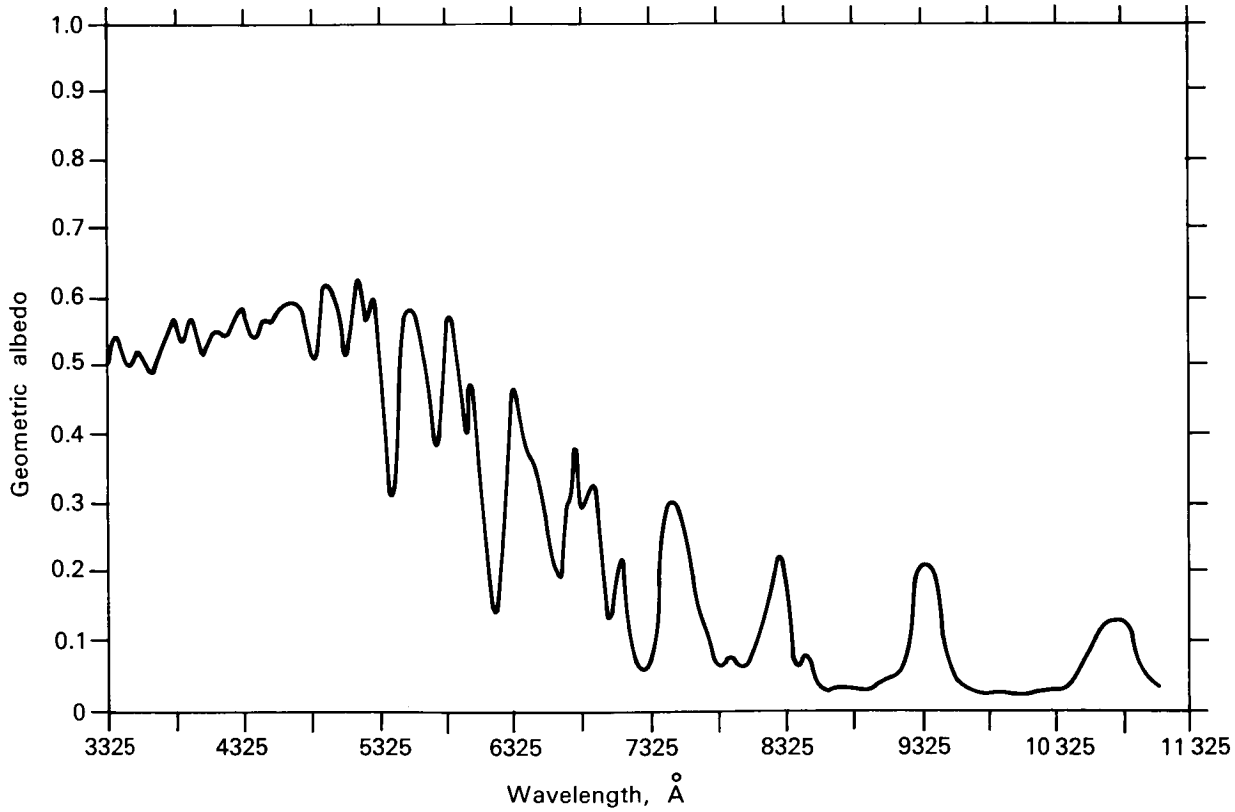

FIGURE 10.—Geometric albedo of Uranus, λ3325–11 100. (Adapted from [530])

Pluto appears as a point source in all but the largest telescopes, and even in the largest telescopes it can be resolved only under the finest observational conditions. Kuiper made a direct measurement in 1950 of 0.23″ (about 5860 km) for Pluto's diameter [260], which may be subject to uncertainties approaching 50%. A far more accurate technique for measuring such small angles is photometric observation of a stellar occultation, but such occultations occur rarely. A "very near miss" recently fixed the extreme upper limit of Pluto's diameter at 6800 km [189].

The mass of Pluto has been difficult to determine, since it requires measuring perturbations on a large body, Neptune, by a smaller one, Pluto. Pluto has made only half a revolution including all known prediscovery observations back to 1846, further complicating determination of its mass. The best available mass figure for Pluto presently is 0.11 that of Earth [414], which, together with a 6400-km diameter, implies density of 4.9 g cm^{-3}. The history of attempts to determine the mass of Pluto has been one of continuous uncertainty, with the "best" value being 0.91 that of Earth until as recently as 1968. Halliday [188] suggested that a small change in the mass of either Saturn or Uranus could easily cause a large change in the mass determined for Pluto. The safest conclusion may be that of Ash et al [22], that "Pluto's mass cannot be determined reliably from existing data."

The rotation period of Pluto was first measured photometrically in 1955 by Walker and Hardie [494]. The latest period for Pluto obtained from phasing more than 20 years of data is 6.38737 ± 0.00018 d [342]. Although the rotation period is quite constant, amplitude and mean opposition V magnitude of the light curves have not been. Andersson and Fix [12] find that the mean brightness of Pluto has decreased 0.20 magnitudes and amplitude of the light curves increased from 0.11 magnitudes 20 years ago to 0.22 magnitudes today. Attributing these changes to variation in the sub-Earth point on a Pluto with albedo features as the latter planet moves along its orbit, they solved for the obliquity of Pluto's axis and found it "probably greater than 50°."

Atmosphere

Pluto's low mass and temperature suggest that it may not have an atmosphere. Many potential atmospheric molecules, such as CO_2, H_2O, and NH_3, would lie frozen on the surface, while others, such as H_2 and He, would escape. The atmosphere might contain extremely small amounts of CH_4 and/or N_2, but even at 50° K, the vapor pressure of these species is extremely low. Heavier inert gases, such as neon and argon, could form a permanent atmosphere, but these are difficult to detect spectroscopically. Hart [196] finds that the spectrophotometry of Fix et al [142] would allow 1 atm of neon but this seems incompatible with 3 atm pressure because of increase in ultraviolet albedo that would result from Rayleigh scattering.

No evidence of an atmosphere could be detected on Pluto in a low-dispersion (720 and 340 Å mm^{-1}) spectroscopic study of the visible red [258]. Much higher dispersion is certainly available today, but the best hope for detecting an atmosphere, which might be largely inert gases, would be by means of a spacecraft occultation experiment.

Photometric Properties

As noted previously (in the discussion on rotation period and axial obliquity), the magnitude of Pluto reduced to mean opposition distance seems to be increasing, as is the amplitude of its diurnal variation. Pluto, because of its large orbital eccentricity, would be more than a magnitude brighter at perihelion than at its mean distance, were it not for this effect attributed to bright polar caps by its discoverers [12]. They [12] also suggested a phase coefficient of 0.05 magnitude/degree be applied to all Pluto photometry.

The relative brightness of Pluto has been measured between 3400 and 5900 Å in 21 passbands having a full width of 128 Å at half-maximum transmission [142]. This work showed a slowly increasing albedo toward the red from λ3800 as well as a steeper increase toward the blue from that point and some hint of structure at 4800 and 5800 Å. Harris' photometry [194] shows a body considerably redder than the Sun at λ6900 and 8200.

The radius of Pluto is so poorly known that attempts to quote a geometric albedo based on the radius are almost meaningless. Harris [194] picked a radius of 0.45 that of Earth, which gives $p_v=0.13$. He then chose a phase integral equal to that for Mars ($q_v=1.04$), to derive a visual Bond albedo $A_v=0.14$. The albedo of Pluto seems to change only slowly with wavelength, so this value was inserted in Table 1 as a guess at the bolometric Bond albedo. It is obvious that an accurate radius and phase integral for at least 1 wavelength must be measured before such numbers can have real meaning. It seems likely that the bolometric Bond albedo for Pluto is sufficiently smaller than Neptune's to give Pluto the higher effective temperature. However, Pluto's slow rotation will assure considerable difference in actual dayside and nightside temperatures, the former reaching perhaps 50° K.

Polarimetry of Pluto by Kelsey and Fix [242] indicates that the planet probably has a microscopically rough surface, and their value of 0.27% polarization at a phase angle of only 0.8° is certainly compatible with a low albedo, since it hints at a deep negative branch for the polarization curve.

Body Structure

Since even density of Pluto is grossly uncertain, meaningful work on the structure of the planet is unlikely until a spacecraft has accurately determined at least its basic physical measurements with some accuracy. A large magnetic field seems unlikely, since Pluto is small and rotates slowly, but after Mercury, who knows?

SATELLITES AND RINGS

Less than a decade ago, satellites of the solar system (except the Moon) were in the backwater of astrophysical research. The extensive photoelectric photometry of Harris [194] and occasional studies by Kuiper and his students constituted the majority of modern knowledge, other than that of their masses and motions. During the past 5 years, satellite study has burgeoned into one of the most active fields of solar system physical research, one which required 100 pages to encompass in the recent review of Morrison and Cruikshank [335]. The emphasis here will be upon the Galilean satellites of Jupiter, and Titan, the bodies most likely to be of biological interest. The aforementioned review is recommended for additional physical information. Reviews of celestial mechanics are in papers by Wilkins and Sinclair [517] and Porter [369]. No review of satellites, however brief, would be complete without some description of the innumerable small satellites seen as the rings of Saturn, which will be discussed along with Saturn's satellites.

Jupiter's Satellites

Jupiter has 12 known satellites, 5 near the planet in circular orbits in the equatorial plane and 7 in far out, highly eccentric, highly inclined orbits.[7] The basic orbital elements are given in Table 16, together with mean brightness and change of brightness caused by rotation. JV, sometimes called Amalthea, and the four large Galilean satellites (discovered by Galileo in 1610) appear to keep one face toward their primary [237, 335], rotating on their axes in the same period as they revolve about Jupiter. Almost nothing is known about the other seven bodies, or even Amalthea, which is so close to Jupiter (1.54 radii from the planetary surface) as to virtually prohibit accurate photometry.

The Galilean satellites are large, important bodies in their own right. Ganymede is larger than the planet Mercury, and all but Europa are larger than the Moon. In understanding these bodies, it is of great importance that accurate physical data are finally becoming available. In 1971, Io occulted β-Scorpii C [219, 347, 457], and in 1972, Ganymede occulted SAO 186800 [77], giving greatly improved radii for the two satellites. With these radii forming a base, it became possible to derive further data from mutual occultations occurring every 6 years when Earth is in the plane of the satellite orbits [67]. Finally, new masses have come from the flight of Pioneer 10 [8]. These data and quantities derived from them are in Table 17.

[7] A thirteenth satellite, lying just inside JVI, was discovered in Sept. 1974.

The occultation by Ganymede, besides an improved radius, apparently gave the first direct evidence of an atmosphere on a Galilean satellite, suggesting a surface pressure on Ganymede of at least 10^{-6} bar but probably not as great as 10^{-3} bar [77]. The star occulted was quite faint, however; and there are some questions on the reliability of the pressure data. The Pioneer 10 S-band radio occultation experiment [250] detected an electron density of 6×10^{4} cm^{-3} at 100±40 km above the surface of Io and a neutral atmosphere corresponding to surface pressure of 10^{-8} to 10^{-10}

TABLE 16.—*Jupiter's Satellites*

Satellite	Semimajor axis, km	Eccentricity [1]	Inclination [1,2]	Sidereal period	V magnitude at mean opposition [5]	Rotational change in V [6]
JV [3]	181 500	0.0028	0°27.3′	11 h 57 min 22.70 s	ca 13.0	([7])
JI (Io) [3]	422 000	0.0000	0°1.6′	1 d 18 h 27 min 33.51 s	4.80	0.16
JII (Europa) [3]	671 400	0.0003	0°28.1′	3 d 13 h 13 min 42.05 s	5.17	0.31
JIII (Ganymede) [3]	1 071 000	0.0015	0°11.0′	7 d 3 h 42 min 33.35 s	4.54	0.15
JIV (Callisto) [3]	1 884 000	0.0075	0°15.2′	16 d 16 h 32 min 11.21 s	5.50	0.15
JVI [4]	11 487 000	0.158	27.6°	250.57 d	14.88	U
JVII [4]	11 747 000	0.207	24.8°	259.65 d	16.	N
JX [4]	11 861 000	0.130	29.0°	263.55 d	18.6	K
JXII [4]	21 250 000	0.169	147°	631 d	18.8	N
JXI [4]	22 540 000	0.207	164°	692 d	18.1	O
JVIII [4]	23 510 000	0.378	145°	739 d	18.8	W
JIX [4]	23 670 000	0.275	153°	758 d	18.3	N

[1] Eccentricities and inclinations for regular satellites are slightly variable. Those for irregular satellites are extremely variable.

[2] To the equatorial plane of Jupiter.

[3] From [400], except photometric data.

[4] From [369], except photometric data.

[5] From [194], except JVI which is from [10, 11].

[6] From [335].

[7] Possibly variable with leading edge brighter.

TABLE 17.—*Galilean Satellites: Physical Data*

Parameter [1]	Io (JI)	Europa (JII)	Ganymede (JIII)	Callisto (JIV)
Mass (Jupiter = 1) [8]	4.696×10^{-5} ± 0.06	2.565×10^{-5} ±0.06	7.845×10^{-5} ± 0.08	5.603×10^{-5} ± 0.17
Mass (Moon = 1)[2]	1.213	0.663	2.027	1.448
Mean diameter, km	3636 ± 5 [347]	2980 ± 100 [3]	$5270^{\pm30}_{\pm200}$ [77]	5000 ± 150 [119]
Mean density, g cm^{-3} [4]	3.54	3.51	1.94	1.63
Mean surface gravity, m s^{-2} [4]	1.80	1.46	1.43	1.14
Escape velocity, km s^{-1} [4]	2.56	2.09	2.75	2.38
Bolometric Bond albedo [335]	0.62 ± 0.13	0.74 ± 0.14 [5]	0.35±0.08	0.11 ± 0.03
Effective temperature, K [6]	96	87	109	118
Maximum temperature, K [7]	135	123	155	167

[1] Where the same source was used for all four satellites, the reference number is given in the parameter column. In all other cases, it follows the individual datum.

[2] Calculated from value above, mass of Moon = 7.347×10^{22} kg [190], and mass of Jupiter = 1.8985×10^{27} kg [8]. Unlike the figure in Table 1, this does not include the satellites' mass.

[3] This figure is the average of three values from mutual occultation observations reported at the 1974 AAS Division of Planetary Sciences Meeting, Palo Alto, Calif.

[4] Calculated from mass and diameter given above. G = 6.673×10^{20} km^3 s^{-2} kg^{-1}.

[5] Corrected from 0.68 for new value of radius given above.

[6] Calculated from $F=4(1-A)^{-1}\sigma T_e^4$, assuming the flux F = 1353 Wm^{-2} at 1 AU and the Stefan-Boltzmann constant $\sigma=5.669\times10^{-8}$ Wm^{-2} deg^{-4}. A is the bolometric Bond albedo.

[7] Calculated from $F=(1-A)^{-1}\sigma T_e^4$. This is the maximum equilibrium temperature that a body of the given albedo, normally illuminated, can have at 5.203 AU from the Sun without an internal heat source.

bar (depending upon composition) on that satellite. The Io optical occultation observations had only resulted in an atmospheric upper limit of about 10^{-7} bar [30, 427].

In 1964, Binder and Cruikshank [54] reported an apparent excess brightness on Io of about 0.1 magnitude as it reappeared after solar eclipse by Jupiter, the excess disappearing in about 15 min. It was suggested that this might be evidence for an atmosphere condensing during eclipse and evaporating in sunlight. It was estimated that about 2×10^{-7} bar of evaporate would be required to satisfy the observations [279]. Since 1964, there have been many photometric studies of Io eclipses, some positive, some negative. If the phenomenon is real, it is certainly intermittent, and the Pioneer 10 results on atmospheric pressure would indicate it is not caused by atmospheric condensation. The results for 1973, using photometers specially designed to reject scattered light from Jupiter, were all negative (no brightening) [151, 324].

The discovery by Brown [69] of sodium D-line emission from the satellite was the most unexpected and spectacular result on the atmosphere of Io. Confirming observations were soon reported by Brown and Chaffee [70], and then Trafton et al [478] found that the sodium radiation came from a large area around Io (more than 10 arc seconds in radius). The amount often averaged ca 10^{11} atoms cm^{-2}, assuming it to be uniform and optically thin over the field of view, although it apparently is variable in time. Meanwhile, Judge and Carlson [239] reported an apparent torus of hydrogen around Jupiter in the orbit of Io with a surface brightness of 10 kilo-Rayleighs (assuming it is all Lyman α-radiation). Presumably, the torus of hydrogen around Io is similar to the torus which McDonough and Brice suggested would be found around Titan [318]. The most acceptable explanation so far suggested for the observations is sputtering of Io's surface by charged particles from the Jovian magnetosphere, followed by resonance fluorescence within the sodium and hydrogen clouds thus created [311].

Photometry of the Galilean satellites has indicated that their surface properties vary considerably from satellite to satellite. This is well illustrated by the broadband photometry of Lee [274], shown in Figure 11 with Morrison and Cruikshank's normalization [335]. More detailed studies at higher spectral resolution have shown that Europa and Ganymede are coated largely with H_2O frost [141, 365] at a temperature near 150° K and of ca 0.1 mm grain size [247]. Kieffer and Smythe [247] estimate fractional abundance at 75% and 60% on JII and JIII, respectively, while H_2O frost is at most a minor constituent on JI and JIV. Io retains its very high and largely featureless albedo even at 5 μm [164]. Kieffer and Smythe [247] suggest strongly hydrated minerals as candidates for the JI surface.

Polarization results also indicate differences among the Galilean satellites, with Callisto standing out with a strong negative branch more than twice as deep as any of its companions [122, 488].

A number of brightness temperature measures have been made through the 8–14 μm and 17–28 μm windows in Earth's atmosphere. Table 18 is taken from Morrison and Cruikshank, with Europa temperatures corrected for the new radius given in Table 17. The 10 μm temperatures are consistently 10° K higher than those at 20 μm, a surprising result. Hansen [192] has shown what appears to be a distinct emission feature at 12 μm on the three Galilean satellites he observed (JI, JIII, and JIV), which may account for the difference but this also needs explanation. Flux curves during eclipse have been obtained by Hansen at 10 μm [191], and Morrison and Cruikshank at 20 μm [334]. In general, results can best be explained by a thin low-conductive layer over a thick layer of high conductivity for JI, JII, and JIII, with some additional complexity for JIV.

The brightness temperatures of Ganymede and Callisto at millimeter and centimeter short wavelengths are given in Table 19. Temperatures have been adjusted (where possible) to the satellite radii given in Table 17; temperatures in parentheses are those published. These measurements are quite difficult to make because of the usual problem of detecting a weak signal in the presence of a nearby strong signal. Of the four measurements shown for Callisto, it is expected that interferometric measurements at 3.71 cm and high signal/noise measurements at

2.82 cm using the 100-m Bonn radio telescope are the most reliable. These are also the most interesting because they indicate brightness temperatures significantly lower than infrared temperatures. Also, the difference in brightness temperatures of the two satellites is larger than would be expected from their albedos [360].

The low brightness temperatures can be explained [360] by radio emission originating below the surface, where the variation of temperature with phase is lower. This implies, if correct, that interior of the satellites is colder than the surface. Brightness temperature measurements at 3.55 mm and 8.2 mm (in contrast to centimeter wave measurements) are considerably higher than both infrared and centimeter radio measurements; their statistical uncertainties, however, are large. The idea has been advanced that high brightness temperatures are the result of a nearly transparent ice surface on these satellites [271]. In the Lewis [279] models, the lapse rate in the ice crust is ca 1° K/km, and a crustal thickness of ca 100 km is required to explain the observations. This theory predicts that brightness temperature does not depend on wavelength, which is inconsistent with available data.

The formation, internal structure, and chemistry of the Galilean satellites have been considered by two groups [279, 280, 281, 368]. These studies indicate that all four bodies are likely to have a core of hydrated silicates, and Ganymede and Callisto may well have thick mantles of frozen or liquid water (liquid, if there is even a small amount of radioactive decay in their interiors). Each should have at least a thin solid crust, possibly ice on all but Io, although on Callisto, the low albedo obviously requires an additional dark material on the surface.

All the Galilean satellites are very interesting, apparently quite different from bodies nearer the

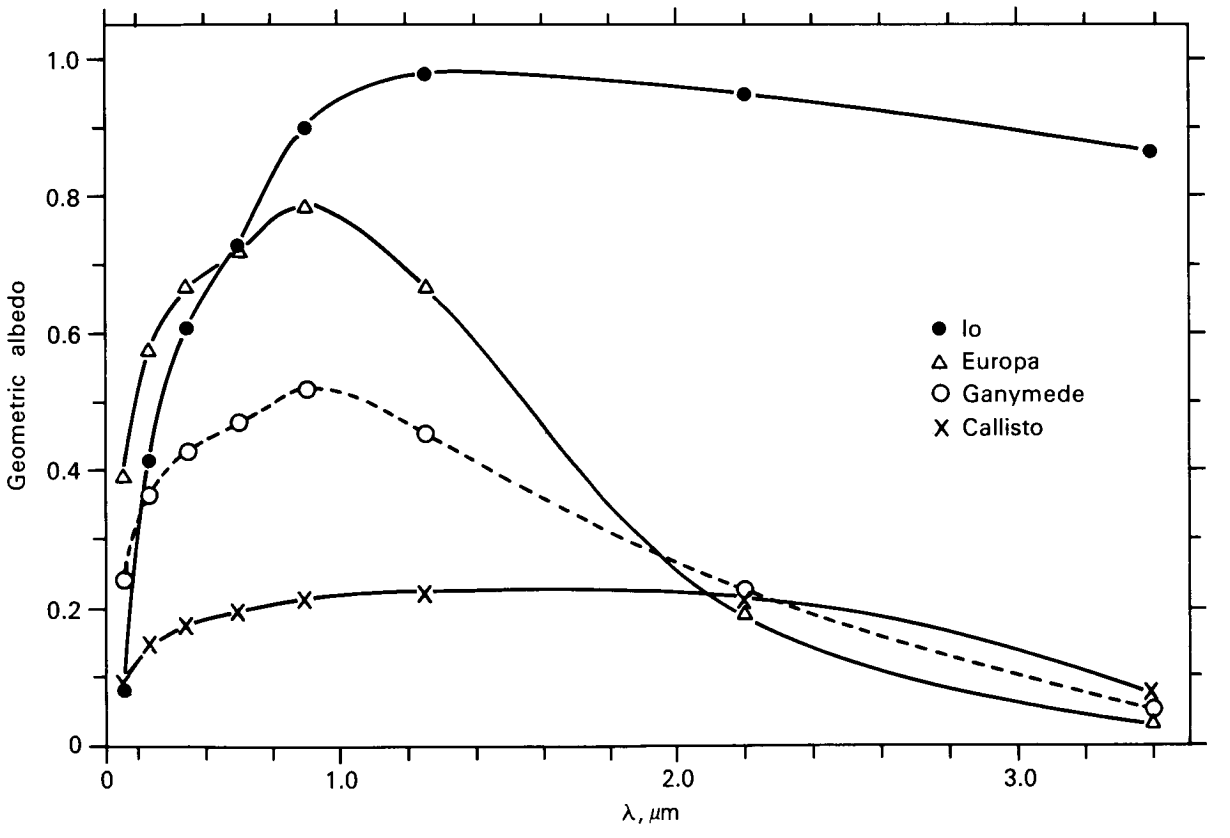

FIGURE 11.—Geometric albedo of the Galilean satellites, 0.4–3.4μm. (Adapted from [274] as normalized by [335])

Sun. Only Io and Europa have densities similar to the terrestrial planets (or perhaps the asteroids), and their albedos are many times higher than nearer, airless bodies. Io also exhibits a number of unique phenomena apparently associated with the Jovian magnetosphere. These satellites are sure to receive increased attention from space probes and ground-based observers during the next decade.

Saturn's Rings and Satellites

The Rings

Saturn has 10 satellites, all but the outermost (Phoebe) in fairly regular orbits, and a glorious set of rings. The rings around Saturn, which appear to be unique in the solar system, were first seen by Galileo in 1610 as queer appendages on either side of the planet. The real nature of the appendages as part of a flat ring around the planet was discovered by Huygens in 1655. In the 1670s, Cassini found that the ring was double, a dark line separating it into two concentric rings. The dark line is now called Cassini's division, the outer ring A, and the inner ring B. In 1850, Bond at Harvard and Davies in England independently discovered a very tenuous third ring, a "crape ring" or Ring C, inside the first two. For many years, there has been considerable controversy about the existence of a fourth, extremely tenuous ring outside the A ring. Some positive evidence of this D ring's existence was obtained by Feibelman during the most recent [136] edge-on aspect, and was recently confirmed by Kuiper [267] who found evidence of material extending nearly to Dione.

Similarly, there have been reports of material inside the crape ring [60, p 382]. Guerin has presented most convincing evidence of this [96, 176, 177] from photographs of Saturn which seem to confirm the presence of at least a small amount of ring material almost to the planet's atmosphere. He calls this material, which is separated from the C ring by a dark division, the D ring. To avoid confusion with material external to the A ring, it has been suggested that any material external to the A ring be called the D′ ring [149]. Radial dimensions of the rings are given in Table 20.

The thickness of the rings is not easily determined, since they are very thin. The only times the rings have been observed when Earth was exactly in their plane occurred in October and December 1966 [60]. Then, through large telescopes, the rings did not completely disappear as it sometimes had been predicted they would. Photometry was undertaken at that time [61, 145] with somewhat discordant results. Both sets of data were analyzed and each found internally consistent. The thickness cannot be less than 500 m, nor is it likely to be greater than about 4 km. Systematic errors seem likely to cause the value to be underestimated [61], consequently a value of 2–3 km seems best until additional observations become available.

It is certain that the rings are not solid. Maxwell showed theoretically in 1857 that a solid ring rotating around a planet would not be stable, and Keeler showed spectroscopically in 1895 that the rings were in differential rotation. On at least six occasions, stars have been seen through the A ring, even though of magnitude 7.2 or fainter [59], giving rather direct proof of the rings' particulate nature. On at least two

TABLE 18.—*Galilean Satellite Temperatures*[1]

Authority	Wavelength, μm	Io (JI)	Europa (JII)[2]	Ganymede (JIII)	Callisto (JIV)
Gillett, Merrill, and Stein	11–12	139 ± 3	132 ± 3	142 ± 3	157 ± 3
Hansen	8–14	137 ± 3	131 ± 3	142 ± 3	152 ± 4
Morrison	8–14	138 ± 4	130 ± 4	145 ± 4	153 ± 5
Morrison, Cruikshank, and Murphy	17–28	128 ± 5	123 ± 5	138 ± 5	151 ± 7
Hansen	17–25	124 ± 4	122 ± 4	132 ± 5	142 ± 6
Morrison	17–28	130 ± 3	123 ± 3	143 ± 4	155 ± 5

[1] From Morrison and Cruikshank [335].

[2] Corrected for new radius of Europa, 1490 ± 50 km.

occasions, eighth magnitude stars were seen part of the time during passage behind the brighter, more dense B ring [59]. The troublesome problem of the mechanical stability of the ring will not be discussed here. (See references [60, 92, 93, 527] for further information.)

Additional information on the rings has come from four sources. Only photometry has been available for a considerable time; infrared radiometry, microwave radiometry, and radar information are very new. The large body of photometric work (reviewed by Morrison and Cruikshank [335]) will only be summarized here.

The visual surface brightness of the B ring and parts of the A ring are somewhat higher than the mean surface brightness of Saturn [95], indicating individual particles of very high albedo, since the rings are not optically thick. Several studies of ring optical depth converge on values of 0.7–1.0 for the B ring and 0.4–0.5 for the A ring [335]. There is a very large opposition effect of 0.2 magnitude in the yellow up to 0.4 magnitude in the infrared and ultraviolet [229]. Since large opposition surges are usually identified with dark surfaces, the effect in Saturn's rings classically (since the 1880s) has been associated with mutual shadowing of the particles but such an effect should be independent of color, which is not what Irvine and Lane observed. The effect may be a combination of shadowing and backscattering.

Recent infrared spectrophotometry has shown that ring particles are largely ice or at least ice-covered [363], accounting for high yellow, red, and infrared albedo. However, a sharp drop in the ring albedo below 6000 Å, very much like the Io's behavior [28, 273], is not the behavior of ordinary pure ice.

Radiometry in the 8–14 μm windows is given in Table 21. It seems clear that ring temperature has increased with increasing Sun angle, implying shadowing was occuring at low angles. Most surprising is the high temperature for bodies of such high albedo. The effective temperature of a *blackbody* at Saturn's distance from the Sun is only 90° K. This would be raised to about 94° K for the B ring by including radiation from Saturn [338]. Estimates of the bolometric Bond albedo for ring particles generally lie between 0.5 and 0.8 or higher [335], implying fairly large, non-isothermal particles which are much warmer on the Sun-Earth side.

Recently, Goldstein and Morris demonstrated that the rings of Saturn are remarkably efficient radar reflectors by transmitting and receiving strong echoes from the rings at 12.6 cm [169]. The measured Doppler spread of echoes matches that expected from the particles in the bright

TABLE 19.—*Microwave Brightness Temperatures of Ganymede and Callisto*

Wavelength [reference]	Ganymede	Callisto
3.55 mm [171]		276 (255 ± 80)
8.2 mm [272]		233 (280 ± 120)
2.82 cm [360]	55 ± 14 (55 ± 14)	88 ± 18 (88 ± 18)
3.71 cm [42]		101 (101 ± 25)

TABLE 20.—*Saturn's Rings, Dimensions* [1]

Parameters	Radii, km	Saturn radii
Equatorial radius, Saturn	60 000 ± 240	1.00
Outer edge, ring D	72 600 ± 2000 [2]	1.21
Guerin division	Width ca 4200 km [2]	
Inner edge, ring C	76 800 ± 2000	1.28
Inner edge, ring B	92 000 ± 850	1.54
Outer edge, ring B	117 800 ± 350	1.97
Cassini division	Width ca 2600 km [3]	
Inner edge, ring A	120 400 ± 400	2.01
Outer edge, ring A	136 450 ± 350	2.28
Semimajor axis, orbit of Janus	168 700 [2]	2.81

[1] From [120], except where otherwise indicated.
[2] From [149].
[3] The edges of A and B rings are not sharp. Direct measurements of the width of the Cassini division often result in much larger values (i.e., ca 3500 km, Dollfus, [120]).

TABLE 21.—*Temperature of Saturn's Rings*

Wavelength, μm	Saturnicentric latitude of the Sun	Ring observed	Brightness temperature, °K	Reference
20	$\lesssim$5°	A and B?	<60	[23]
12.7	18°	A and B	82.7	[5]
20	26°	A	89	[338]
20	26°	B	94	[338]
11	26°	B	91	[335]
20	26°	B	96	[335]

inner ring, thereby strongly supporting the results. The received radar echo power was $62 \pm 6\%$ of what would have been received from an isotropic reflector, without loss, in the same projected geometric cross section as the A and B rings and at the same distance—an entirely unexpected result. This reflectivity compares to 6% for Mercury, 12% for Venus, 8% for Mars, and 5 to 15% for the asteroids, Icarus and Toro. Interpretation is still very speculative, although it is generally agreed that radar observations require that reflecting objects be a centimeter-size or larger.

Goldstein and Morris [169] hypothesize that the scattering objects are likely to be rough with diameters on the order of a meter or larger. Pollack et al postulate that centimeter-sized particles of high albedo yield the observed high reflectivity through multiple scattering [367], and it is pointed out that radio brightness temperatures of the rings provide important constraints to the models. A third hypothesis proposed does not require a large single-scattering albedo. Pettengill and Hagfors [362] point out that backscattering from transparent spheres can show considerable gain over simple external reflection from the front surface of an equivalent sphere. Such gain results from internal scattering processes. For Saturn's rings, it is proposed, smooth ice fragments larger than 8 cm in radius will reproduce the radar result.

There are a number of single antenna and a few interferometer brightness temperature measurements of Saturn and its rings. Single antenna measurements yield the combined radiation from the Saturn-ring system, whereas interferometric measurements allow the ring brightness contribution to be separated and measured directly. One method of studying the ring influence is to observe dependence of the single disk antenna brightness temperatures on the planetocentric latitude of Earth (relative to the plane of the rings). A second method is to estimate the disk contribution from atmospheric models and attribute the residuals to the rings.

In a recent compilation of single antenna data [234] which relate to brightness temperature of the rings, it is shown that, with the exception of data at 1-mm wavelength, there are no statistically significant variations of brightness temperature with planetocentric angle. Measurements are consistent with absence of the rings, thereby showing that brightness temperatures of the rings must be low. Observing at a wavelength of 1 mm, Rather et al [381] measured a brightness temperature for Saturn that is $45° \pm 15°$ K larger than that observed for Jupiter, inferring a brightness temperature of $35° \pm 15°$ K for the rings. Because of the large size of the scatterers implied by radar observations, Pollack et al [367] infer that low brightness temperature must be due to emissivity effect. Janssen [234] combining the Rather et al data with earlier data, finds that the 1-mm data are consistent with an emissivity of 0.4. Briggs [66] estimates an upper limit of 80 cm to the particle size by assuming they are pure water ice.

High resolution interferometric observations of Saturn have been carried out at 3.7, 11, and 21 cm wavelengths [41, 43, 66] showing that nearly all of Saturn's emission originates from the planetary disk. Berge and coworkers estimate brightness temperature of the rings to be less than 10° and 40° K at 20 cm and 10 cm, respectively. Briggs, in agreement with Berge, found that average ring brightness temperature is less than 20° K at 3.7, 11, and 21 cm. Further, he found that when his interferometric fringes were perpendicular to Saturn's polar axis, the apparent size of the planet decreased. Such effect was not seen when the fringes were aligned with the polar axis. Briggs interpreted these data by a model in which the rings obscure part of Saturn's disk, thereby reducing the apparent size of the disk. Ring particles which are good scatterers and poor emitters can diffuse radiation from the disk while having a low brightness, which is consistent with both radio and radar data.

Several lines of evidence have converged to indicate that ring particles must be at least a few centimeters in diameter. Two not previously mentioned are the Poynting-Robertson effect which would sweep the ring free of all original particles smaller than about 3 cm in 5×10^9 years [61,505], and sputtering which would erode several centimeters of ice in a similar time [195]. Thus any small particles would have to be of more recent origin, nor can the rings be a monolayer, since shadowing and multiple scattering appear

to be required. Thus a number of "classical" models suggesting micron-sized particles or a monolayer of various thicknesses apparently have been ruled out by recent studies. No completely consistent ring models exist as yet, however, and there may still be surprises in physical study of one of the most beautiful objects of the solar system.

The Satellites

The satellites of Saturn are laid out fairly regularly except for Phoebe, which is in an elongated retrograde orbit. The basic orbital elements are given in Table 22. Janus was discovered in 1966 when Saturn's rings were "edge-on." Even with the ring lights almost zero, Janus is difficult to see, with a magnitude of only 13.5 or 14, located next to a very bright planet [118, 425, 462]. Absolute confirmation that the object observed is indeed a satellite and not a ring condensation will probably have to wait until the rings are again edge-on, although the best of the photographs are very convincing.

The satellites of Saturn are rather substantial bodies, for the most part, all larger than the seven irregular satellites of Jupiter, and at least five (perhaps seven) of them of greater size than the largest asteroid. Titan (to be discussed in detail) is more massive and somewhat larger than the Moon. The basic physical data for all the satellites (except Janus) will be found in Table 23. Additional photometric and radiometric data for a number of Saturn's satellites are reviewed in Morrison and Cruikshank [335] and will not be repeated, except for mention of Iapetus and Titan.

TABLE 22.—*Saturn's Satellites*[1]

Satellite	Semimajor axis, km	Eccentricity	Inclination [2]	Period, d
Janus [3]	168 700	ca 0	ca 0	0.815
Mimas	185 800	0.0201	1°31.0′	0.942422
Enceladus	238 300	0.00444	0°01.4′	1.370218
Tethys	294 900	0	1°05.6′	1.887802
Dione	377 900	0.00221	0°01.4′	2.736916
Rhea	527 600	0.00098	0°21′	4.517503
Titan	1 222 600	0.029	0°20′	15.945452
Hyperion	1 484 100	0.104	(17–56′) [4]	21.276665
Iapetus	3 562 900	0.02828	14.72°	79.33082
Phoebe	12 960 000	0.16326	150.05°	550.45

[1] From [369], except data for Janus.
[2] To plane of ring.
[3] From [149].
[4] Varies from 17′ to 56′ [400].

Iapetus

Iapetus was discovered by Cassini in 1671, who immediately reported a great brightness variation, suggesting . . . "but it seems, that one part of his surface is not so capable of reflecting to us the light of the Sun which maketh it visible, as the other part is" [1]. That, indeed, has proved to be the case. Murphy et al [339] found anticorrelation between visible brightness and infrared flux, with Iapetus having a temperature of $117° \pm 4°$ K and visual albedo of 0.04 ± 0.01 near minimum light, and a temperature of $110° \pm 4°$ K and 0.25 ± 0.05 visual albedo near maximum light. They suggest that the albedo at maximum is about 0.28. Zellner's [535] polarization studies are consistent with a bright trailing hemisphere and a dark leading hemisphere. Neither of the above studies is consistent with an elongated shape.

The most detailed photometry of Iapetus (that of Millis [323]) showed successive minima differing by 0.3 magnitude, which is attributed to change in solar phase angle, the resulting phase coefficient and opposition effect being comparable to that of the Moon, Callisto, and some asteroids—all having dark surfaces. A much smaller phase coefficient was found for the bright side, comparable to bright Io and Europa. The first good color curves obtained [323] showed 0.07 variation in B–V and 0.045 in U–B. Iapetus, then, is truly a remarkable object with one hemisphere six times as bright as the other. The best theory so far, proposed by Cook and Franklin [94], is that a thin ice crust was largely eroded from one side by meteoroidal bombardment of its leading hemisphere.

Titan

Titan is certainly the most interesting of Saturn's satellites because of its extensive atmosphere. In 1944 Kuiper [258] first discovered methane on the satellite, empirically estimating its abundance in a presumed pure methane atmosphere at 200 m-amagat in 1952

[261]. There the matter stood for 20 years until Trafton's [469] surprising announcement of the possible presence of H_2 on Titan. He further suggested [470] that even the spectrophotometric observations of McCord et al [316] showed that either methane must be an order of magnitude more abundant than previously thought or a minor constituent. Hydrogen observations [469] suggested the presence of ca 5 km-amagat of H_2 (with a very large uncertainty).

Very recent radiometry by Low and Rieke [287], however, shows no evidence of the 17 μm pressure-induced H_2 feature, so the abundance is probably much lower than 5 km-amagat. Trafton also found [475] that there is at least one additional spectroscopically active gas on Titan absorbing in the 1.05–1.1 μm area. There is evidence of an additional absorber near 1.65 μm [297]. Further, there is a prominent emission feature near 12 μm [162], probably best explained as the 12.2 μm ethane (C_2H_6) band [101]. Both ethane (C_2H_6) and ethylene (C_2H_4) have bands in the 1.65 μm region, but Trafton [475] was unable to find evidence for absorptions of either in the 1.06 μm region. He suggests an isotope of CH_4 as one possible explanation of these lines [475].

Evidence of clouds on Titan further complicates spectroscopic interpretation. Polarization observations [489, 536] suggest the presence of an opaque cloud deck. Further, there is a rapid decrease in Titan's albedo through blue, violet, and near ultraviolet [25, 72], entirely opposite to the effect of molecular (Rayleigh) scattering. Albedo decrease virtually requires the presence of an aerosol, preferably a fine dust which absorbs ca λ^{-1} [28].

A major boundary condition on models of Titan's atmosphere is furnished by photometric and thermal data. Younkin's [531] high resolution spectrophotometry from 0.50 to 1.08 μm permitted derivation of geometric albedos. With

TABLE 23.—*Saturn's Satellites, Physical Data*

Parameter[1]	Mimas	Enceladus	Tethys	Dione	Rhea
Mass (Saturn = 1)[2]	$6.59 \pm 0.15 \times 10^{-8}$	$1.48 \pm 0.61 \times 10^{-7}$	$10.95 \pm 0.22 \times 10^{-7}$	$20.39 \pm 0.53 \times 10^{-7}$	$3.2 \pm 5.6 \times 10^{-6}$
Mass (Moon = 1)[3]	0.00051	0.001	0.0085	0.0158	ca 0.025
Mean diameter, km[16]	ca 400[5]	550 ± 300[4]	1200 ± 200[4]	1150 ± 231	1450 ± 200[4]
Mean diameter (Moon = 1)[8]	ca 0.1	0.16	0.35	0.33	0.42
Mean density, g cm^{-3}[9]	ca 1.0	ca. 1.0	0.7	1.5	ca 1.1
V mag at mean opposition[10]	12.1	11.77	10.27	10.44	9.76
Rotational change in V	Unknown	ca 0.4[12]	0.16[5]	0.20[5]	0.19[5]

Parameter[1]	Titan	Hyperion	Iapetus	Phoebe
Mass (Saturn = 1)[2]	$2.4619 \pm 0.0029 \times 10^{-4}$	ca 2.0×10^{-7}	$3.94 \pm 1.93 \times 10^{-6}$	Unknown
Mass (Moon = 1)[3]	1.905	0.0015	0.02	
Mean diameter, km	4850 ± 300[4]	160 – 920[5,7]	1800 ± 200[5]	60–320[5,7]
Mean diameter (Moon = 1)[8]	1.40		0.52	
Mean density, g cm^{-3}[9]	2.34		ca 0.7	
V mag at mean opposition[10]	8.35[15]	14.16	11.03	16.56[11]
Rotational change in V	0.00[5]	Unknown	1.92[13]	0.25[11,14]

[1] All references are given in these footnotes.
[2] From Duncombe, Klepczynski, and Seidelmann [128].
[3] Calculated using mass of Moon = 7.347×10^{22} kg (190).
[4] From Dollfus [119].
[5] From Morrison and Cruikshank [335].
[6] From Murphy, Cruikshank, and Morrison [339].
[7] Lower limit assumes a geometric albedo of 1.0; the upper limit, 0.03.
[8] Calculated using diameter of Moon = 3475 km [190].
[9] Calculated from data above.
[10] From Harris [194] except for Titan and Phoebe.
[11] From Andersson [10, 11].
[12] From Franz and Millis [150].
[13] From Millis [323]. (See discussion in text).
[14] Phoebe is apparently not "locked' to Saturn. Its period of rotation is apparently less than 1 d [10, 11].
[15] From Blanco and Catalano [58].
[16] Elliot, Veverka, and Goguen reported new radii for five satellites at IAU Colloquium No. 28, Planetary Satellites, Ithaca, N.Y., Aug. 1974. These will cause major changes in all physical data. For example, their values for Titan and Iapetus are 5832 ± 53 and 1595 ± 139 respectively.

existing measurements from 0.30 to 0.50 μm and a synthetic spectrum based upon similar Jupiter and Saturn results from 1.08 to 4.0 μm, Younkin [531] derives a bolometric geometric albedo of 0.21 and suggests using a bolometric Bond albedo of 0.27 ± 0.04. The effective temperature of Titan then is $84° \pm 2°$ K.

Detailed thermal measurements (from Low and Riecke [287]), given in Table 24, show a surprising picture. Even a nonrotating blackbody (zero albedos) normal to the Sun can reach only 127° K at Titan's distance from the Sun. It would appear that there must be either a fairly effective atmospheric greenhouse mechanism or an atmospheric nonequilibrium radiator in operation. The peak at 8μm is to be expected from methane inversion as on Jupiter and Saturn. The peak at 12 μm may be C_2H_6 as noted above. The rest can potentially be modeled in at least two ways.

A series of greenhouse models for Titan was computed [366] in which the best fit to the data then available suggested roughly a 50–50 mix of H_2 and CH_4 with a surface temperature and pressure of at least 150° K and 0.4 atm. The greenhouse was created by pressure-induced transitions in the gases, but there was visible opacity from methane clouds. The biggest problem is that the pressure-induced H_2 feature that would then fill the region near 17 μm simply does not seem to be present [287].

Danielson, Caldwell, and Larach suggest that an aerosol layer of micron-sized particles would absorb a large part of incident thermal radiation [101], but could not reradiate it effectively at wavelengths several times their size, hence creating thermal inversion and explaining high 5 μm temperatures. The surface would be near 80° K, heated by direct solar radiation and reemitted atmospheric radiation. The greatest problem is that the Bond albedo appears to be higher (0.27) than they assumed (0.20).

Low and Rieke suggest a slight modification: retaining the particle inversion layer but adding a bit of greenhouse would keep the surface temperature up to 80°–90° K, as required to keep too much CH_4 from condensing out in spite of the higher albedo [287]. Detailed calculations have not yet been made for a combined greenhouse-inversion model of Titan's atmosphere, but it seems plausible. Reliable quantitative models must await radio surface temperatures and positive identification of the unknown absorbers in Titan's atmosphere.[8]

The nature of Titan's crust is expected to be the factor which determines the presence and composition of the atmosphere. This problem and that of hydrogen escape have been considered by Hunten [222], who showed that a pure H_2 atmosphere would escape extremely rapidly but that 10–25% H_2 could probably be retained in a steady state, produced perhaps from photolysis of NH_3. Although an atmosphere on Titan may have a sufficient velocity to escape from Titan, it probably does not have a Saturn escape velocity [318]. Consequently, atoms and molecules lost by Titan are forced by the planet's gravitational field to orbit Saturn until ionized, or until recaptured by Titan.

There is no direct observational knowledge of the surface and interior of Titan. For example, in spite of very high precision photometry, no variation in Titan's brightness has been detected which could be attributed to rotation. Titan is usually assumed to keep one face toward Saturn, rotating and revolving synchronously, but this is no more than an educated guess. According to Lewis' models [279, 281], the surface may be largely methane hydrate ice, although obviously this is a function of what the surface temperature proves to be. The interior may contain a hydrous silicate mantle overlain with a hydrous ammonia solution immediately below the solid crust [279, 281], while there may be a troilite (FeS) core. The uncomfortable fact remains that the only real observational datum on the interior of Titan is its density, and even that is uncertain by perhaps 20% because of the uncertainty in the satellite's radius.[8]

Satellites of Uranus

Uranus has five satellites which form an extremely regular system, for which basic data is

[8] The new 5832 km radius for Titan (see Table 23) reduces the temperature discrepancy significantly and decreases the density by 60%.

given in Table 25. The satellites are too small for direct measurement of size at the distance of Uranus, and none has been detected in the middle infrared to allow a radiometric radius determination. If ice-covered, with a very high albedo, they could be as small as 200 km (Miranda) to 700 km (Titania) in diameter. Given extremely dark surfaces, diameters could be 1300 km (Miranda) to 4000 km (Titania). If Kuiper's uncertain masses (see Table 25) are taken literally, the true diameters must be near the lower limits to keep the densities above 1 g/cm^3.

Satellites of Neptune

Neptune has only two satellites. The apparently large and massive Triton is in retrograde motion in an orbit with no detected eccentricity, while tiny Nereid is in direct motion in a large, highly eccentric orbit. Basic data for the two satellites are given in Table 26. Very rough mass and diameter figures exist for Triton, $1.3 \pm 0.3 \times 10^{-3}$ of Neptune [253] and 3770 ± 1300 km [119], respectively.

Triton is apparently large enough to hold an atmosphere, although none has yet been detected; an upper limit of 8 m-amagat of methane has been set [441].

The maximum surface temperature on Triton (assuming little atmospheric opacity) is noted at below the condensation temperature of methane hydrate [335], but above that of pure methane. Any atmosphere may have to consist largely of inert gases.

TABLE 24.—*Infrared Photometry of Titan* [1]

λ, μm	$\Delta\lambda$, μm	p[2]	T_B[3], °K
1.65	0.3	ca. 0.01	--
2.2	0.6	0.05	--
3.6	1.0	0.01	--
5.0	1.0	$\leq$ 0.10	165
8.8	1.0	--	136
10.3	1.3	--	125
10.6	5.0	--	124
11.6	0.8	--	128
12.6	1.0	--	129
17	2	--	101
19	1	--	97
21	8	--	93
22.5	5	--	91
24.5	1	--	86
34	12	--	82

[1] From [287].
[2] Geometric albedo.
[3] Assumes a diameter of 5100 km rather than 4850 km as given in Table 23. The new value of 5832 km (see footnote 16, Table 23) will reduce all of these significantly.

ASTEROIDS

Discovery and Logistics

A belief in basic order in the universe is inherent in science. Especially strong in the past was a corollary belief in simple mathematical symmetry in all things as well. This led in 1766 to Titius' discovery of a simple mathematical progression describing the distances of the then known planets from the Sun. The regularity (highly publicized later by Bode) is often known as Bode's law. Uranus, discovered in 1781, fit the law very well with one exception: the law predicted a planet at a heliocentric distance of 2.8 AU and none was known.

A cooperative search for the "missing planet" was then proposed. Even before the letter asking his cooperation reached him, Piazzi discovered a small planet while working on a star catalog [283]. This body was discovered January 1, 1801 and found to be at a mean distance of 2.77 AU. It was named Ceres. The next year, while making additional observations of Ceres, Olbers discovered a second small planet which was named Pallas [283]. He immediately suggested they might be parts of a larger planet which had exploded [283]. The same year, Huth suggested that between Mars and Jupiter the matter which formed the planets had simply collected into many smaller bodies rather than one large one [283]. In 1804, Harding found Juno; in 1807, Olbers added Vesta; and in 1845 and 1847, Hencke added Astraea and Hebe [283]. Two more small bodies were found in 1847, and no year since then has passed without at least one discovery [400].

Astronomers agreed in 1851 to officially designate the small planets, *minor planets* [283], but Herschel's term *asteroid* (starlike) has been more commonly used. When an asteroid is discovered and reported, it is given a provisional

designation [157]. If recovered at a second apparition, it is given a number in chronological order on the list of confirmed objects and named by its discoverer [157]. All names were feminized at one time, but this convention is no longer followed [157]. By early 1974, the list of numbered asteroids had reached 1846. An annual ephemeris of the numbered asteroids is published by the Institute for Theoretical Astronomy in Leningrad, while all minor planet observations, ephemerides of objects which have not yet received numbers, and lists of orbital elements and residuals of differential corrections are published by the Cincinnati Observatory in *Minor Planet Circulars* [198].

Statistics and Groups

There have been two systematic searches for asteroids, from which statistical conclusions are relatively free from the selection effects resulting from using only the catalog of numbered objects. The first was the McDonald Survey, from 1950 through 1952, with a 25-cm f/7 four element photographic objective [268]. It reached to about the 16th apparent magnitude (in the blue). The second was the Palomar-Leiden Survey using plates taken in 1960 with a 122-cm f/2.5 Schmidt camera [212]. It reached through the 20th apparent magnitude, but only in a small group of selected areas which biased against high eccentricity and high inclination objects [256]. The total number of asteroids brighter than photographic (B) magnitude 21.2 at mean opposition is $4.8 \pm 0.3 \times 10^5$ [157]. Schubart [411] estimates the total mass of *all* asteroids to be only about 2.4×10^{21} kg, which is 4×10^{-4} of Earth's mass.

The great majority of asteroids have orbits with semimajor axes lying between 2.17 and 3.3 AU, the lower limit apparently the result of interactions with Mars. Williams [518] suggests that the asteroid belt once extended to much smaller heliocentric distances but was swept clean by collisions and close approaches to Mars, except for isolated groups. The upper limit of the main belt is the 2:1 resonance with Jupiter, the location where the mean daily motion of a body is exactly half that of Jupiter. The average inclination of asteroid orbits is about 4° near the inner edge of the main belt rising to 11° near the outer edge, with the larger asteroids less well-confined to the ecliptic than the smaller ones [157]. The mean orbital eccentricity of asteroids

TABLE 25.—*Satellites of Uranus*[1]

Satellite	Semimajor axis, km	Eccentricity	Inclination[2], deg	Period, d	Mass[3] (Uranus = 1)	V magnitude at mean opposition[4]
Miranda[5]	129 800	0.017	3.4	1.41348	1×10^{-6}	16.5
Ariel	190 900	0.0028	ca 0	2.52038	15×10^{-6}	14.4
Umbriel	266 000	0.0035	ca 0	4.14418	6×10^{-6}	15.3
Titania	436 000	0.0024	ca 0	8.70587	50×10^{-6}	14.01
Oberon	583 400	0.0007	ca 0	13.46325	29×10^{-6}	14.20

[1] Adapted from [263], except as otherwise noted.
[2] To what is thought the plane of Uranus' Equator. Dunham [129] reports that small mutual inclinations, in fact, exist for all the satellite orbits.
[3] Very uncertain values, derived with the assumption of equal densities and albedos for all five bodies.
[4] Taken from [194].
[5] Orbital elements from [513].

TABLE 26.—*Satellites of Neptune* [1]

Satellite	Semimajor axis, km	Eccentricity	Inclination, deg	Period, d	V magnitude at mean opposition[2]
Triton	355 550	0	159.945	5.876844	13.55
Nereid	5 567 000	0.74934	27.71	359.881	ca 18.7

[1] From [369], except as otherwise noted. [2] From [194].

in the Palomar-Leiden Survey is 0.147, the complete range being 0 to 0.385 [212, 256].

Numerous asteroid groups are of special interest both within and outside the main asteroid belt. The Trojan asteroids occupy the L_4 and L_5 Lagrangian solutions to the three-body problem in the Sun-Jupiter system, following and preceding Jupiter by roughly 60° in its orbit. A special search of the preceding (L_5) point indicated it contained about 700 members brighter than mean opposition magnitude of 20.9 [213]. Preliminary results show only about 300 near the following point.[9] There is a stable resonance at the 3:2 commensurability with Jupiter (at 4.0 AU), which contains 23 numbered members and 10 discoveries of the Palomar-Leiden survey known as the Hilda group [211]. One asteroid called (279) Thule is in the 4:3 commensurability (at 4.3 AU) [211]; two asteroids (1362) Griqua, and (1101) Clematis are librating about the 2:1 resonance [302]; and 24 known members (15 numbered) in the Hungaria group are in the 9:2 resonance (at 1.9 AU) [302].

Asteroids crossing Earth's orbit are called Apollo asteroids after the first one discovered to do this. Seventeen are known, but several will be recovered only by chance [155, 305]. Apollo itself was recovered in a deliberate search by McCrosky in 1973, the first time it was seen since its discovery in 1932 [305]. Asteroids coming nearer than the perihelion distance of Mars (1.38 AU) but not crossing Earth's orbit, are called Amor asteroids [155]. Sixteen are known, but at least one, and perhaps two or more are lost [155]. One very special object is (944) Hidalgo; at the greatest mean distance of any known asteroid (5.8 AU) with an eccentricity of 0.66, it moves in to 2.0 and out to 9.7 AU [302], is the only minor planet known to come closer than 1 AU to Jupiter; it reached 0.38 AU in 1673 [302]. Hidalgo's orbit is also at high inclination, 42.5°, the largest known for many years. Hidalgo shares with Apollo and Amor asteroids the virtually ubiquitous property of high-eccentricity orbits. Only (433) Eros (eccentricity 0.22) of these groups has an eccentricity less than 0.36; (1566) Icarus holds the record at 0.83.

[9] T. Gehrels, private communication.

Most Apollo and Amor asteroids do not have particularly high inclination orbits, but this may have been a partially observational selection. Recent discoveries include Apollos 1973 EA at 40°, 1972 XA at 41°, and 1973 NA at 67° [305]. One Amor asteroid, (1580) Betulia, has an inclination of 52°. It was found that a number of the lower inclination Apollo and Amor asteroids are in resonance with, or librate about a resonance with Earth, although the "captures" may not be of very long duration [227].

In 1866, Kirkwood noted an apparent structure in the main asteroid belt, notably gaps at commensurabilities with Jupiter's period. The "Kirkwood gaps" at 2:1, 3:1, and 5:2 are particularly prominent [84], although (as previously noted) there are occasional asteroids exactly in, or librating about, a commensurability.

In a series of papers from 1918 through 1933, Hirayama recognized families of asteroids within the main belt with very similar "proper" orbital elements. "Proper" elements represent the motions of a body freed from most secular perturbations ([68], pp. 524–529). These Hirayama families are generally assumed to be collision fragments [211]. When clustering occurs in the angular variables as well, Alfvén has called the result a "jet stream." A complete listing of the Hirayama families and of many jet streams among the numbered asteroids has been given by Arnold [19]. Additional families were found in the Palomar-Leiden survey [211].

Origin and Evolution

Classical theories of the origin of asteroids were those enunciated by Olbers and Huth within a year after the discovery of Ceres. Kuiper [262] consolidated these ideas, suggesting perhaps 100 (originally 5–10 [259]) bodies were formed by accretion while the rest resulted from collisions. In 1953, Kuiper [262] noted that some accretion must still be continuing while Alfvén, going much farther, describes gravitational focusing into "jet streams" as a major accretion mechanism still operating to the present [3]. A number of scientists have worked on the mechanics of the problem [33, 103, 480, 482]. A recent comprehensive study by Napier and Dodd

[340] indicates that collisions among some of the original asteroids are the most probable origin of the main belt.

The source of asteroids crossing into the inner solar system and of meteorites recovered on Earth is of great importance. There is evidence that some, but probably not all, of the Apollo asteroids may be nuclei of extinct comets [302, 303]. Evidence from spectrophotometry of asteroids (to be discussed) indicates that at least one Apollo, 1685 Toro, shares characteristics with main belt asteroids of the Flora group and with common chondritic meteorites [86, 238]. There has been a severe problem, however, that cosmic ray exposure ages of stone meteorites are very short compared to the time normally required to perturb them from the main belt into an Earth-crossing orbit without an extreme collision, which would create an obviously shocked body.

Two mechanisms have been suggested very recently which seem to supply sufficient stony meteorites from low velocity collisions with low exposure to cosmic rays [519, 538]. Both mechanisms furnish material only from the immediate vicinity of resonances, which would imply that all stony meteorites may originate from a limited number of asteroidal sources. Most iron meteorites are old enough to come from several places in the belt. Many meteors, entering Earth's atmosphere from well-known streams associated with comets, appear generally to be quite fragile and burn up long before reaching the ground. More substantial bodies could exist in cometary debris, however, and there is no problem dynamically in bringing them to Earth. There is quite general agreement, then, that meteorites originate in the asteroid belt and/or comets, but which types come from where is still a much debated and researched question. Standard references on the subject include [7, 17, 18, 197, 509, 510].

Physical Data

The masses and diameters of the asteroids are of fundamental importance, but masses exist for only three asteroids, and one of those is very uncertain. In 1968, Hertz [199] published a mass of $1.2 \pm 0.1 \times 10^{-10}$ solar masses for (4) Vesta determined from a series of close encounters with (197) Arete. In 1974, Schubart [412] reported new masses for (1) Ceres and (2) Pallas derived from their mutual interaction, that for Ceres being $5.9 \pm 0.3 \times 10^{-10}$ solar masses and for Pallas $1.3 \pm 0.4 \times 10^{-10}$ solar masses. The mass of Ceres is roughly half the total mass of the asteroid belt [411].

Useful direct measurements of diameters have been made only for the first four asteroids. There are two other known methods to determine diameters: one using both infrared radiometry and visual photometry to determine albedo and diameter [332], the other, polarimetry to determine albedo, which, when coupled with visual photometry, gives a diameter [490]. Results from all three methods are compared in Table 27. Infrared and polarization results agree well but are obviously systematically larger than direct measures. Ceres has also been detected at 3.7 cm [65]. Use of the polarization diameter gives a disk brightness temperature of $160° \pm 53°$ K, which is in good agreement with the expected temperature from solar insolation [65]. The larger diameters for Ceres and Vesta imply densities of 2–2½ g cm^{-3}, but uncertainty in both masses and radii is sufficient to make this number of little value. Diameters have been measured for other asteroids and used to determine geometric albedos (to be discussed).

A great deal of information about asteroids has come from their light curves at one or more wavelengths. Since most asteroids have either an irregular shape or variation in reflectivity over their surfaces (or both), it usually requires careful photometry to find the period in which light fluctuations repeat (to phase the light curve), hence the rotation period. This has been accom-

TABLE 27.—*Asteroid Diameters*

Asteroid	Direct measurement[1], km	Infrared measurement[2], km	Polarization measurement[3], km
(1) Ceres	770	1000	1050
(2) Pallas	490	530	560
(3) Juno	195	240	225
(4) Vesta	390	530	515

[1] Barnard's values as quoted by Dollfus [122].
[2] From Chapman and Morrison [84].
[3] Zellner's values as quoted by Chapman and Morrison [84].

plished to varying accuracy for some 50 asteroids; results through 1971 have been summarized by Taylor [458]. Well-determined rotation periods vary from 2.273 for (1566) Icarus to 18.813 for (532) Herculina [458], but a few objects appear to have much longer periods. Different aspects of the asteroid are seen by observing over a reasonable fraction of a revolution period—the amplitude of the light curve decreasing as one looks more at the pole.

Techniques have been developed for measuring the coordinates of the pole and the sense of rotation [458, 487] and results have been summarized by Vesely [487]. Some of the techniques used for small amounts of data unfortunately do not lead to unique answers when the shape is somewhat extreme, which is true for many asteroids. Determination of shape as well as rotation axis is considered by Dunlap [131]. In principle, albedo variations on the surface can also be modeled from light curves of sufficient detail and accuracy. Here, curves at more than 1 wavelength are useful, since albedo markings may vary with wavelength while shape will not.

Some description of the composition of asteroids has become possible for the first time, with the advent of precision spectrophotometry, placed on an absolute scale by means of polarization or infrared radius determinations. A summary of work through mid-1972 has been given by Chapman et al [87], while Chapman and Morrison provide a popular account of more recent work [84]. Two gross classes of asteroids are: red objects with moderate blue geometric albedo (0.1–0.2) and higher red geometric albedo (0.14–0.23); and dark, neutral objects with nearly flat spectral response, having geometric albedos from 0.09 down to 0.03. The latter sometimes show slight slope or structure and a decreasing albedo below 4000 Å. The former often show distinct spectral features. The first (red) class is of largely silicate-type material, and the second (dark, neutral) class is of carbonaceous chondritic-type material.

Chapman and Salisbury [85] have made detailed comparisons of laboratory spectral reflectivities between 41 meteorites and 36 asteroids. Only the Earth orbit crosser (1685) Toro [86] and (43) Ariadne [238] and (8) Flora [84] from the inner edge of the main belt resemble ordinary chondritic meteorites. Matches to enstatite chondrites were found [85] for (16) Psyche and (29) Amphitrite, to a basaltic achondrite for (4) Vesta, to a carbonaceous chondrite for (2) Pallas, and to Chantonnay (a shocked, brecciated L6 chondrite) for (192) Nausikaa. However, it is most striking that many asteroids resemble no known meteorite while many meteorites resemble no studied asteroid [85]. This is consistent with the idea that most common stony meteorites are derived from a very few atypical asteroids. Research on asteroids is only beginning to reach maturity. Detailed studies have been under way for only 5 years and many important new geochemical results can be expected in the near future.

COMETS

History and Nomenclature

Ancient Chinese records contain the earliest clear reference to a comet, one which appeared during a war about 1055 BC [209]. Records of Halley's Comet go back, possibly, to 240 BC or even to 467 BC [209, 304], and no apparition has gone unreported since it was seen in 86 BC [283, 304].

Two schools of thought existed among the ancient Chaldeans [283]: one group held that comets were like planets but moving far enough from Earth to be invisible most of the time; the other group believed comets were "fires produced by an eddy of violently rotating air." Aristotle considered them atmospheric, the *product* of dry and windy weather [283]. In peoples' minds they soon came to be the *cause* of winds, and then of things associated with winds, such as floods and severe fires. At first they were omens, later only bad omens, so that for 2 millennia people were frightened of comets. As late as 1910, during the appearance of P/Halley, confidence men did a large business in comet pills and gas masks to ward off "its noxious influence" [6].

Comets had been "respectable" among educated people for several hundred years before 1910. Tycho Brahe showed that the great comet of 1577 was more distant than the Moon because observations over all Europe clearly indicated the comet's smaller parallax [283]. As early as

1665, Borelli observed that the comet of 1664 had apparently moved in an elliptical orbit "or another curved line" rather than a straight line [283]. However, using the new gravitational theory of his friend Newton, it was Edmond Halley, who showed that comets were relatively well-behaved members of the solar system. He demonstrated that the comet of 1682 had an orbit nearly identical to comets sighted in 1607 and 1531, and that four earlier comets had appeared at intervals of about 76 years [283]. He then predicted its reappearance in 1758, which, of course, occurred.

In current practice each comet, in order of discovery or recovery in a given calendar year, is provisionally designated by that year and successive letters of the alphabet, i.e., 1974a, 1974b. In about 2 years, after their orbits are well-determined, comets are redesignated with the year and a roman numeral in the order of their perihelion passages, i.e., 1971 I, 1971 II. Each comet is also designated by the name of its discoverer(s) but not by more than three names. If the comet's period is less than 200 years, the name is usually preceded by P (for periodic), and it may often be preceded or followed by its most recent observed perihelion passage designation, i.e., 1910 II P/Halley. If the discoverer has more than one periodic comet to his credit, the name is followed by a number, i.e. P/Temple 1 and P/Temple 2. In a few instances, where a comet has been lost for several returns, the name of its recoverer has been added, thus P/Swift 1, having been lost for eight successive apparitions and recovered by Gehrels on the ninth in 1973, is now designated P/Swift-Gehrels. At times a comet has been designated by the name of a scientist who has intensively investigated its orbit, the most prominent being P/Halley and P/Encke.

Cometary Orbits

Edmond Halley proved that at least one or more comets moved in orbits that were highly eccentric ellipses. Other comets, apparently the great majority, seemed to move in parabolas or even hyperbolas. Comets were therefore designated periodic and nonperiodic, but as astrometry became more precise, this dichotomy began to seem more and more artificial. Marsden's recent catalog [304] lists 503 comets with periods greater than 200 years. Of the 392 observed from 1800 through 1969, only 10 orbits were even formally hyperbolic when traced back beyond Neptune and referred to the solar system barycenter. Only 1899 I had a hyperbolic excess greater than three times the formal standard error, and Marsden feels this one would be removed from the hyperbolic list if allowance were made for nongravitational effects [304]. Marsden, along with the majority of orbit specialists (but by no means all) believes that all comets are initially bound to the solar system, although they may be lost (given a hyperbolic velocity) through planetary perturbations. Comets today are usually termed short period (periodic) or long period, the split being at a period of 200 years, although this is an arbitrary, nonphysical distinction. Five known comets have periods between 100 and 200 years and seven between 200 and 300 years; but this does mean the short period category includes all comets seen more than once.

A more physical distinction of comets could be based upon orbital characteristics. Table 28 groups the inclinations and periods of all comets seen at more than one return. Clearly, the vast majority of short period comets are very short period and show great preference for the plane of the ecliptic. No comet with a period of less than 13 years has an inclination greater than 32°. The long period comets, on the other hand, show absolutely no preference for the ecliptic orbit. Their lines of apsides are located almost randomly, though showing some clumpiness and a slight (many say significant) preference toward the galactic plane [292, 521] (see also, Volume I, Part 1, Chapter 1). Another significant difference is that the median perihelion distance of the 503

TABLE 28.—*Orbital Characteristics of 65 Comets Appearing More than Once*

Inclination	No.	Period	No.
$i < 30°$	55	$P < 10$ yr	46
$i < 60°$	60	$P < 20$ yr	55
$i < 90°$	62	$P < 50$ yr	58

long period comets is 0.84 AU, only about half that of the short period comets (1.5 AU) [304]. The meaning of these dynamical differences will be considered in the section, **Origin and Evolution.**

Empirical Behavior of Comets

A comet, at very great distances from the Sun, is usually completely stellar in appearance, if it can be seen at all. As it reaches heliocentric distance of about 3 AU, it begins to develop a small nebulosity, called the coma. Spectroscopically, the initial nebulosity is largely emission from the (0–0) band of the violet system of CN near 3880 Å [453]. At about 2 AU, emission from the complex λ4050 group of C_3 begins to develop, as does the α-ammonia system of NH_2 (with weak bands scattered throughout the visible and near-infrared), but these bands are seen only in a much smaller area around the nucleus than CN [453]. At 1.8 AU, the Swan bands of C_2 begin to develop (primarily (1–0) at λ4737, (0–0) at λ5165, and (0–1) at λ5636), having a greater spatial extent than C_3 but not so great as CN [21, 453]. By 1.5 AU, all radicals normally present can be seen (OH, CH, NH), as well as other overtones of C_2 and CN (0–1 of CN usually appears at about 2 AU) [453].

In 1970, Code et al [89] reported the presence of a large corona of H about Comet Tago-Sato-Kosaka, detected from its Lyman-α emission at 1216 Å by the Orbiting Astronomical Observatory. Since that time, hydrogen has been observed about comets Bennett, Encke, and Kohoutek, and it is obvious that atomic hydrogen is a major feature of all active comets, although its time of onset has not been reported observationally. Lines of metastable oxygen [OI] in the region λ6300–6400 have been observed in comets since the available spectral dispersion became high enough to separate them from terrestrial airglow lines and other cometary emissions. These have now been observed at more than 1.5 AU [442]. At about 0.7 AU, the D-lines of Na usually appear in emission [453]. Comets approaching very close to the Sun, such as Ikeya-Seki 1965 VIII, also show emission lines of K, Cr, Mn, Fe, Ni, and Cu, plus ionized Ca [372].

The coma, although brightening as it approaches the Sun, generally shrinks in apparent size after reaching a maximum near 1.4 AU [453]. Meanwhile, the continuum of reflected sunlight, completely dominant beyond 3 AU and corresponding only to the stellarlike nucleus or occasionally a small area around it [123, 257], may grow in extent and dominate the entire central spectrum (as for comet Bennett), or, it may remain so weak as to be virtually undetectable (as for P/Encke), making the spectrum seem to be pure emission features.

The brighter comets nearer the Sun than 1.5 AU usually develop tails (type I) which seem to be composed largely, if not totally, of ions, emission features of CO^+ and N_2^+ being dominant [453]. CO_2^+, CH^+, NH^+, and H_2O^+ are also seen in ion tails. On rare occasion, an outstanding ion tail may develop even at a far greater distance. Comet Humason 1962 VIII showed great tail activity at more than 2.5 AU, with CO^+ and N_2^+ completely dominating the coma spectrum as well as that of the tail [174, 396]. Strong CO^+ emission was seen even at 5 AU [452]. Normally, beginning at about 1 AU, a comet may also develop a tail (type II) which shows only a continuum of reflected sunlight, apparently scattered from very small particles (ca 1 μm). Apparent type II tails have occasionally also been observed at very great distances (3.95–5.0 AU) [350, 417]. The ion tails usually appear very straight, often with intricate filamentary structure and/or a turbulent appearance, while the "dust" tails are more featureless and often curved. Depending upon geometry, the two tails may appear separate or superimposed, in cases where a comet exhibits both types.

Any attempt to discuss an "average" comet or to predict its behavior is valid only in a statistical sense. Comets are individual entities. Their behavior is a complex function of dust-to-gas ratio, gas composition, and age (number of times they have come nearer than ca 4 AU to the Sun) at the very least; many additional variables can be hypothesized. The early attempts to forecast the brightness of comet Kohoutek (1973f) near perihelion are excellent examples. Long-period comets almost always brighten less rapidly with distance than short-period ones, and any hope

that Kohoutek would brighten as r^{-6}, or even r^{-4}, all the way from 5 AU was extremely optimistic. Long-period comets typically brighten at ca $r^{-2.8}$ [123] to the extent that a simple power law can describe their behavior. The complexities of the situation have been well described by Sekanina [416] for one comet, P/Encke.

Cometary Models

There is no universally accepted model of comets. The most widely accepted one by far is the icy conglomerate model of Whipple [511], which has been amplified considerably, especially by Delsemme and coworkers [108] and Sekanina [415]. It works well for the average comet, and cometary observations will be discussed here in terms of this model. Competing ideas about comets will be discussed briefly in the section, Origin and Evolution.

A comet has been pictured by Whipple [511] as a solid, low-density structure of frozen gases well-mixed with dust and larger debris. As it approaches the Sun, volatile substances begin to vaporize, forming a dust and gas atmosphere which is seen as the coma. Streaming back under the influences of radiation pressure and the solar wind, the dust and ionized gases form tails. The relatively sudden onset of activity at 3 AU has been explained by the discovery that water is the major component of comets, which controls the vaporization rate [108]. Whipple was led to the icy conglomerate model in order to explain the apparent secular acceleration of P/Encke. The nongravitational "jet propulsion" effect of gases vaporizing from part of the sunward hemisphere of a rotating nucleus seems quite an adequate explanation for Encke as well as other comets [307]. Sekamina has suggested that some or all comets may have a rocky core [415]. Thus, as comets grow older their activity would decline, being dependent toward the end upon the amount of gas which could diffuse to the surface. The end product then might be an Apollo-type asteroid, as discussed previously [303].

A major problem is the determination of the parent molecules of all radicals and ions actually observed in comets, that is, the composition of the frozen gases in the nucleus. Observed abundances and extent of H and OH are compatible with photodissociation of an H_2O parent [48]. Water was finally detected, at 22.23 GHz, in 1974 [232]. Microwave studies also revealed the presence of two other stable, neutral species in comet Kohoutek: methyl cyanide (CH_3CN) [484] and hydrogen cyanide (HCN) [434]. It is not clear whether either can be the parent of CN, since the photodissociation lifetime of CH_3CN seems too long [371] and that of HCN is unknown. The parent molecules could be much more volatile than water and still controlled by water vaporization if trapped as clathrates, as suggested by Delsemme and coworkers [110]. The interesting possibility of releasing a halo of icy grains from the nucleus, thereby increasing the effective area of release of material, is considered by Delsemme and Miller [110, 111, 112]. This has the added attraction of explaining the photometric nucleus, an optically thick region in the coma much larger than the "real" nucleus could possibly be.

As soon as the radical or ion is formed, its excitation is well-understood for most species. It is resonance fluorescence excitation of a collisionless gas [452], except possibly in the innermost region of the coma [297]. This has been shown quantitatively in CN, for example, where the strength of individual rotational lines in the comet is completely dependent upon the heliocentric velocity of the comet, as the Doppler effect shifts the wavelength and therefore the available intensity of exciting solar radiation, particularly when shifting through a Fraunhofer line [21, 104, 297, 452]. The intensity shift with changing velocity is known as the Swings effect. The Greenstein effect is similar but much smaller, resulting from the actual velocities (ca 1 km s^{-1}) of the gases in the comet [21, 297, 452]. Rotational temperatures for C_2 are always quite high (3000°–5000° K) as compared to heteronuclear molecules (200°–500° K) because a homopolar molecule cannot make pure rotational transitions, but there is no fundamental difference in excitation mechanism [452]. Resonance fluorescence works well for ions, too, as demonstrated by Arpigny for CO^+ [20]. Only for metastable oxygen does resonance fluorescence seem completely inadequate [452]. It is generally believed that this

574-269 O - 76 - 18

excitation results directly from the dissociation of the parent [51].

The flow of hydrogen from comet Bennett 1970 II was measured after perihelion from 0.6 to 1.04 AU [48]. The flow rate followed roughly an r^{-2} law (r = heliocentric distance), being 0.7×10^{29} H atoms s^{-1} $sterad^{-1}$ at 0.81 AU [48]. P/Encke produced ca 5×10^{26} H atoms s^{-1} $sterad^{-1}$ at 0.715 AU before perihelion in 1970 [48]. Assuming that all hydrogen comes from water and all water finally is completely broken down (OH also dissociates), the number of water molecules emitted by the nuclei was half these values. An old periodic comet, Encke, a bit closer to the Sun and before perihelion, was producing less than 10^{-2} as much water as a "new" comet, Bennett, after perihelion. This clearly indicates that either Encke is much smaller than Bennett, or no longer "an infinite source" controlled only by solar insolation, or both.

Limits on cometary nuclei size can be set by measuring their apparent brightness at an inactive time (beyond 3 AU) and assuming various reflectivities. A compilation of such data by Roemer [397] suggests P/Encke is between 1.2 and 7.0 km in diameter, for example, while Humason is a giant between 19 and 110 km, and Tuttle-Giacobini-Kresák, a dwarf between 0.2 and 0.8 km. Studies by Delsemme and Rud [113] suggest Bennet has a diameter of about 7.5 km and a Bond albedo of 0.66, while the mean Bond albedo of Encke must be much smaller, with water-ice covering only a small fraction of the surface or no longer controlling H production. A nucleus of density 1 g cm^{-3} and 4 km in diameter would have a mass of 3×10^{13} kg, one 50 km in diameter, a mass of 5×10^{17} kg. The range 10^{12}–10^{18} kg is about that usually given for the smallest to largest possible comets.

Modeling of cometary tails has a long history. The mechanical theory of dust tails was well-developed by Soviets Bredikhin, Orlov, and others many years ago. The problem is essentially that of the motion of particles given various initial conditions moving under the dual forces of gravitation and solar radiation pressure [62], although details of dust emission mechanisms are still very much open to question [37, 526]. Apparent objections to the purely mechanical theory stemming from observations [350] of nonradial tails at great distances can be explained by emission of icy grains at very large heliocentric distances [417].

Levin [275] has suggested that dust tails should remain divided into two categories, Bredikhin's type II and type III, and that one of these contains a large amount of neutral gas as well as dust, but this does not create a severe physical theory crisis. Type I tails are altogether different. Their structures appear to show accelerations far too large to have been induced by radiation; in fact, Biermann [49] was led to predict the solar wind, long before its actual detection, to explain these accelerations. A fairly detailed model of the interaction of a typical long-period comet with the solar wind has been presented by Biermann, Brosowski, and Schmidt [50]. It predicts the existence of a shock front about 10^6 km in front of the nucleus where the flow becomes subsonic and of a contact surface at about 10^5 km inside which the solar wind cannot penetrate. Wallis [498], on the other hand, suggests a collisionless charge exchange that slows the solar wind. Others have suggested that the contact surface may be unstable. Photoionization is insufficient to explain ion densities observed in a comet, and so apparently is charge exchange [107]. A critical velocity theory of ionization has been proposed (e.g., [418]). No real understanding exists of the mechanisms of interaction between a comet and the solar wind, hence there is no generally accepted mechanism for the formation and behavior of ion tails.

A discussion of comets within the framework of the icy conglomerate model should not neglect mention of a few of its problems. Some comets (previously noted) show activity at a heliocentric distance of 5 AU or more, much too distant to be caused by H_2O vaporization. If a comet has never before been near the Sun, then it could easily have a layer of more volatile species which would be activated at great distance. A comet with an excess ratio of volatile substances to water could not trap them all as clathrates, and would exhibit activity outside of control by water. These are the explanations usually offered for "new" comets. There are, however, "problem children," the best known being P/Schwassmann-Wachmann 1,

which is known to be in a nearly circular orbit (eccentricity 0.132) *beyond* Jupiter (perihelion 5.54 AU, aphelion 7.21 AU). This object, normally of magnitude ca 19, suddenly, in less than a day, brightens by as much as 7 magnitudes (a factor of more than 600) [391]. At least 20 outbursts were observed between 1939 and 1950, and these must be fairly common, since the comet is observed only rarely [391]. Crude spectra obtained on two occasions showed only a pure continuum of scattered sunlight; the cause of these outbursts is unknown.

The only other comet in nearly circular orbit at large distance, P/Oterma ($e=0.144$, $q=3.39$ until recent perturbations by Jupiter) has never shown such activity [391]. There have been rather extreme brightness fluctuations in a number of comets nearer the Sun. P/Tuttle-Giacobini-Kresák flared by 8–10 magnitudes in less than 5 days in May 1973 [398], just a day or two before its perihelion passage at 1.15 AU. It continued lesser outbursts for several weeks. "Pockets of gas," or sometimes solar activity are occasionally used as explanations [13]. Even rather prosaic objects such as P/d'Arrest cause occasional problems. P/d'Arrest appears to have a well-condensed photometric nucleus after perihelion, but before perihelion, it is extremely difficult to locate and is invariably faint and diffuse [492]. This behavior has no reasonable explanation in terms of the icy conglomerate model. At least three diffuse comets (P/Westphal 1913 VI, Ensor 1926 III, and Pajdusakova 1954 II) have disappeared as they approached the Sun. Perhaps they simply "ran out of gas." It will be most interesting to find if P/Westphal reappears on schedule in late 1975.

Origin and Evolution

The nature and origin of comets has a long if not too satisfactory history. The idea that comets originate in interstellar space is often called the Laplace hypothesis, since Laplace made the first mathematical study of capture probabilities. However, the idea of interstellar formation goes at least back to Kepler [391]. The idea of formation within the solar system by ejection from the major planets is usually attributed to Lagrange [391]; at times all forms of origin within the solar system are termed Lagrangian, although Vsekhsvyatskiy [493] is virtually alone in still championing the Lagrangian hypothesis in its original form. Until Whipple's icy conglomerate model, it was generally agreed that comets were a loose swarm of separate particles with slight mutual gravitation [400]. At about the same time as Whipple's theory appeared, Lyttleton [292] presented a study of origin by accretion from interstellar clouds. In the resulting comet, mutual gravitation is unimportant near the Sun, and each tiny particle pursues its own independent Keplerian orbit except for collisions.

Respected scientists, during the past 6 years, have advocated all four combinations of interstellar and solar system origin with "compact" and "loose-swarm" nucleus, plus various in-between theories. Witkowski supports a compact nucleus of interstellar origin [522]; Lyttleton, a very loose swarm of interstellar origin [292, 294]; Robey, a loose structure of plasma created from the Sun [395]; Alfvén, current creation of compact structures from loose ones by his jetstream mechanism [4, 481]. However, a large majority of comet specialists now favor compact structures created somewhere within the gravitational influence of the Sun, and further discussion is limited to such theories.

There are apparently two distinct dynamic families of comets (noted previously, under Cometary Orbits). Everhart [134, 135] has shown that there is no evolutionary path linking the two families, but suggests that both distributions (and a third group with very large perihelia, which we could never observe) could be derived from a source at near infinity (relative to solar binding energy) with all comets entering the system in near parabolic orbits [135]. Those with perihelia near Jupiter and Saturn could then be perturbed into short-period comets, while those with smaller perihelia would remain almost unperturbed and constitute the long-period family [135]. Between 3×10^4 and 10^5 comets would be required, with perihelia near Jupiter at present, in order to keep the supply of short-period comets in steady state [109].

The question then arises: What is the origin and behavior of the possible source of comets "near infinity?" Oort [348] proposed that comets

originated at the same time and in the same general region as planets, and that perturbations threw them outward into a vast cloud between 30 000 and 100 000 AU. The orbits would there be randomized by stellar perturbations so that all sense of their origin in the ecliptic plane would be lost [348]. Whipple [512], Safronov [401], Nezhinskiy [344], and others have supported this idea. One big drawback is the inefficiency of the process. Another is that the resulting distribution of comets in heliocentric distance apparently would be completely unlike that observed today [135]. Cameron [74] suggests that comets originated in independent subdisks of the solar nebula already far beyond Pluto and reached even greater aphelion distances as a result of mass loss in the solar nebula and Sun during the Sun's T Tauri stage. O'Dell [345] has considered an interesting variation in which comets form as a vast cluster (ca 10^{33}) of small bodies (radius ca 70 μm) at great distance, accumulating interstellar volatile substances on their surfaces. Approaching the Sun, they collapse into a structure not readily distinguishable from Whipple's icy conglomerate comet.

Purported observational evidence for the existence of the "Oort Cloud" [348] has been strongly challenged by Lyttleton [293]. Improved evidence of its existence [306] is based upon improved orbital elements for comets of very long period and with relatively large perihelion distance (so nongravitational forces from escaping volatile substances are insignificant), but even the improved result isn't terribly convincing, being based upon too few data points. In part, the argument is semantic. Lyttleton has clearly shown that there is no evidence for a "shell" in which the number of comets per unit volume is very high, but there does seem to be a grouping in "binding energy space" ($E \propto 1/a$, where a is the semimajor axis). Whether this is considered a mathematical artifact or physically significant depends upon the author.

The possibility of storing some comets nearer the Sun, perhaps among the giant planets, has been considered. The action on them by the giant planets is so strong that such orbits are soon transformed [135, 240]. Everhart [135] estimates that most orbits between Jupiter and Neptune would be emptied in about 10^7 years with no new supply available. The best theory at present, then, seems to be one in which the comets originated as a part of the primordial nebula, at least in the region beyond Saturn, and more probably beyond Pluto, and are kept in "cold storage" most of their lives. They are never seen at all unless their perihelion distance falls below about 6 AU, and they are seen regularly only if captured into short-period orbits by the action of the giant planets.

The average short-period comet, with a period of 10 years, may live 10^4 years or so before all its volatile substances are lost. What becomes of it then? It may totally dissipate, leaving nothing but a meteor stream. In Sekanina's [415] mantle-core model, there should be a rocky remnant, however, perhaps appearing as an Apollo asteroid [302, 303] (as discussed previously). Until there has been more study of both comets and asteroids, from the ground and from spacecraft, there can be no final answer to this question.

REFERENCES

1. ALEXANDER, A. F. O'D. *The Planet Saturn.* London, Faber and Faber, 1962.
2. ALEXANDER, A. F. O'D. *The Planet Uranus.* New York, Am. Elsevier, 1965.
3. ALFVÉN, H., and G. ARRHENIUS. Structure and evolutionary history of the solar system., I. *Astrophys. Space Sci.* 8:338–421, 1970.
4. ALFVÉN, H., and A. MENDIS. Nature and origin of comets. *Nature* 246:410–411, 1973.
5. ALLEN, D. A., and T. L. MURDOCK. Infrared photometry of Saturn, Titan, and the rings. *Icarus* 14:1–2, 1971.
6. ALTER, D. Comets and people. *Griffith Obs.* XX:74–82, 1956.
7. ANDERS, E. Interrelations of meteorites, asteroids, and comets. *In*, Gehrels, T., Ed. *Physical Studies of Minor Planets*, pp. 429–446. Washington, NASA, 1971. (NASA SP-267)
8. ANDERSON, J. D., G. W. NULL, and S. K. WONG. Gravity results from Pioneer 10 Doppler data. *J. Geophys. Res.* 79:3661–3664, 1974.
9. ANDERSON, R. C., J. G. PIPES, A. L. BROADFOOT, and L. WALLACE. Spectra of Venus and Jupiter from 1800 to 3200 Å. *J. Atmos. Sci.* 26:874–888, 1969.
10. ANDERSSON, L. Photometry of Jupiter VI and Phoebe

(Saturn IX). *Bull. Am. Astron. Soc.* 4:313, 1972.
11. ANDERSSON, L. New findings about Jupiter's and Saturn's satellites. *Sky Telesc.* 45:22–23, 1973.
12. ANDERSSON, L. E., and J. D. FIX. Pluto: new photometry and a determination of the axis of rotation. *Icarus* 20:279–283, 1974.
13. ANDRIENKO, D. A., A. A. DEMENKO, I. M. DEMENKO, and I. D. ZOSIMOVICH. Comet brightness variations and the conditions in interplanetary space. *Sov. Astron.-A. J.* 15:666–671, 1972.
14. APPLEBY, J. F. Multicolor photoelectric photometry of Neptune. *Astron. J.* 78:110–112, 1973.
15. APPLEBY, J. F., and W. M. IRVINE. Multicolor photoelectric photometry of Uranus. *Astron. J.* 76:617–619, 1971.
16. ARMSTRONG, K. R., D. A. HARPER, Jr., and F. J. LOW. Far-infrared brightness temperatures of the planets. *Astrophys. J.* 178:L89–L92, 1973.
17. ARNOLD, J. R. The origin of meteorites as small bodies. II. The model. *Astrophys. J.* 141:1536–1547, 1965.
18. ARNOLD, J. R. The origin of meteorites as small bodies. III. General considerations. *Astrophys. J.* 141:1548–1556, 1965.
19. ARNOLD, J. R. Asteroid families and "jet streams." *Astron. J.* 74:1235–1242, 1969.
20. ARPIGNY, C. The resonance-fluorescence excitation of the CO^+ comet-tail bands in comet Humason (1961e). *Ann. Astrophys.* 27:406–416, 1964.
21. ARPIGNY, C. Comet spectra. *In*, Kuiper, G. P., and E. Roemer, Eds. *Comets, Scientific Data and Missions, Proceedings of the Tucson Comet Conference*, Apr., 1970, pp. 84–111. Tucson, Univ. Ariz., 1972.
22. ASH, M. E., I. I. SHAPIRO, and W. B. SMITH. The system of planetary masses. *Science* 174:551–556, 1971.
23. AUMANN, H. H., C. M. GILLESPIE, Jr., and F. J. LOW. The internal powers and effective temperatures of Jupiter and Saturn, *Astrophys. J.* 157:L69–L72, 1969.
24. AVRAMCHUK, V. V. Spectrophotometry of the λ6190 methane and λλ6441 and 6478 ammonia absorption bands on the disk of Jupiter. *Sov. Astron.-A. J.* 14:462–468, 1970.
25. BALASUBRAHMANYAN, V. K., and D. VENKATESAN. Solar activity and the great red spot of Jupiter. *Astrophys. Lett.* 6:123–126, 1970.
26. BANOS, C. J. Contribution to the study of Jupiter's atmosphere. *Icarus* 15:58–67, 1971.
27. BANOS, C. J., and C. E. ALISSANDRAKIS. Isodensitometry of Jupiter's red spot and Jupiter. *Astron. Astrophys.* 15:424–432, 1971.
28. BARKER, E. S., and L. M. TRAFTON. Ultraviolet reflectivity and geometrical albedo of Titan. *Icarus* 20:444–454, 1973.
29. BARROW, C. H., and D. P. MORROW. The polarization of the Jupiter radiation at 18 Mc/S. *Astrophys. J.* 152: 593–608, 1968.
30. BARTHOLDI, P., and F. OWEN. The occultation of Beta Scorpii by Jupiter and Io. II. Io. *Astron. J.* 77:60–65, 1972.
31. BASH, F. N., F. D. DRAKE, E. GUNDERMANN, and C. E. HEILES. 10-cm observations of Jupiter, 1961–1963. *Astrophys. J.* 139:975–985, 1964.
32. BAUM, W. A., and A. D. CODE. A photometric observation of the occultation of σ Arietis by Jupiter. *Astron. J.* 58:108–112, 1953.
33. BAXTER, D. C., and W. B. THOMPSON. Jetstream formation through inelastic collisions. *In*, Gehrels, T., Ed. *Physical Studies of Minor Planets*, pp. 319–326. Washington, D.C., NASA, 1971. (NASA SP-267)
34. BEER, R., and F. W. TAYLOR. The abundance of CH_3D and the D/H ratio in Jupiter. *Astrophys. J.* 179:309–327, 1973.
35. BEER, R., C. B. FARMER, R. H. NORTON, J. V. MARTONCHIK, and T. G. BARNES. Jupiter: observation of deuterated methane in the atmosphere. *Science* 175:1360–1361, 1972.
36. BELTON, M. J. S., and H. SPINRAD. H_2 pressure-induced lines in the spectra of the major planets. *Astrophys. J.* 185:363–372, 1973.
37. BENVENUTI, P. Dust emission structure in comets with type II tails. *Astrophys. Space Sci.* 27:203–209, 1974.
38. BERGE, G. L. Circular polarization of Jupiter's decimeter radiation. *Astrophys. J.* 142:1688–1693, 1965.
39. BERGE, G. L. An interferometric study of Jupiter's decimeter radio emission. *Astrophys. J.* 146:767–798, 1966.
40. BERGE, G. L. Some recent observations and interpretations of the Jupiter decimeter emission. *In*, *Proceedings of the Jupiter Radiation Belt Workshop*, pp. 223–242. Pasadena, Calif., Jet Propul. Lab., 1972.
41. BERGE, G. L., and D. O. MUHLEMAN. High-angular-resolution observations of Saturn at 21.1 cm wavelength. *Astrophys. J.* 185:373–381, 1973.
42. BERGE, G. L., and D. O. MUHLEMAN. The brightness temperature of Callisto at 3.71 cm wavelength. Presented at 5th Annu. Meet., Am. Astron. Soc., Planet. Sci. Div., Palo Alto, April 1974. *Am. Astron. Soc. Bull.* 6(3, pt. 2), 1974. (Abstr. No. 106)
43. BERGE, G. L., and R. B. READ. The microwave emission of Saturn. *Astrophys. J.* 152:755–764, 1968.
44. BERGSTRALH, J. T. Methane absorption in the atmosphere of Saturn: rotational temperature and abundance from the $3\nu_3$ band. *Icarus* 18:605–611, 1973.
45. BERGSTRALH, J. T. Methane absorption in the Jovian atmosphere. I. The Lorentz half-width in the $3\nu_3$ band at 1.1 μm. *Icarus* 19:499–506, 1973.
46. BERGSTRALH, J. T., and J. S. MARGOLIS. Recomputation of the absorption strengths of the methane $3\nu_3$ J-manifolds at 9050 cm^{-1}. *J. Quant. Spectrosc. Radiat. Transfer* 11:1285–1287, 1971.
47. BERGSTRALH, J. T., and J. W. YOUNG. Spectroscopic evidence of variability in Saturn's atmosphere. *Am. Astron. Soc. Bull.* 6(3, pt. 2), 1974. Abstr. No. 88)
48. BERTAUX, J. L., J. E. BLAMONT, and M. FESTOU. Interpretation of hydrogen Lyman-alpha observations of comets Bennett and Encke. *Astron. Astrophys.* 25:415–430, 1973.
49. BIERMANN, L. Comet tails and solar corpuscular radiation. *Z. Astrophys.* 29:274–286, 1951. (Ger.)

50. BIERMANN, L., B. BROSOWSKI, and H. U. SCHMIDT. The interaction of the solar wind with a comet. *Solar Phys.* 1:254–284, 1967.
51. BIERMANN, L., and E. TREFFTZ. On the mechanisms of ionization and excitation in cometary atmospheres. *Z. Astrophys.* 59:1–28, 1964.
52. BIGG, E. K. Influence of the satellite Io on Jupiter's decametric emission. *Nature* 203:1008–1010, 1964.
53. BINDER, A. B. Spectrophotometry of the 1.5 μm window of Jupiter. *Astron. J.* 77:93–99, 1972.
54. BINDER, A. B., and D. P. CRUIKSHANK. Evidence of an atmosphere on Io. *Icarus* 3:299–305, 1964.
55. BINDER, A. B., and D. W. MCCARTHY, Jr. The infrared spectral albedo of Uranus. *Astrophys. J.* 171:L1–L3, 1972.
56. BINDER, A. B., and D. W. MCCARTHY, Jr. IR spectrophotometry of Jupiter and Saturn. *Astron. J.* 78:939–950, 1973.
57. BISHOP, E. V., and W. C. DE MARCUS. Thermal histories of Jupiter models. *Icarus* 12:317–330, 1970.
58. BLANCO, C., and S. CATALANO. Photoelectric observations of Saturn satellites Rhea and Titan. *Astron. Astrophys.* 14:43–47, 1971.
59. BOBROV, M. S. On the observation of the occultation of stars by Saturn's rings. *Sov. Astron.-A.J.* 6:525–531, 1963.
60. BOBROV, M. S. Physical properties of Saturn's rings. *In*, Dollfus, A., Ed. *Surface and Interiors of Planets and Satellites*, pp. 377–461. New York, Academic, 1970.
61. BOBROV, M. S. Thickness of Saturn's rings from observations in 1966. *Sov. Astron.-A.J.* 16:348–354, 1972.
62. BOBROVNIKOFF, N. T. Comets. *In*, Hynek, J. A., Ed. *Astrophysics: A Topical Symposium*, pp. 302–356. New York, McGraw-Hill, 1951.
63. BRANSON, N. J. B. A. High resolution radio observations of the planet Jupiter. *Mon. Not. Roy. Astron. Soc.* 139(2):155–162, 1968.
64. BRICE, N. M., and G. A. IOANNIDIS. The magnetosphere of Jupiter and Earth. *Icarus* 13:173–183, 1970.
65. BRIGGS, F. H. Radio emission from Ceres. *Astrophys. J.* 184:637–639, 1973.
66. BRIGGS, F. H. The microwave properties of Saturn's rings. *Astrophys. J.* 189:367–377, 1974.
67. BRINKMANN, R. T. Jovian satellite-satellite eclipses and occultations. *Icarus* 19:15–29, 1973.
68. BROUWER, D., and G. M. CLEMENCE. *Methods of Celestial Mechanics*. New York, Academic, 1961.
69. BROWN, R. A. Optical line emission from Io. *In, Exploration of the Solar System, 65th Symposium, International Astronomical Union*, Torun, Pol., Sept. 1972.
70. BROWN, R. A., and F. H. CHAFFEE, Jr. High-resolution spectra of sodium emission from Io. *Astrophys. J.* 187:L125–L126, 1974.
71. BURNS, J. A. Jupiter's decametric radio emission and the radiation belts of its Galilean satellites. *Science* 159:971–972, 1967.
72. CALDWELL, J., D. R. LARACH, and R. E. DANIELSON. The continuum albedo of Titan. *Bull. Am. Astron. Soc.* 5:305, 1973.
73. CAMERON, A. G. W. Abundances of the elements in the solar system. *Space Sci. Rev.* 15:121–146, 1973.
74. CAMERON, A. G. W. Accumulation processes in the primitive solar nebula. *Icarus* 18:407–450, 1973.
75. CAMERON, A. G. W. Formation of the outer planets. *Space Sci. Rev.* 14:383–391, 1973.
76. CAPONE, L. A., and S. S. PRASAD. Jovian ionospheric models. *Icarus* 20:200–212, 1973.
77. CARLSON, R. W., J. C. BHATTACHARYYA, B. A. SMITH, T. V. JOHNSON, B. HIDAYAT, S. A. SMITH, G. E. TAYLOR, B. O'LEARY, and R. T. BRINKMANN. An atmosphere on Ganymede from its occultation of SAO 186800 on 7 June 1972. *Science* 182:53–55, 1973.
78. CARR, T. D. Jupiter's magnetospheric rotation period. *Astrophys. Lett.* 7:157–162, 1971.
79. CARR, T. D., and S. GULKIS. The magnetosphere of Jupiter. *In*, Goldberg, L., D. Layzer, and J. G. Phillips, Eds. *Annual Review of Astronomy and Astrophysics*, Vol. 7, pp. 577–618, 1969.
80. CARR, T. D., A. G. SMITH, F. F. DONIVAN, and H. I. REGISTER. The twelve-year periodicities of the decametric radiation of Jupiter. *Radio Sci.* 5(2): 495–503, 1970.
81. CHADHA, M. S., J. J. FLORES, J. G. LAWLESS, and C. PONNAMPERUMA. II. Organic synthesis in a simulated Jovian atmosphere. *Icarus* 15:39–44, 1971.
82. CHANG, D. B., and L. DAVIS, Jr. Synchrotron radiation as the source of Jupiter's polarized decimeter radiation. *Astrophys. J.* 136:567–581, 1962.
83. CHAPMAN, C. R. Jupiter's zonal winds—variation with latitude. *J. Atmos. Sci.* 26:986–990, 1969.
84. CHAPMAN, C. R., and D. MORRISON. The minor planets: sizes and mineralogy. *Sky Telesc.* 47:92–95, 1974.
85. CHAPMAN, C. R., and J. W. SALISBURY. Comparisons of meteorite and asteroid spectral reflectivities. *Icarus* 19:507–522, 1973.
86. CHAPMAN, C. R., T. B. MCCORD, and C. PIETERS. Minor planets and related objects. X. Spectrophotometric study of the composition of (1685) Toro. *Astron. J.* 78:502–505, 1973.
87. CHAPMAN, C. R., T. B. MCCORD, and T. V. JOHNSON. Asteroid spectral reflectivities. *Astron. J.* 78:126–140, 1973.
88. CHASE, S. C., R. D. RUIZ, G. MÜNCH, G. NEUGEBAUER, M. SCHROEDER, and L. M. TRAFTON. Pioneer 10 infrared radiometer experiment: preliminary results. *Science* 183:315–317, 1974.
89. CODE, A. D., T. E. HOUCK, and C. F. LILLIE. Comet Tago-Sato-Kosaka (1969g). *IAU Circ.* (Cambridge, Mass.), No. 2201, Jan. 21, 1970.
90. COHEN, C. J., and E. C. HUBBARD. Libration of the close approaches of Pluto to Neptune. *Astron. J.* 70:10–13, 1965.
91. CONSEIL, L., Y. LEBLANC, G. ANTONINI, and D.

QUEMADA. The effect of the solar wind velocity on the Jovian decametric emission. *Astrophys. Lett.* 8:133–137, 1971.

92. COOK, A. F., and F. A. FRANKLIN. Rediscussion of Maxwell's Adams Prize Essay on the stability of Saturn's rings. *Astron. J.* 69:173–200, 1964.
93. COOK, A. F., and F. A. FRANKLIN. Rediscussion of Maxwell's Adams Prize Essay on the stability of Saturn's rings, II. *Astron. J.* 71:10–19, 1966.
94. COOK, A. F., and F. A. FRANKLIN. An explanation of the light curve of Iapetus. *Icarus* 13:282–291, 1970.
95. COOK, A. F., F. A. FRANKLIN, and F. D. PALLUCONI. Saturn's rings—a survey. *Icarus* 18:317–337, 1973.
96. COUPINOT, G. The rings of Saturn in 1969. Morphological and photometric studies. II. Deconvolution of the raw photometric curves. *Icarus* 19:212–223, 1973.
97. CRUIKSHANK, D. P. A search for ammonia in the atmosphere of Saturn. *Bull. Am. Astron. Soc.* 3:282, 1971.
98. CRUIKSHANK, D. P., and A. B. BINDER. Minor constituents in the atmosphere of Jupiter. *Astrophys. Space Sci.* 3:347–356, 1969.
99. DANIELSON, R. E. The infrared spectrum of Jupiter. *Astrophys. J.* 143:949–960, 1966.
100. DANIELSON, R. E. The structure of the Uranus atmosphere. Presented at 5th Annu. Meet., Planet. Sci. Div., Am. Astron. Soc., Palo Alto, Calif., Apr. 1974. *Am. Astron. Soc. Bull.* 6(3, Pt. 2):380, 1974. (Abstr. No. 076)
101. DANIELSON, R. E., J. J. CALDWELL, and D. R. LARACH. An inversion in the atmosphere of Titan. *Icarus* 20:437–443, 1973.
102. DANIELSON, R. E., M. G. TOMASKO, and B. D. SAVAGE. High-resolution imagery of Uranus obtained by stratoscope, II. *Astrophys. J.* 178:887–900, 1972.
103. DANIELSSON, L. The profile of a jetstream. *In*, Gehrels, T., Ed. *Physical Studies of Minor planets*, pp. 353–362. Washington, D.C., NASA, 1971. (NASA SP–267)
104. DANKS, T., and C. ARPIGNY. Relative band intensities in the red and violet systems of CN in comets. *Astron. Astrophys.* 29:347–356, 1973.
105. DAVIES, R. D., and D. WILLIAMS. Observations of the continuum emission from Venus, Mars, Jupiter, and Saturn at 21.2 cm wavelength. *Planet. Space Sci.* 14:15–32, 1966.
106. DEBERGH, C., M. VION, M. COMBES, J. LECACHEUX, and J. P. MAILLARD. New infrared spectra of the Jovian planets from 12 000 to 4000 cm^{-1} by Fourier transform spectroscopy. II. Study of Saturn in the 3 ν_3 CH_4 band. *Astron. Astrophys.* 28:457–466, 1973.
107. DELSEMME, A. H. Review of cometary science. *In*, Roberts, D. L., Ed. *The Proceedings of the Cometary Science Working Group*. Chicago, Ill. Inst. Tech. Res., 1971.
108. DELSEMME, A. H. Gas and dust in comets. *Space Sci. Rev.* 15:89–101, 1973.
109. DELSEMME, A. H. Origin of the short-period comets. *Astron. Astrophys.* 29:377–381, 1973.
110. DELSEMME, A. H., and D. C. MILLER. Physico-chemical phenomena in comets. II. Gas adsorptions in the snows of the nucleus. *Planet. Space Sci.* 18:717–730, 1970.
111. DELSEMME, A. H., and D. C. MILLER. Physico-chemical phenomena in comets. III. The continuum of comet Burnham (1960 II). *Planet. Space Sci.* 19:1229–1257, 1971.
112. DELSEMME, A. H., and D. C. MILLER. Physico-chemical phenomena in comets. IV. The C_2 emission of comet Burnham (1960 II). *Planet. Space Sci.* 19:1259–1274, 1971.
113. DELSEMME, A. H., and D. A. RUD. Albedos and cross-sections for the nuclei of comets 1969 IX, 1970 II and 1971 I. *Astron. Astrophys.* 28:1–6, 1973.
114. DESCH, M. D., and T. D. CARR. Decametric and hectometric observations of Jupiter from the RAE–1 satellite. Presented at 5th Annu. Meet., Am. Astron. Soc., Planet. Sci. Div., Palo Alto, Calif., April 1974. *Am. Astron. Soc. Bull.* 6(3, Pt. 2):378, 1974. (Abstr. No. 068)
115. DICKEL, J. R., J. J. DEGIOANNI, AND G. C. GOODMAN. The microwave spectrum of Jupiter. *Radio Sci.* 5:517–527, 1970.
116. DOLLFUS, A. Visual and photographic studies of planets at the Pic du Midi. *In*, Kuiper, G. P., and B. M. Middlehurst, Eds. *Planets and Satellites, The Solar System*, Vol. 3, pp. 534–571. Chicago, Univ. Chicago Press, 1961.
117. DOLLFUS, A. Movements in the atmosphere of Saturn in 1960. Coordinated observations by the International Astronomical Union. *Icarus* 2:109–114, 1963. (Fr.)
118. DOLLFUS, A. Saturn X (Janus). *IAU Circ.* (Cambridge, Mass.), No. 1995, Feb. 1, 1967.
119. DOLLFUS, A. Diameters of the planets and satellites. *In*, Dollfus, A., Ed. *Surfaces and Interiors of Planets and Satellites*, pp. 45–139. New York, Academic, 1970. (Fr.)
120. DOLLFUS, A. New optical measurements of the diameters of Jupiter, Saturn, Uranus, and Neptune. *Icarus* 12:101–117, 1970.
121. DOLLFUS, A. Diameter measurements of asteroids. *In*, Gehrels, T., Ed. *Physical Studies of Minor Planets*, pp. 25–31. Washington, D.C., NASA, 1971. (NASA SP–267)
122. DOLLFUS, A. Physical studies of asteroids by polarization of the light. *In*, Gehrels, T., Ed. *Physical Studies of Minor Planets*, pp. 95–116. Washington, D.C., NASA, 1971. (NASA SP–267)
123. DONN, B. The characteristics of distant comets. *Ann. Astrophys.* 25:319–323, 1962.
124. DOUGLAS, J. N., and H. C. SMITH. Interplanetary scintillation in Jovian decametric radiation. *Astrophys. J.* 148:885–903, 1967.
125. DRAKE, F. D., and H. HVATUM. Nonthermal microwave radiation from Jupiter. *Astron. J.* 64:329–330, 1959.
126. DULK, G. A. Characteristics of Jupiter's decametric radio source measured with arc-second resolution. *Astrophys. J.* 159:671–684, 1970.

127. DULK, G. A., and T. A. CLARK. Almost-continuous radio emission from Jupiter at 8.9 and 10 MHz. *Astrophys. J.* 145:945–948, 1966.

128. DUNCOMBE, R. L., W. J. KLEPCZYNSKI, and P. K. SEIDELMANN. The masses of the planets, satellites, and asteroids. *Fundam. Cosm. Phys.* 1:119–165, 1974.

129. DUNHAM, D. Motions of the satellites of Uranus. *Bull. Am. Astron. Soc.* 3:415, 1971.

130. DUNHAM, T., Jr. Spectroscopic observations of the planets at Mount Wilson. *In,* Kuiper, G. P., Ed. *The Atmospheres of the Earth and Planets,* rev. ed., pp. 288–305. Chicago, Univ. Chicago Press, 1952.

131. DUNLAP, J. L. Laboratory work on the shapes of asteroids. *In,* Gehrels, T., Ed. *Physical Studies of Minor Planets,* pp. 147–154. Washington, D.C., NASA, 1971. (NASA SP–267).

132. ELLIS, G. R. A. The decametric radio emissions of Jupiter. *Radio Sci.* 69D:1513–1530, 1965.

133. ENCRENAZ, T., and T. OWEN. New observations of the hydrogen quadrupole lines on Saturn and Uranus. *Astron. Astrophys.* 28:119–124, 1973.

134. EVERHART, E. The origin of short-period comets. *Astrophys. Lett.* 10:131–135, 1972.

135. EVERHART, E. Examination of several ideas of comet origins. *Astron. J.* 78:329–337, 1973.

136. FEIBELMAN, W. A. Concerning the 'D' ring of Saturn. *Nature* 214:793–794, 1967.

137. FIELD, G. B. The source of radiation from Jupiter at decimeter wavelengths. *J. Geophys. Res.* 64:1169–1177, 1959.

138. FIELD, G. B. The source of radiation from Jupiter at decimeter wavelengths 2. Cyclotron radiation by trapped electrons. *J. Geophys. Res.* 65:1661–1671, 1960.

139. FIELD, G. B. The source of radiation from Jupiter at decimeter wavelengths. 3. Time dependence of cyclotron radiation. *J. Geophys. Res.* 66:1395–1405, 1961.

140. FIELD, G. B. REMARKS ON JUPITER. *In,* Brown, H., G. J. Stanley, D. O. Muhleman, and G. Münch, Eds. *Proceedings, CalTech-JPL Lunar and Planetary Conference,* Sept. 1965, pp. 141–142. Pasadena, Calif. Inst. Tech., Jet Propul. Lab., 1966. (NASA CR–76142; JPL–TM–33–266)

141. FINK, U., H. P. LARSON, and N. H. DEKKERS. Infrared spectra of the Galilean satellites of Jupiter. *Astrophys. J.* 179:L155–L159, 1973.

142. FIX, J. D., J. S. NEFF, and L. A. KELSEY. Spectrophotometry of Pluto. *Astron. J.* 75:895–896, 1970.

143. FLASAR, F. M. Gravitational energy sources in Jupiter. *Astrophys. J.* 186:1097–1106, 1973.

144. FOCAS, J. H. Activity in Jupiter's atmospheric belts between 1904 and 1963. *Icarus* 15:56–57, 1971.

145. FOCAS, J. H., and A. DOLLFUS. Optical properties and thickness of the rings of Saturn observed on edge in 1966. *Astron. Astrophys.* 2:251–265, 1969. (Fr.)

146. FOUNTAIN, J. W., D. L. COFFEEN, L. R. DOOSE, T. GEHRELS, W. SWINDELL, and M. G. TOMASKO. Jupiter's clouds: equatorial plumes and other cloud forms in the Pioneer 10 images. *Science* 184:1279–1281, 1974.

147. FOX, K., and I. OZIER. The importance of methane to pressure-induced absorption in the atmospheres of the outer planets. *Astrophys. J.* 166:L95–L100, 1971.

148. FOX, K., T. OWEN, A. W. MANTZ, and K. N. RAO. A tentative identification of $^{13}CH_4$ and an estimate of $^{12}C/^{13}C$ in the atmosphere of Jupiter. *Astrophys. J.* 176:L81–L84, 1972.

149. FRANKLIN, F. A., G. COLOMBO, and A. F. COOK. A dynamical model for the radial structure of Saturn's rings, II. *Icarus* 15:80–92, 1971.

150. FRANZ, O. G., and R. L. MILLIS. UBV photometry of Enceladus, Tethys, and Dione. *Bull. Am. Astron. Soc.* 5:304, 1973.

151. FRANZ, O. G., and R. L. MILLIS. A search for post-eclipse brightening of Io with an area-scanning photometer. Presented at 5th Annu. Meet., Am. Astron. Soc., Planet. Sci. Div., Palo Alto, Calif., April 1974. *Am. Astron. Bull.* 6(3, Pt. 2):383, 1974. (Abstr. No. 096)

152. FREEMAN, K. C., and G. LYNGA. Data for Neptune from occultation observations. *Astrophys. J.* 160:767–780, 1970.

153. GALKIN, L. S., L. A. BUGAENKO, O. I. BUGAENKO, and A. V. MOROZHENKO. The spectrum of Uranus in the region 4800–7500 Å. *In,* Sagan, C., T. C. Owen, and H. J. Smith, Eds. *Planetary Atmospheres,* pp. 392–393. Dordrecht, Holland, D. Reidel, 1971. (IAU Symp. No. 40)

154. GEHRELS, T. The transparency of the Jovian polar zones. *Icarus* 10:410–411, 1969.

155. GEHRELS, T. Physical parameters of asteroids and interrelations with comets. *In,* Elvius, A., Ed. *From Plasma to Planet,* pp. 169–178. Stockholm, Almqvist & Wiksell; New York, Wiley, 1972. (Nobel Symp. Ser. No. 21)

156. GEHRELS, T., B. M. HERMAN, and T. OWEN. Wavelength dependence of polarization. XIV. Atmosphere of Jupiter. *Astron. J.* 74:190–199, 1969.

157. GEHRELS, T., J. R. GILL, and J. W. HAUGHEY. Introduction. *In,* Gehrels, T., Ed. *Physical Studies of Minor Planets,* pp. xiii–xxvii. Washington, D.C., NASA, 1971. (NASA SP–267)

158. GERARD, E. Long-term variations of the decimeter radiation of Jupiter. *Radio Sci.* 5:513–516, 1970.

159. GIERASCH, P. J. Jupiter's cloud bands. *Icarus* 19:482–494, 1973.

160. GILLE, J. C., and T. LEE. The spectrum and transmission of ammonia under Jovian conditions. *J. Atmos. Sci.* 26:932–940, 1969.

161. GILLETT, F. C., and W. J. FORREST. The 7.5- to 13.5-micron spectrum of Saturn. *Astrophys. J.* 187:L37–L39, 1974.

162. GILLETT, F. C., W. J. FORREST, and K. M. MERRILL. 8–13 micron observations of Titan. *Astrophys. J.* 184:L93–L95, 1973.

163. GILLETT, F. C., F. J. LOW, and W. A. STEIN. The 2.8-

14-micron spectrum of Jupiter. *Astrophys. J.* 157:925–934, 1969.

164. GILLETT, F. C., K. M. MERRILL, and W. A. STEIN. Albedo and thermal emission of Jovian satellites I–IV. *Astrophys. Lett.* 6:247–249, 1970.
165. GILLETT, F. C., and J. A. WESTPHAL. Observations of 7.9 micron limb brightening on Jupiter. *Astrophys. J.* 179:L153–L154, 1973.
166. GIVER, L. P., and H. SPINRAD. Molecular hydrogen features in the spectra of Saturn and Uranus. *Icarus* 5:586–589, 1966.
167. GLEDHILL, J. A. Magnetosphere of Jupiter. *Nature* 214:155–156, 1967.
168. GOLDREICH, P. An explanation of the frequent occurrence of commensurable mean motions of the solar system. *Mon. Not. Roy. Astron. Soc.* 130:159–181, 1965.
169. GOLDSTEIN, R. M., and G. A. MORRIS. Radar observations of the rings of Saturn. *Icarus* 20:260–262, 1973.
170. GOLITSYN, G. S. A similarity approach to the general circulation of planetary atmospheres. *Icarus* 13:1–24, 1970.
171. GORGOLEWSKI, S. Possible detection of thermal radio emission at 3.5 mm from Callisto. *Astrophys. Lett.* 7:37, 1970.
172. GRABOSKE, H. C., Jr., J. B. POLLACK, A. S. GROSSMAN, and R. J. OLNESS. *The Structure and Evolution of Jupiter: The Fluid Contraction Stage.* Livermore, Calif., Lawrence Livermore Lab., 1973. (Prepr. UCRL–74860)
173. GRABOSKE, H. C., Jr., R. J. OLNESS, and A. S. GROSSMAN. *Thermodynamics of Dense Hydrogen-Helium Fluids.* Livermore, Calif., Lawrence Livermore Lab., 1973. (Prepr. UCRL–74859)
174. GREENSTEIN, J. The spectrum of comet Humason (1961e). *Astrophys. J.* 136:688–690, 1962.
175. GROSSMAN, A. S., and H. C. GRABOSKE, Jr. Evolution of low-mass stars. III. Effects of nonideal thermodynamic properties during the pre-main-sequence contraction. *Astrophys. J.* 164:475–490, 1971.
176. GUERIN, P. The new ring of Saturn. *Sky Telesc.* 40:88, 1970.
177. GUERIN, P. The rings of Saturn in 1969. Morphological and photometric study. I. Photograph acquisition and evaluation. *Icarus* 19:202–211, 1973.
178. GULKIS, S. Lunar occultation observations of Jupiter at 74 cm and 128 cm. *Radio Sci.* 5:505–511, 1970.
179. GULKIS, S. *Radio Emission from the Major Planets—The Thermal Component.* Presented at 17th Annu. Meet., Am. Astronaut. Soc., Seattle, Wash., June 1971. (AAS 71–109)
180. GULKIS, S., and T. D. CARR. Radio rotation period of Jupiter. *Science* 154:257–259, 1966.
181. GULKIS, S., B. GARY, M. KLEIN, and C. STELZRIED. Observations of Jupiter at 13-cm wavelength during 1969 and 1971. *Icarus* 18:181–191, 1973.
182. GULKIS, S., T. R. MCDONOUGH, and H. CRAFT. The microwave spectrum of Saturn. *Icarus* 10:421–427, 1969.
183. GULKIS, S., M. J. KLEIN, and R. L. POYNTER. Jupiter's microwave spectrum—implications for the upper atmosphere. *In, Exploration of the Solar System,* Torun, Pol., 1973, pp. 273–280. (In press)
184. GULKIS, S., and R. POYNTER. Thermal radio emission from Jupiter and Saturn. *Phys. Earth Planet. Inter.* 6:36–43, 1972.
185. GURNETT, D. A. Sheath effects and related charged-particle acceleration by Jupiter's satellite Io. *Astrophys. J.* 175:525–533, 1972.
186. HALL, C. F. Pioneer 10. *Science* 183:301–302, 1974.
187. HALL, J. S., and L. A. RILEY. Polarization measurements of Jupiter and Saturn. *J. Atmos. Sci.* 26:920–923, 1969.
188. HALLIDAY, I. Comments on the mean density of Pluto. *Pub. Astron. Soc. Pac.* 81:285–287, 1969.
189. HALLIDAY, I., R. H. HARDIE, O. G. FRANZ, and J. B. PRISER. An upper limit for the diameter of Pluto. *Pub. Astron. Soc. Pac.* 78:113–124, 1966.
190. HAINES, E. L., Ed. Selenodesy and lunar dynamics. *In, Lunar Scientific Model,* Vol. 1.Pasadena, Calif., Jet Propul. Lab., 1971. (JPL Intern. Work. Doc. 900–278)
191. HANSEN, O. L. Ten micron observations of Io, Europa, and Ganymede. *Icarus* 18:237–246, 1973.
192. HANSEN, O. L. 12-micron emission features of the Galilean satellites and Ceres. *Astrophys. J.* 188:L31–L33, 1974.
193. HARPER, D. A., Jr., F. J. LOW, G. H. RIEKE, and K. R. ARMSTRONG. Observations of planets, nebulae, and galaxies at 350 microns. *Astrophys. J.* 177:L21–L25, 1972.
194. HARRIS, D. L. Photometry and colorimetry of planets and satellites. *In,* Kuiper, G. P., and B. M. Middlehurst, Eds. *Planets and Satellites, The Solar System,* Vol. III, pp. 272–342. Chicago, Univ. Chic., 1961.
195. HARRISON, H., and R. I. SCHOEN. Evaporation of ice in space: Saturn's rings. *Science* 157:1175–1176, 1967.
196. HART, M. H. A possible atmosphere for Pluto. *Icarus* 21:242–247, 1974.
197. HARTMANN, W. K., and A. C. HARTMANN. Asteroid collisions and evolution of asteroidal mass distribution and meteoritic flux. *Icarus* 8:361–381, 1968.
198. HERGET, P. The work at the minor planet center. *In,* Gehrels, T., Ed. *Physical Studies of Minor Planets,* pp. 9–12. Washington, D.C., NASA, 1971. (NASA SP–267)
199. HERTZ, H. G. The mass of Vesta. *Science* 160:299–300, 1968.
200. HERZBERG, G. Laboratory absorption spectra obtained with long paths. *In,* Kuiper, G. P., Ed. *The Atmospheres of the Earth and Planets,* rev. ed., pp. 406–416. Chicago, Univ. Chic., 1952.
201. HESS, S. L. Variations in atmospheric absorption over the disks of Jupiter and Saturn. *Astrophys. J.* 118:151–160, 1953.
202. HIDE, R. Origin of Jupiter's great red spot. *Nature* 190:895–896, 1961.
203. HIDE, R. On the hydrodynamics of Jupiter's atmosphere.

Mem. Soc. Roy. Sci. Liège, Ser. 5, 7:481–505, 1963.

204. HIDE, R. Dynamics of the atmospheres of the major planets with an appendix on the viscous boundary layer at the rigid bounding surface of an electrically-conducting rotating fluid in the presence of a magnetic field. *J. Atmos. Sci.* 26:841–853, 1969.
205. HIDE, R. Motions in planetary atmospheres: a review. *Meteorol. Mag.* 100:268–276, 1971.
206. HIDE, R. On geostrophic motion of a non-homogeneous fluid. *J. Fluid Mech.* 49:745–751, 1971.
207. HIDE, R. Jupiter and Saturn. *Proc. Roy. Soc. London A* 336:63–84, 1974.
208. HIDE, R., and A. IBBETSON. An experimental study of "Taylor columns." *Icarus* 5:279–290, 1966.
209. HO PENG YOKE. Ancient and mediaeval observations of comets and novae in Chinese sources. *In*, Beer, A., Ed. *Vistas in Astronomy*, Vol. 5, pp. 127–225. Oxford, Pergamon, 1962.
210. HOPKINS, N. B., and W. M. IRVINE. Variations in the color of Jupiter. *In*, Sagan, C., T. C. Owen, and H. J. Smith, Eds. *Planetary Atmospheres, 40th Symposium, International Astronomical Union*, pp. 349–352. Dordrecht, Holland, D. Reidel, 1971.
211. HOUTEN, C. J. VAN. Descriptive survey of families, Trojans, and jetstreams. *In*, Gehrels, T., Ed. *Physical Studies of Minor Planets*, pp. 173–175. Washington, D.C., NASA, 1971. (NASA SP–267)
212. HOUTEN, C. J. VAN, I. VAN HOUTEN-GROENEVELD, P. HERGET, and T. GEHRELS. The Palomar-Leiden survey of faint minor planets. *Astron. Astrophys. Suppl.* 2:339–448, 1970.
213. HOUTEN, C. J. VAN, I. VAN HOUTEN-GROENEVELD, and T. GEHRELS. Minor planets and related objects. V. The density of Trojans near the preceding Langrangian point. *Astron. J.* 75:659–662, 1970.
214. HUBBARD, W. B. Thermal models of Jupiter and Saturn. *Astrophys. J.* 155:333–344, 1969.
215. HUBBARD, W. B. Structure of Jupiter: chemical composition, contraction, and rotation. *Astrophys. J.* 162:687–697, 1970.
216. HUBBARD, W. B. Observational constraint on the structure of hydrogen planets. *Astrophys. J.* 182:L35–L38, 1973.
217. HUBBARD, W. B. The significance of atmospheric measurements for interior models of the major planets. *Space Sci. Rev.* 14:424–432, 1973.
218. HUBBARD, W. B., and R. SMOLUCHOWSKI. Structure of Jupiter and Saturn. *Space Sci. Rev.* 14:599–662, 1973.
219. HUBBARD, W. B., and T. C. VAN FLANDERN. The occultation of beta Scorpii by Jupiter and Io. III. Astrometry. *Astron. J.* 77:65–74, 1972.
220. HUNT, G. E. Interpretation of hydrogen quadrupole and methane observations of Jupiter and the radiative properties of the visible clouds. *Mon. Not. Roy. Astron. Soc.* 161:347–363, 1973.
221. HUNT, G. E., and J. S. MARGOLIS. Formation of spectral lines in planetary atmospheres. V. Collision narrowed profiles of quadrupole lines in hydrogen atmospheres. *J. Quant. Spectrosc. Radiat. Transfer* 13:417–426, 1973.
222. HUNTEN, D. M. The escape of H_2 from Titan. *J. Atmos. Sci.* 30:726–732, 1973.
223. HUNTEN, D. M., and G. MÜNCH. The helium abundance on Jupiter. *Space Sci. Rev.* 14:433–443, 1973.
224. INGE, J. L. Short-term Jovian rotation profiles, 1970–1972. *Icarus* 20:1–6, 1973.
225. [International Astronomical Union] *IAU Inf. Bull.* (Cambridge, Mass.), No. 8, Mar. 1962.
226. IONNIDIS, G. A., and N. M. BRICE. Plasma densities in the Jovian magnetosphere: plasma slingshot or Maxwell demon? *Icarus* 14:360–373, 1971.
227. IP, W.-H., and R. MEHRA. Resonances and librations of some Apollo and Amor asteroids with the Earth. *Astron. J.* 78:142–147, 1973.
228. IRVINE, W. M., and A. P. LANE. Monochromatic albedos for the disk of Saturn. *Icarus* 15:18–26, 1971.
229. IRVINE, W. M., and A. P. LANE. Photometric properties of Saturn's rings. *Icarus* 18:171–176, 1973.
230. IRVINE, W. M., T. SIMON, D. H. MENZEL, J. CHARON, G. LECOMTE, P. GRIBOVAL, and A. T. YOUNG. Multicolor photometry of the brighter planets. II. Observations from Le Houga Observatory. *Astron. J.* 73:251–264, 1968.
231. IRVINE, W. M., T. SIMON, D. H. MENZEL, C. PIKOOS, and A. T. YOUNG. Multicolor photoelectric photometry of the brighter planets. III. Observations from Boyden Observatory. *Astron. J.* 73:807–828, 1968.
232. JACKSON, W. M., T. CLARK, and B. DONN. Comet Bradfield (1974b). *IAU Circ.* (Cambridge, Mass.), No. 2674, May 24, 1974.
233. JAMES T. C. Calculations of collision narrowing of the quadrupole lines in molecular hydrogen. *J. Opt. Soc. Am.* 59:1602–1606, 1969.
234. JANSSEN, M. A. Short wavelength radio observations of Saturn's rings, pp. 83–96. *In, The Rings of Saturn.* Proceedings of the Saturn's Rings Workshop, Pasadena, Calif., 1974. (NASA SP–343)
235. JENKINS, E. B. Far-ultraviolet spectroscopy of Jupiter. *Icarus* 10:379–385, 1969.
236. JOHNSON, H. L. The infrared spectra of Jupiter and Saturn at 1.2–4.2 microns. *Astrophys. J.* 159:L1–L5, 1970.
237. JOHNSON, T. V. Galilean satellites: narrowband photometry 0.30–1.10 microns. *Icarus* 14:94–111, 1971.
238. JOHNSON, T. V., and D. L. MATSON. Spectrophotometry of (43) Ariadne: a possible chondritic composition. *Bull. Am. Astron. Soc.* 5:308, 1973.
239. JUDGE, D. L., and R. W. CARLSON. Pioneer 10 observations of the ultraviolet glow in the vicinity of Jupiter. *Science* 183:317–318, 1974.
240. KAZIMIRCHAK-POLONSKAYA, E. I. The major planets as powerful transformers of cometary orbits. *In*, Chebotarev, G. A., E. I. Kazimirchak-Polonskaya, and B. G. Marsden, Eds. *The Motion, Evolution of Orbits, and Origin of Comets*, pp. 371–397. Dordrecht,

Holland, D. Reidel, 1972.

241. KEAY, C. S. L., F. J. LOW, G. H. RIEKE, and R. B. MINTON. High-resolution maps of Jupiter at five microns. *Astrophys. J.* 183:1063–1073, 1973.
242. KELSEY, L. A., and J. D. FIX. Polarimetry of Pluto. *Astrophys. J.* 184:633–636, 1973.
243. KEMP, J. C., J. B. SWEDLUND, R. E. MURPHY, and R. D. WOLSTENCROFT. Circularly polarized visible light from Jupiter. *Nature* 231:169–170, 1971.
244. KEMP, J. C., and R. D. WOLSTENCROFT. Elliptical polarization by surface-layer scattering. *Nature* 231:170–171, 1971.
245. KEMP, J. C., R. D. WOLSTENCROFT, and J. B. SWEDLUND. Circular polarization—Jupiter and other planets. *Nature* 232:165–168, 1971.
246. KHARE, B. N., and C. SAGAN. Red clouds in reducing atmospheres. *Icarus* 20:311–321, 1973.
247. KIEFFER, H. H., and W. D. SMYTHE. Frost spectra: comparison with Jupiter's satellites. *Icarus* 21:506–512, 1974.
248. KIESS, C. C., C. H. CORLISS, and H. K. KIESS. High dispersion spectra of Jupiter. *Astrophys. J.* 132:221–231, 1960.
249. KLEIN, M. J., S. GULKIS, and C. T. STELZRIED. Jupiter: new evidence of long term variations of its decimeter flux density. *Astrophys. J.* 176:L85–L88, 1972.
250. KLIORE, A., D. L. CAIN, G. FJELDBO, and B. L. SEIDEL. *The Atmospheres of Io and Jupiter Measured by the Pioneer 10 Radio Occultation Experiment.* Presented at 17th COSPAR meet., Sao Paulo, Brazil, June 1974.
251. KOMESAROFF, M. M., and P. M. MCCULLOCH. The radio rotation period of Jupiter. *Astrophys. Lett.* 1:39–41, 1967.
252. KOMESAROFF, M. M., D. MORRIS, and J. A. ROBERTS. Circular polarization of Jupiter's decimetric emission and the Jovian magnetic field strength. *Astrophys. Lett.* 7:31–36, 1970.
253. KOVALEVSKY, J. Determination of the masses of the planets and satellites. *In*, Dollfus, A., Ed. *Surfaces and Interiors of Planets and Satellites*, pp. 1–44. New York, Academic, 1970. (Fr.)
254. KOVALEVSKY, J., and F. LINK. Diameter, flattening and optical properties of the upper atmosphere of Neptune as derived from the occultation of the star BD–17° 4388. *Astron. Astrophys.* 2:398–412, 1969. (Fr.)
255. KRAUS, J. D. Planetary and solar radio emission at 11 meters wavelength. *Proc. IRE* 46:266–274, 1958.
256. KRESÁK, L. Orbital selection effects in the Palomar-Leiden asteroid survey. *In*, Gehrels, T., Ed. *Physical Studies of Minor Planets*, pp. 197–210. Washington, D.C., NASA, 1971. (NASA SP–267)
257. KRESÁK, L. Short-period comets at large heliocentric distances. *Bull. Astron. Inst. Czech.* 24:264–283, 1973.
258. KUIPER, G. P. Titan: a satellite with an atmosphere. *Astrophys. J.* 100:378–383, 1944.
259. KUIPER, G. P. On the origin of asteroids. *Astron J.* 55:164, 1950.
260. KUIPER, G. P. The diameter of Pluto. *Pub. Astron. Soc. Pac.* 62:133–137, 1950.
261. KUIPER, G. P. Planetary atmospheres and their origins. *In*, Kuiper, G. P., Ed. *The Atmospheres of the Earth and Planets*, rev. ed., pp. 306–405. Chicago, Univ. Chic., 1952.
262. KUIPER, G. P. Note on the origin of the asteroids. *Proc. Natl. Acad. Sci.* 39:1159–1161, 1953.
263. KUIPER, G. P. On the origins of the satellites and the Trojans. *In*, Beer, A., Ed. *Vistas in Astronomy*, Vol. 2, pp. 1631–1666. New York, Pergamon, 1956.
264. KUIPER, G. P. Further studies on the origin of Pluto. *Astrophys. J.* 125:287–289, 1957.
265. KUIPER, G. P. Lunar and planetary laboratory studies of Jupiter, I. *Sky Telesc.* 43:4–8, 1972.
266. KUIPER, G. P. Lunar and planetary laboratory studies of Jupiter, II. *Sky Telesc.* 43:75–81, 1972.
267. KUIPER, G. P. On the origin of the solar system, I. *Celestial Mech.* 9:321–348, 1974.
268. KUIPER, G. P., Y. FUJITA, T. GEHRELS, I. GROENEVELD, J. KENT, G. VAN BIESBROECK, and C. J. VAN HOUTEN. Survey of asteroids. *Astrophys. J. Suppl.* 3:289–427. 1958.
269. KUZ'MIN, A. D., A. P. NAUMOV, and T. V. SMIROVA. Estimate of ammonia concentration in subcloud atmospheres of Saturn from radio-astronomy measurements. *Sol. Syst. Res.* 6:10–13, 1972.
270. KUZ'MIN, A. D., and B. Ya. LOSOVSKIY. Measurements of 8.2 mm radio emission from Saturn and estimates of the rings' optical thickness. *Sol. Syst. Res.* 5:62–65, 1971.
271. KUZ'MIN, A. D., and B. Ya. LOSOVSKIY. On the radio emission of Callisto. *Icarus* 18:222–223, 1973.
272. KUZ'MIN, A. D., and B. Ya. LOSOVSKIY. Measurements of the radio emission of Jupiter's satellite Callisto. *Sov. Phys. Dokl.* 18:511–512, 1974.
273. LEBOFSKY, L. A., T. V. JOHNSON, and T. B. MCCORD. Saturn's rings: spectral reflectivity and compositional implications. *Icarus* 13:226–230, 1970.
274. LEE T. Spectral albedos of the Galilean satellites. *Commun. Lunar Planet. Lab.* (Univ. Ariz.) 9(3):179–180, 1972.
275. LEVIN, B. J. On the Bredikhin's classification of cometary tails and the nature of the type II tails. *Mem. Soc. Roy. Sci. Liège*, Ser. 5, XII:323–328, 1966.
276. LEVIN, B. Yu. Some remarks on the liberation of gases from cometary nuclei. *In*, Chebotarev, G. A., E. I. Kazimirchak-Polonskaya, and B. G. Marsden., Eds. *The Motion, Evolution of Orbits, and Origin of Comets*, pp. 260–270. Dordrecht, Holland, D. Reidel, 1972.
277. LEWIS, J. S. The clouds of Jupiter and the NH_3-H_2O and NH_3-H_2S systems. *Icarus* 10:365–378, 1969.
278. LEWIS, J. S. Observability of spectroscopically active compounds in the atmosphere of Jupiter. *Icarus* 10:393–409, 1969.
279. LEWIS, J. S. Satellites of the outer planets: their physical and chemical nature. *Icarus* 15:174–185, 1971.
280. LEWIS, J. S. Chemistry of the outer solar system. *Space*

Sci. Rev. 14:401–411, 1973.

281. LEWIS, J. S. The chemistry of the solar system. *Sci. Am.* 230(3):51–60, 65, 1974.
282. LEWIS, J. S., and R. G. PRINN. Jupiter's clouds: structure and composition. *Science* 169:472–473, 1970.
283. LEY, W. *Watchers of the Skies.* New York, Viking, 1963.
284. LOW, F. J. The infrared brightness temperature of Uranus. *Astrophys. J.* 146:326–328, 1966.
285. LOW, F. J. Observations of Venus, Jupiter, and Saturn at $\lambda 20\mu$. *Astron. J.* 71:391, 1966.
286. LOW, F. J., and A. W. DAVIDSON. The thermal emission of Jupiter and Saturn. *Bull. Am. Astron. Soc.* 1:200, 1969.
287. LOW, F. J., and G. H. RIEKE. Infrared photometry of Titan. *Astrophys. J.* 190:L143–L145, 1974.
288. LOW, F. J., G. H. RIEKE, and K. R. ARMSTRONG. Ground-based observations at 34 microns. *Astrophys. J.* 183:L105–L109, 1973.
289. LUTZ, B. L. Molecular hydrogen on Uranus. Observation of the 3–0 quadrupole band. *Astrophys. J.* 182:989–998, 1973.
290. LUTZ, B. L., and D. A. RAMSAY. New observations on the Kuiper bands of Uranus. *Astrophys. J.* 176:521–524, 1972.
291. LYTTLETON, R. A. On the possible results of an encounter of Pluto with the Neptunian system. *Mon. Not. Roy. Astron. Soc.* 97:108–115, 1936.
292. LYTTLETON, R. A. *The Comets and Their Origin.* London, Cambridge Univ. Press, 1953.
293. LYTTLETON, R. A. On the distribution of major-axes of long-period comets. *Mon. Not. Roy. Astron. Soc.* 139:225–230, 1968.
294. LYTTLETON, R. A. Does a continuous solid nucleus exist in comets? *Astrophys. Space Sci.* 15:175–184, 1972.
295. MAILLARD, J. P., M. COMBES, T. ENCRENAZ, and J. LECACHEUX. New infrared spectra of the Jovian planets from 12000 to 4000 cm^{-1}. I. Study of Jupiter in the $3\nu_3$ CH_4 band. *Astron. Astrophys.* 25:219–232, 1973.
296. MAKALKIN, A. B. The structure of models of Neptune. *Solar Syst. Res.* 6:153–157, 1973.
297. MALAISE, D. J. Collisional effects in cometary atmospheres. I. Model atmospheres and synthetic spectra. *Astron. Astrophys.* 5:209–227, 1970.
298. MARGOLIS, J. S. Studies of methane absorption in the Jovian atmosphere. III. The reflecting-layer model. *Astrophys. J.* 167:553–558, 1971.
299. MARGOLIS, J. S., and K. FOX. Infrared absorption spectrum of CH_4 at 9050 cm^{-1}. *J. Chem. Phys.* 49:2451–2452, 1968.
300. MARGOLIS, J. S., and K. FOX. Studies of methane absorption in the Jovian atmosphere. I. Rotational temperature from the $3\nu_3$ band. *Astrophys. J.* 157:935–943, 1969.
301. MARGOLIS, J. S., and G. E. HUNT. On the level of H_2 quadrupole absorption in the Jovian atmosphere. *Icarus* 18:593–598, 1973.
302. MARSDEN, B. G. On the relationship between comets and minor planets. *Astron. J.* 75:206–217, 1970.
303. MARSDEN, B. G. Evolution of comets into asteroids? *In*, Gehrels, T., Ed. *Physical Studies of Minor Planets*, pp. 413–421. Washington, D.C., NASA, 1971. (NASA SP-267)
304. MARSDEN, B. G. *Catalogue of Cometary Orbits.* Cambridge, Mass., Smithsonian Astrophys. Obs., 1972.
305. MARSDEN, B. G. The recovery of Apollo. *Sky Telesc.* 46:155–158, 1973.
306. MARSDEN, B. G., and Z. SEKANINA. On the distribution of "original" orbits of comets of large perihelion distance. *Astron. J.* 78:1118–1124, 1973.
307. MARSDEN, B. G., Z. SEKANINA, and D. K. YEOMANS. Comets and nongravitational forces, V. *Astron. J.* 78:211–225, 1973.
308. MARSHALL, L., and W. F. LIBBY. Stimulation of Jupiter's radio emission by Io. *Nature* 214:126–128, 1967.
309. MARTIN, T. Z., D. P. CRUIKSHANK, and C. B. PILCHER. Ammonia in the atmosphere of Saturn. Presented at 5th Annu. Meet., Am. Astron. Soc., Planet Sci. Div., Palo Alto, April 1974. *Am. Astron. Bull.* 6(3, Pt.2):380, 1974. (Abstr. No. 074)
310. MASON, H. P. The abundance of ammonia in the atmosphere of Jupiter. *Astrophys. Space Sci.* 7:424–436, 1970.
311. MATSON, D. L., T. V. JOHNSON, and F. P. FANALE. Sodium D-line emission from Io: sputtering and resonant scattering hypothesis. *Astrophys. J.* 192:L43–L46, 1974.
312. MAXWORTHY, T. A review of Jovian atmospheric dynamics. *Planet. Space Sci.* 21:623–641, 1973.
313. MAYER, C. H., T. P. MCCULLOUGH, and R. M. SLOANAKER. Observations of Mars and Jupiter at a wavelength of 3.5 cm. *Astrophys. J.* 127:11–16, 1958.
314. MCBRIDE, J. O. P., and R. W. NICHOLLS. The vibrational-rotational spectrum of ammonia gas, I. *J. Phys. B.* 5:408–417, 1972.
315. MCBRIDE, J. O. P., and R. W. NICHOLLS. The vibrational-rotational spectrum of ammonia gas. II. A rotational analysis of the 6450 Å band. *Can. J. Phys.* 50:93–102, 1972.
316. MCCORD, T. B., T. V. JOHNSON, and J. H. ELIAS. Saturn and its satellites: narrow-band spectrophotometry (0.3–1.1 μ). *Astrophys. J.* 165:413–424, 1971.
317. MCCULLOCH, P. M., and M. M. KOMESAROFF. Location of the Jovian magnetic dipole. *Icarus* 19:83–86, 1973.
318. MCDONOUGH, T. R., and N. M. BRICE. A new kind of ring around Saturn? *Nature* 243:513, 1973.
319. MCGOVERN, W. E., and S. D. BURK. Upper atmospheric thermal structure of Jupiter with convective heat transfer. *J. Atmos. Sci.* 29:179–189, 1972.
320. MELBOURNE, W. G., J. D. MULHOLLAND, W. L. SJOGREN, and F. M. STURMS, Jr. *Constants and Related Information for Astrodynamic Calculations.* Pasadena, Calif., Jet Propul. Lab., 1968. (NASA CR-97666; JPL TR-32-1306)
321. MELROSE, D. B. Rotational effects on the distribution

of thermal plasma in the magnetosphere of Jupiter. *Planet. Space Sci.* 15:381–393, 1967.

322. MENDIS, D. A., and W. I. AXFORD. Satellites and magnetospheres of the outer planets. *In*, Donath, F. A., F. G. Stehli, and G. W. Wetherill, Eds. *Annual Review of Earth and Planetary Sciences*, Vol. 2, pp. 419–474. Palo Alto, Calif., Univ. Calif., 1974.
323. MILLIS, R. L. UBV photometry of Iapetus. *Icarus* 18:247–252, 1973.
324. MILLIS, R. L., D. T. THOMPSON, B. J. HARRIS, P. BIRCH, and R. SEFTON. A search for post-eclipse brightening of Io with multiple-aperture photometers. Presented at 5th Annu. Meet., Am. Astron. Soc., Planet. Sci. Div., Palo Alto, Apr. 1974. *Am. Astron. Soc. Bull.* 6(3, pt. 2):383, 1974. (Abstr. No. 095)
325. MOLTON, P. M., and C. PONNAMPERUMA. Organic synthesis in a simulated Jovian atmosphere. III. Synthesis of aminonitriles. *Icarus* 21:166–174, 1974.
326. MOORE, J. H. Spectroscopic observations of the rotation of Saturn. *Pub. Astron. Soc. Pac.* 51:274–281, 1939.
327. MOORE, J. H., and D. H. MENZEL. Preliminary results of spectrographic observations for rotation of Neptune. *Pub. Astron. Soc. Pac.* 40:234–238, 1928.
328. MOORE, J. H., and D. H. MENZEL. The rotation of Uranus. *Pub. Astron. Soc. Pac.* 42:330–335, 1930.
329. MOROZ, V. I., and D. P. CRUIKSHANK. Distribution of ammonia on Jupiter. *J. Atmos. Sci.* 26:865–869, 1969.
330. MOROZHENKO, A. V. Polarimetric observations of the giant planets. III. Jupiter. *Sov. Astron.-A.J.* 17:105–107, 1973.
331. MOROZHENKO, A. V., and E. G. YANOVITSKIY. The optical properties of Venus and the Jovian planets. I. The atmosphere of Jupiter according to polarimetric observations. *Icarus* 18:583–592, 1973.
332. MORRISON, D. Determination of radii of satellites and asteroids from radiometry and photometry. *Icarus* 19:1–14, 1973.
333. MORRISON, D., and D. P. CRUIKSHANK. Temperatures of Uranus and Neptune at 24 microns. *Astrophys. J.* 179:329–331, 1973.
334. MORRISON, D., and D. P. CRIUKSHANK. Thermal properties of the Galilean satellites. *Icarus* 18:224–236, 1973.
335. MORRISON, D., and D. P. CRUIKSHANK. Physical properties of the natural satellites. *Space Sci. Rev.* 15:641–739, 1974.
336. MÜNCH, G., and H. SPINRAD. On the spectrum of Saturn. *Mem. Soc. Roy. Sci. Liège, Ser. 5*, 7:541–542, 1963.
337. MÜNCH, G., and R. L. YOUNKIN. Molecular absorptions and color distributions over Jupiter's disk. *Astron. J.* 69:553, 1964.
338. MURPHY, R. E. Temperatures of Saturn's rings. *Astrophys. J.* 181:L87–L90, 1973.
339. MURPHY, R. E., D. P. CRUIKSHANK, and D. MORRISON. Radii, albedos, and 20-micron brightness temperatures of Iapetus and Rhea. *Astrophys. J.* 177:L93–L95, 1972.
340. NAPIER, W. McD., and R. J. DODD. On the origin of the asteroids. *Mon. Not. Roy. Astron. Soc.* 166:469–489, 1974.
341. [Nautical Almanac Office]. *Explanatory Supplement to the Astronomical Ephemeris*. London, HMSO, 1961.
342. NEFF, J. S., W. A. LANE, and J. D. FIX. An investigation of the rotational period of the planet Pluto. *Pub. Astron. Soc. Pac.* 86:225–230, 1974.
343. NEWBURN, R. L., Jr., and S. GULKIS. A survey of the outer planets Jupiter, Saturn, Uranus, Neptune, Pluto and their satellites. *Space Sci. Rev.* 14:179–271, 1973.
344. NEZHINSKIY, E. M. On the stability of the Oort cloud. *In*. Chebotarev, G. A., E. I. Kazimirchak-Polonskaya, and B. G. Marsden, Eds. *The Motion, Evolution of Orbits, and Origin of Comets*, pp. 335–340. Dordrecht, Holland, D. Reidel, 1972.
345. O'DELL, C. R. A new model for cometary nuclei. *Icarus* 19:137–146, 1973.
346. OHRING, G. The temperature and ammonia profiles in the Jovian atmosphere from inversion of the Jovian emission spectrum. *Astrophys. J.* 184:1027–1040, 1973.
347. O'LEARY, B., and T. C. VAN FLANDERN. Io's triaxial figure. *Icarus* 17:209–215, 1972.
348. OORT, J. H. Empirical data on the origin of comets. *In*, Middlehurst, B. M., and G. P. Kuiper, Eds. *The Moon, Meteorites, and Comets, The Solar System*, Vol. IV, pp. 665–673. Chicago, Univ. Chic., 1963.
349. ÖPIK, E. J. Jupiter: chemical composition, structure, and origin of a giant planet. *Icarus* 1:200–257, 1962.
350. OSTERBROCK, D. E. A study of two comet tails. *Astrophys. J.* 128:95–105, 1958.
351. OWEN, T. Comparisons of laboratory and planetary spectra. III. The spectrum of Jupiter from 7750 to 8800 Å. *Astrophys. J.* 142:782–786, 1965.
352. OWEN, T. An identification of the 6800 Å methane band in the spectrum of Uranus and a determination of atmospheric temperature. *Astrophys. J.* 146:611–613, 1966.
353. OWEN, T. Comparisons of laboratory and planetary spectra. IV. The identification of the 7500 Å bands in the spectra of Uranus and Neptune. *Icarus* 6:108–113, 1967.
354. OWEN, T. The spectra of Jupiter and Saturn in the photographic infrared. *Icarus* 10:355–364, 1969.
355. OWEN, T., B. L. LUTZ, C. C. PORCO, and J. H. WOODMAN. On the identification of the 6420 Å absorption feature in the spectra of Uranus and Neptune. *Astrophys. J.* 189:379–381, 1974.
356. OWEN, T., and H. P. MASON. New studies of Jupiter's atmosphere. *J. Atmos. Sci.* 26:870–873, 1969.
357. OWEN, T., and J. A. WESTPHAL. The clouds of Jupiter: observational characteristics. *Icarus* 16:392–396, 1972.
358. OWEN, T., and J. H. WOODMAN. On the atmospheric temperature of Jupiter derived from the $3\nu_3$ methane band. *Astrophys. J.* 154:L21–L23, 1968.
359. PALLUCONI, F. D. The planet Saturn (1970). *In*, *NASA*

Space Vehicle Design Criteria (Environment). Washington, D.C., NASA, 1972. (NASA SP-8091)

360. PAULINY-TOTH, I. I. K., A. WITZEL, and S. GORGOLEWSKI. The brightness temperatures of Ganymede and Callisto at 2.8 cm wavelength. *Astron. Astrophys.* 34:129–132, 1974.
361. PEAK, B. M. *The Planet Jupiter.* London, Faber and Faber, 1958.
362. PETTENGILL, G. H., and T. HAGFORS. Comments on radar scattering from Saturn's rings. *Icarus* 21:188–190, 1974.
363. PILCHER, C. B., C. R. CHAPMAN, L. A. LEBOFSKY, and H.H. KIEFFER. Saturn rings: identification of water frost. *Science* 167:1372–1373, 1970.
364. PILCHER, C. B., and T. B. MCCORD. Narrow-band photometry of the bands of Jupiter. *Astrophys. J.* 165:195–201, 1971.
365. PILCHER, C. B., S. T. RIDGWAY, and T. B. MCCORD. Galilean satellites; identification of water frost. *Science* 178:1087–1089, 1972.
366. POLLACK, J. B. Greenhouse models of the atmosphere of Titan. *Icarus* 19:43–58, 1973.
367. POLLACK, J. B., A. SUMMERS, and B. BALDWIN. Estimates of the size of the particles in the rings of Saturn. *Icarus* 20:263–278, 1973.
368. POLLACK, J. B., and R. T. REYNOLDS. Implications of Jupiter's early contraction history for the composition of the Galilean satellites. *Icarus* 21:248–253, 1974.
369. PORTER, J. G. The satellites of the planets. *Br. Astron. Assoc. J.* 70:33–59, 1960.
370. PORTER, W. S. The constitutions of Uranus and Neptune. *Astron. J.* 66:243–245, 1961.
371. POTTER, A. E., and B. DEL DUCA. Lifetime in space of possible parent molecules of cometary radicals. *Icarus* 3:103–108, 1964.
372. PRESTON, G. W. The spectrum of comet Ikeya-Seki (1965f). *Astrophys. J.* 147:718–742, 1967.
373. PRICE, M. J. The scattering mean free path in the Uranian atmosphere. *Icarus* 20:455–464, 1973.
374. PRINN, R. G. UV radiative transfer and photolysis in Jupiter's atmosphere. *Icarus* 13:424–436, 1970.
375. PRINN, R. G., and J. S. LEWIS. Uranus atmosphere: structure and composition. *Astrophys. J.* 179:333–342, 1973.
376. PRINZ, R. The atmospheric activity of the planet Jupiter. I. From 1964 to 1968 in yellow light. *Icarus* 15:68–73, 1971.
377. PRINZ, R. The atmospheric activity of the planet Jupiter. II. Short-term variations in five spectral ranges. *Icarus* 15:74–79, 1971.
378. RABE, E. On the origin of Pluto and the masses of the protoplanets. *Astrophys. J.* 125:290–295, 1957.
379. RABE, E. Further studies on the orbital development of Pluto. *Astrophys. J.* 126:240–244, 1957.
380. RAMSEY, W. H. On the constitutions of Uranus and Neptune. *Planet. Space Sci.* 15:1609–1623, 1967.
381. RATHER, I., P. ADE, and P. CLEGG. *Brightness Temperature Measurements of Saturn, Jupiter, Mars, and Venus at 1 mm Wavelength.* (To be published)
382. REESE, E. J. Jupiter's red spot in 1968–1969. *Icarus* 12:249–257, 1970.
383. REESE, E. J. *Summary of Jovian Latitude and Rotation-Period Observations from 1898 to 1970.* Las Cruces, N. Mex. State Univ., Dep. Astron., 1971. (TN-71-36)
384. REESE, E. J. Jupiter: its red spot and other features in 1969–1970. *Icarus* 14:343–354, 1971.
385. REESE, E. J. Recent photographic measurements of Saturn. *Icarus* 15:466–479, 1971.
386. REESE, E. J. Jupiter: its red spot and disturbances in 1970–1971. *Icarus* 17:57–72, 1972.
387. REESE, E. J., and B. A. SMITH. Evidence of vorticity in the great red spot of Jupiter. *Icarus* 9:474–486, 1968.
388. REESE, E. J., and H. G. SOLBERG, Jr. *Recent Measures of the Latitude and Longitude of Jupiter's Red Spot.* Las Cruces, N. Mex. State Univ., 1965. (TN-557-65-7)
389. REGISTER, H. I. *Decameter-Wavelength Radio Observations of the Planet Jupiter, 1957–1968.* Gainesville, Fla., Univ. Fla., 1968. (Doct. diss.)
390. REYNOLDS, R. T., and A. L. SUMMERS. Models of Uranus and Neptune. *J. Geophys. Res.* 70:199–208, 1965.
391. RICHTER, N. B. *The Nature of Comets.* London, Methuen, 1963.
392. RIDGWAY, S. T. Jupiter: identification of ethane and acetylene. *Astrophys. J.* 187:L41–L43, 1974.
393. RIDGWAY, S. T. The infrared spectrum of Jupiter, 750-1200 cm^{-1}. Presented at 5th Annu. Meet., Am. Astron. Sci., Planet. Sci. Div., Palo Alto, Apr. 1974. *Am. Astron. Soc. Bull.* 6(3, pt.2):376, 1974. (Abstr. No. 056)
394. ROBERTS, J. A., and R. D. EKERS. The position of Jupiter's Van Allen belt. *Icarus* 5:149–153, 1966.
395. ROBEY, D. H. *A Theory on the Nature and Origin of Comets with Implications for Space Mission Planning.* Presented at Annu. Meet., Am. Astronaut. Soc., Anaheim, Calif., June 1970. New York, AAS, 1970. (AAS-70-029)
396. ROEMER, E. Comet notes. *Pub. Astron. Soc. Pac.* 74:537–539, 1962.
397. ROEMER, E. The dimensions of cometary nuclei. *Mem. Soc. Roy. Sci. Liège,* Ser. 5, XII:23–28, 1966.
398. ROEMER, E. Comet notes. *Mercury* 2(4):19–21, 1973.
399. ROTTMAN, G. J., H. W. MOOS, and C. S. FREER. The far-ultraviolet spectrum of Jupiter. *Astrophys. J.* 184:L89–L92, 1973.
400. RUSSELL, H. M., R. S. DUGAN, and J. Q. STEWART. *Astronomy,* Vol. 1, rev. ed. Boston, Mass., Ginn, 1945.
401. SAFRONOV, V. S. Ejection of bodies from the solar system in the course of the accumulation of the giant planets and the formation of the cometary cloud. *In,* Chebotarev, G. A., E. I. Kazimirchak-Polonskaya, and B. G. Marsden, Eds. *The Motion, Evolution of Orbits, and Origin of Comets,* pp. 329–334. Dordrecht, Holland, D. Reidel, 1972.
402. SAGAN, C. On the nature of the Jovian red spot. *Mem. Soc. Roy. Sci. Liège, Ser. 5,* 7:506–515, 1963.

403. SAGAN, C. A truth table analysis of models of Jupiter's great red spot. *Comments Astrophys. Space Phys.* 3:65–72, 1971.

404. SAGAN, C. The solar system beyond Mars: an exobiological survey. *Space Sci. Rev.* 11:827–866, 1971.

405. SAGAN, C., and B. N. KHARE. Experimental Jovian photochemistry: initial results. *Astrophys. J.* 168:563–569, 1971.

406. SAGAN, C., J. VEVERKA, L. WASSERMAN, J. ELLIOT, and W. LILLER. Jovian atmosphere: structure and composition between the turbopause and the mesopause. *Science* 184:901–903, 1974.

407. SALPETER, E. E. On convection and gravitational layering in Jupiter and in stars of low mass. *Astrophys. J.* 181:L83–L86, 1973.

408. SAVAGE, B. D., and J. J. CALDWELL. Ultraviolet photometry from the orbiting astronomical observatory. XIII. The albedos of Jupiter, Uranus, and Neptune. *Astrophys. J.* 187:197–208, 1974.

409. SAVAGE, B. D., and R. E. DANIELSON. Models of the atmosphere of Jupiter. *In*, Brancazio, P. J., and A. G. W. Cameron, Eds. *Infrared Astronomy*, pp. 211–244. New York, Gordon and Breach, 1968.

410. SCHATTEN, K. H., and N. F. NESS. The magnetic-field geometry of Jupiter and its relation to Io-modulated Jovian decametric radio emission. *Astrophys. J.* 165: 621–632, 1971.

411. SCHUBART, J. Asteroid masses and densities. *In*, Gehrels, T., Ed. *Physical Studies of Minor Planets*, pp. 33–39. Washington, D.C., NASA, 1971. (NASA SP–267)

412. SCHUBART, J. The masses of the first two asteroids. *Astron. Astrophys.* 30:289–292, 1974.

413. SEAQUIST, E. R. Circular polarization of Jupiter at 9.26 cm. *Nature* 224:1011–1012, 1969.

414. SEIDELMANN, P. K., W. J. KLEPCZYNSKI, R. L. DUNCOMBE, and E. S. JACKSON. Determination of the mass of Pluto. *Astron. J.* 76:488–492, 1971.

415. SEKANINA, Z. Dynamical and evolutionary aspects of gradual deactivation and disintegration of short-period comets. *Astron. J.* 74:1223–1234, 1969.

416. SEKANINA, Z. Secular decrease in the absolute brightness of the comet Encke. *In*, Konopleva, V. P., Ed. *Astrometry and Astrophysics, No. 4, Physics of Comets*, pp. 43–62. Washington, D.C., NASA, 1970. (NASA TT–F–599)

417. SEKANINA, Z. Existence of icy comet tails at large distances from the Sun. *Astrophys. Lett.* 14:175–180, 1973.

418. SHERMAN, J. C. The critical velocity of gas-plasma interaction and its possible heterogonic relevance. *In*, Elvius, A., Ed. *From Plasma to Planet*, pp. 315–341. Stockholm, Almqvist & Wiksell (New York, Wiley), 1972. (Nobel Symp. Ser. No. 21)

419. SHERRILL, W. M. Polarization measurements of the decameter emission from Jupiter. *Astrophys. J.* 142:1171–1185, 1965.

420. SHIMIZU, M. The upper atmosphere of Jupiter. *Icarus* 14:273–281, 1971.

421. SIMPSON, J. A., D. HAMILTON, G. LENTZ, R. B. MCKIBBEN, A. MOGRO-CAMPERO, M. PERKINS, K. R. PYLE, A. J. TUZZOLINO, and J. J. O'GALLAGHER. Protons and electrons in Jupiter's magnetic field: results from the University of Chicago experiment on Pioneer 10. *Science* 183:306–309, 1974.

422. SIMPSON, J. A., D. C. HAMILTON, R. B. MCKIBBEN, A. MOGRO-CAMPERO, K. R. PYLE, and A. J. TUZZOLINO. The protons and electrons trapped in the Jovian dipole magnetic field region and their interaction with Io. *J. Geophys. Res.* 79:3522–3544, 1974.

423. SINTON, W. M. *Physical Researches on the Brighter Planets*. Bedford, Mass., AF Cambridge Res. Lab., 1964. (AFCRL–64–926) (Final rep.)

424. SINTON, W. M. Limb and polar brightening of Uranus at 8870 Å. *Astrophys. J.* 176:L131–L133, 1972.

425. Sky and Telescope. A tenth satellite of Saturn? *Sky Telesc.* 33(2):71, 93, 1967.

426. SLATTERY, W. L., and W. B. HUBBARD. Statistical mechanics of light elements at high pressure. III. Molecular hydrogen *Astrophys. J.* 181:1031–1038, 1973.

427. SMITH, B. A., and S. A. SMITH. Upper limits for an atmosphere on Io. *Icarus* 17:218–222, 1972.

428. SMITH E. J., L. DAVIS, Jr., D. E. JONES, D. S. COLBURN, P. J. COLEMAN, Jr., P. DYAL, and C. P. SONETT. Magnetic field of Jupiter and its interaction with the solar wind. *Science* 183:305–306, 1974.

429. SMITH, E. J., A. M. A. FRANDSEN, L. DAVIS, Jr., D. E. JONES, P. J. COLEMAN, Jr., D. S. COLBURN, P. DYAL, and C. P. SONETT. The planetary magnetic field and magnetosphere of Jupiter: Pioneer 10. *J. Geophys. Res.* 79:3501–3513, 1974.

430. SMOLUCHOWSKI, R. Internal structure and energy emission of Jupiter. *Nature* 215:691–695, 1967.

431. SMOLUCHOWSKI, R. Jupiter's convection and its red spot. *Science* 168:1340–1342, 1970.

432. SMOLUCHOWSKI, R. Dynamics of the Jovian interior. *Astrophys. J.* 185:L95–L99, 1973.

433. SMOLUCHOWSKI, R. *The Interior Structure of Jupiter (Consequences of Pioneer 10 Data).* Presented at USA–USSR Conf. on Cosmochem. of the Moon and Planets, Moscow, June 1974.

434. SNYDER, L. E., D. BUHL, and W. F. HUEBNER. Detection of HCN in Comet Kohoutek (1973f). Presented at 5th Annu. Meet., Am. Astron. Soc., Planet. Sci. Div., Palo Alto, Apr. 1974. *Am. Astron. Soc. Bull.* 6(3, pt.2):389, 1974. (Abstr. No. 152)

435. SOLBERG, H. G., Jr. Jupiter's red spot in 1965–1966. *Icarus* 8:82–89, 1968.

436. SOLBERG, H. G., Jr. Jupiter's red spot in 1965–1966. *Icarus* 9:212–216, 1968.

437. SOLBERG, H. G., Jr. Jupiter's red spot in 1967–1968. *Icarus* 10:412–416, 1969.

438. SOLBERG, H. G., Jr. A three-month oscillation in the longitude of Jupiter's red spot. *Planet. Space Sci.* 17:1573–1580, 1969.

439. SPINRAD, H. Pressure-induced dipole lines of molecular hydrogen in the spectra of Uranus and Neptune. *Astrophys. J.* 138:1242–1245, 1963.

440. SPINRAD, H. Spectroscopic research on the major planets. *Appl. Opt.* 3:181–186, 1964.

441. SPINRAD, H. Lack of a noticeable methane atmosphere on Triton. *Pub. Astron. Soc. Pac.* 81:895–896, 1969.

442. SPINRAD, H., H. E. SMITH, and J. LEIBERT. Comet Kohoutek (1973f). *IAU Circ.* (Cambridge, Mass.), No. 2591, Nov. 7, 1973.

443. STANNARD, D. *The Radio Astronomy of Jupiter.* Presented at Neil Brice Mem. Symp., Franscati, Italy, May 1974.

444. STANSBERRY, K. G., and R. S. WHITE. Jupiter's radiation belt. *J. Geophys. Res.* 79:2331–2342, 1974.

445. STONE, P. H. The symmetric baroclinic instability of an equatorial current. *Geophys. Fluid Dyn.* 2:147–164, 1971.

446. STONE, P. H. A simplified radiative-dynamical model for the static stability of rotating atmospheres. *J. Atmos. Sci.* 29:405–418, 1972.

447. STONE, P. H. The dynamics of the atmospheres of the major planets. *Space Sci. Rev.* 14:444–459, 1973.

448. STONE, P. H., and D. H. BAKER, Jr. Concerning the existence of Taylor-columns in atmospheres. *Q. J. Roy. Meteorol. Soc.* 94:576–580, 1968.

449. STREETT, W. B. Phase equilibria in molecular hydrogen-helium mixtures at high pressures. *Astrophys. J.* 186:1107–1125, 1973.

450. STREETT, W. B., H. I. RINGERMACHER, and G. VERONIS. On the structure and motions of Jupiter's red spot. *Icarus* 14:319–342, 1971.

451. STROBEL, D. F., and G. R. SMITH. On the temperature of the Jovian thermosphere. *J. Atmos. Sci.* 30:718–725, 1973.

452. SWINGS, P. Cometary spectra. *Q. J. Roy. Astron. Soc.* 6:28–69, 1965.

453. SWINGS, P., and L. HASER. *Atlas of Representative Cometary Spectra.* Louvain, Belg., Univ. Liège, 1956.

454. TAYLOR, D. J. Spectrophotometry of Jupiter's 3400–10 000 Å spectrum and a bolometric albedo for Jupiter. *Icarus* 4:362–373, 1965.

455. TAYLOR, F. W. Methods and approximations for the computation of transmission profiles in the ν_4 band of methane in the atmosphere of Jupiter. *J. Quant. Spectrosc. Radiat. Transfer* 12:1151–1156, 1972.

456. TAYLOR, F. W. Temperature sounding experiments for the Jovian planets. *J. Atmos. Sci.* 29:950–958, 1972.

457. TAYLOR, G. E. The determination of the diameter of Io from its occultation of β Scorpii C on May 14, 1971. *Icarus* 17:202–208, 1972.

458. TAYLOR, R. C. Photometric observations and reduction of lightcurves of asteroids. *In*, Gehrels, T., Ed. *Physical Studies of Minor Planets*, pp. 117–131. Washington, D.C., NASA, 1971. (NASA SP-267)

459. TEIFEL, V. G. Spectrophotometry of the methane absorption bands at 0.7–1.0 μ on the disk of Jupiter. *Sov. Astron.-A. J.* 10:121–123, 1966.

460. TEIFEL, V. G. Molecular absorption and the possible structure of the cloud layers of Jupiter and Saturn. *J. Atmos. Sci.* 26:854–859, 1969.

461. TEIFEL, V. G., L. A. USOLTZEVA, and G. A. KHARITONOVA. The spectral characteristics and probable structure of the cloud layer of Saturn. *In*, Sagan, C., T. C. Owen, and H. J. Smith, Eds. *Planetary Atmospheres*, pp. 375–383. Dordrecht, Holland, D. Reidel, 1971. (IAU Symp. No. 40)

462. TEXEREAU, J. Observing Saturn's edgewise rings, October 1966. *Sky Telesc.* 33:226–227, 1967.

463. THORNE, K. S. Dependence of Jupiter's decimeter radiation on the electron distribution in its Van Allen belts. *Radio Sci.* 69D:1557–1560, 1965.

464. THOMBAUGH, C. W. The trans-Neptunian planet search. *In*, Kuiper, G. P. and B. M. Middlehurst, Eds. *Planets and Satellites, The Solar System*, Vol. III, pp. 12–30. Chicago, Univ. Chic., 1961.

465. TRAFTON, L. Model atmospheres of the major planets. *Astrophys. J.* 147:765–781, 1967.

466. TRAFTON, L. M. Photometric observations of Saturn's 1.1μ CH_4 band. *Bull. Am. Astron. Soc.* 3:282, 1971.

467. TRAFTON, L. A semiempirical model for the mean transmission of a molecular band and application to the 10μ and 16μ bands of NH_3. *Icarus* 15:27–38, 1971.

468. TRAFTON, L. On the methane opacity for Uranus and Neptune. *Astrophys. J.* 172:L117–L120, 1972.

469. TRAFTON, L. On the possible detection of H_2 in Titan's atmosphere. *Astrophys. J.* 175:285–293, 1972.

470. TRAFTON, L. The bulk composition of Titan's atmosphere. *Astrophys.* J. 175:295–306, 1972.

471. TRAFTON, L. Saturn: a study of the $3\nu_3$ methane band. *Astrophys. J.* 182: 615–636, 1973.

472. TRAFTON, L. Scanner observations of the quadrupole H_2 lines in the spectrum of Uranus. *Bull. Am. Astron. Soc.* 5:290–291, 1973.

473. TRAFTON, L. Neptune: observations of the H_2 quadrupole lines in the (4–0) band. *In, Exploration of the Solar System, 65th Symposium, International Astronomical Union*, Torun, Pol., Sept. 1973.

474. TRAFTON, L. Neptune's internal heat source: an explanation in terms of the dissipation of Triton's orbit. Presented at 5th Annu. Meet., Am. Astron. Soc., Planet. Sci. Div., Palo Alto, Calif., Apr. 1974. *Am. Astron. Soc. Bull.* 6(3, pt. 2):380, 1974. (Abstr. No. 078)

475. TRAFTON, L. Titan: unidentified strong absorptions in the photometric infrared. *Icarus* 21:175–187, 1974.

476. TRAFTON, L., and G. MÜNCH. The structure of the atmospheres of the major planets. *J. Atmos. Sci.* 26:813–825, 1969.

477. TRAFTON, L., and P. H. Stone. Radiative-dynamical equilibrium states for Jupiter. *Astrophys. J.* 188:649–655, 1974.

478. TRAFTON, L., T. PARKINSON, and W. MACY, Jr. The spatial extent of sodium emission around Io. *Astrophys. J.* 190:L85–L89, 1974.

479. TRAUB, W. A., and N. P. CARLETON. Observations of spatial and temporal variations of the Jovian H_2

quadrupole lines. Presented at 5th Annu. Meet., Am. Astron. Soc., Planet. Sci. Div., Palo Alto, Apr. 1974. *Am. Astron. Soc. Bull.* 6(3, pt. 2):376, 1974. (Abstr. No. 054)

480. TRULSEN, J. Collisional focusing of particles in space causing jetstreams. *In*, Gehrels, T., Ed. *Physical Studies of Minor Planets*, pp. 327–335. Washington, D.C., NASA, 1971. (NASA SP–267)
481. TRULSEN, J. Formation of comets in meteor streams. *In*, Chebotarev, G. A., E. I. Kazimirchak-Polonskaya, and B. G. Marsden, Eds. *The Motion, Evolution of Orbits, and Origin of Comets*, pp. 487–490. Dordrecht, Holland, D. Reidel, 1972.
482. TRULSEN, J. Numerical simulation of jetstreams. II. The two-dimensional case. *Astrophys. Space Sci.* 18:3–20, 1972.
483. ULICH, B. L. Absolute brightness temperature measurements at 2.1 mm wavelength. *Icarus* 21:254–261, 1974.
484. ULICH, B. L., and E. K. CONKLIN. Detection of methyl cyanide in comet Kohoutek. *Nature* 248:121–122, 1974.
485. VAN ALLEN, J. A., D. N. BAKER, B. A. RANDALL, and D. D. SENTMAN. The magnetosphere of Jupiter as observed with Pioneer 10. I. Instrument and principal findings. *J. Geophys. Res.* 79:3559–3577, 1974.
486. VAN ALLEN, J. A., D. N. BAKER, B. A. RANDALL, M. F. THOMSEN, D. D. SENTMAN, and H. R. FLINDT. Energetic electrons in the magnetosphere of Jupiter. *Science* 183:309–311, 1974.
487. VESELY, C. D. Summary on orientations of rotation axes. *In*, Gehrels, T., Ed. *Physical Studies of Minor Planets*, pp. 133–140. Washington, D.C., NASA, 1971. (NASA SP–267)
488. VEVERKA, J. Polarization measurements of the Galilean satellites of Jupiter. *Icarus* 14:355–359, 1971.
489. VEVERKA, J. Titan: polarimetric evidence for an optically thick atmosphere. *Icarus* 18:657–660, 1973.
490. VEVERKA, J., and M. NOLAND. Asteroid reflectivities from polarization curves: calibration of the "slope-albedo" relationship. *Icarus* 19:230–239, 1973.
491. VEVERKA, J., L. WASSERMAN, and C. SAGAN. On the upper atmosphere of Neptune. *Astrophys. J.* 189:569–575, 1974.
492. VSEKHSVYATSKIY, S. K. *Physical Characteristics of Comets*. Jerusalem, Isr. Prog. Sci. Transl., 1964. (NASA T–80; OTS 62–11031)
493. VSEKHSVYATSKIY, S. K. The origin and evolution of the comets and other small bodies in the solar system. *In*, Chebotarev, G. A., E. I. Kazimirchak-Polonskaya, and B. G. Marsden, Eds. *The Motion, Evolution of Orbits, and Origin of Comets*, pp. 413–425. Dordrecht, Holland, D. Reidel, 1972.
494. WALKER, M. F., and R. HARDIE. A photometric determination of the rotational period of Pluto. *Pub. Astron. Soc. Pac.* 67:224–231, 1955.
495. WALKER, R. G. *Infrared Photometry of Stars and Planets*. Cambridge, Mass., Harvard Univ., 1967. (Doct. diss.)
496. WALLACE, L., J. J. CALDWELL, and B. D. SAVAGE. Ultraviolet photometry from the orbiting astronomical observatory. III. Observations of Venus, Mars, Jupiter, and Saturn longward of 2000 Å. *Astrophys. J.* 172:755–769, 1972.
497. WALLACE, L., M. PRATHER, and M. J. S. BELTON. The thermal structure of the atmosphere of Jupiter. Presented at 5th Annu. Meet., Am. Astron. Soc., Planet. Sci. Div., Palo Alto, Apr. 1974. *Am. Astron. Soc. Bull.* 6(3 pt.2):377, 1974. (Abstr. No. 060)
498. WALLIS, M. K. The physics of cometary plasma. *Planet. Space Sci.* 15:1407–1418, 1967.
499. WAMSTEKER, W. The wavelength dependence of the albedos of Uranus and Neptune from 0.3 to 1.1 micron. *Astrophys. J.* 184:1007–1016, 1973.
500. WARWICK, J. W. The position and sign of Jupiter's magnetic moment. *Astrophys. J.* 137:1317–1318, 1963.
501. WARWICK, J. W. Radio emission from Jupiter. *Ann. Rev. Astron. Astrophys.* 2:1–22, 1964.
502. WARWICK, J. W. Radiophysics of Jupiter. *Space Sci. Rev.* 6:841–891, 1967.
503. WARWICK, J. W. *Particles and Fields Near Jupiter*. Washington, D.C., NASA, 1970. (NASA CR–1685)
504. WASSERMAN, L., and J. VEVERKA. On the reduction of occultation light curves. *Icarus* 20:322–345, 1973.
505. WATSON, K., B. C. MURRAY, and H. BROWN. The stability of volatiles in the solar system. *Icarus* 1:317–327, 1963.
506. WEIDENSCHILLING, S. J., and J. S. LEWIS. Atmospheric and cloud structures of the Jovian planets. *Icarus* 20:465–476, 1973.
507. WESTPHAL, J. A. Observations of Jupiter's cloud structure near 8.5 μ. *In*, Sagan, C., T. C. Owen, and H. J. Smith, Eds. *Planetary Atmospheres*, pp. 359–362. Dordrecht, Holland, D. Reidel, 1971. (IAU Symp. 40)
508. WESTPHAL, J. A., K. MATTHEWS, and R. J. TERRILE. Five micron pictures of Jupiter. *Astrophys. J.* 188: L111–L112, 1974.
509. WETHERILL, G. W. Collisions in the asteroid belt. *J. Geophys. Res.* 72:2429–2444, 1967.
510. WETHERILL, G. W. Cometary versus asteroidal origin of chondritic meteorites. *In*, Gehrels, T., Ed. *Physical Studies of Minor Planets*, pp. 447–460. Washington, D.C., NASA, 1971. (NASA SP–267)
511. WHIPPLE, F. L. On the structure of the cometary nucleus. *In*, Middlehurst, B. M., and G. P. Kuiper, Eds. *The Moon, Meteorites, and Comets, The Solar System*, Vol. IV, pp. 639–664. Chicago, Univ. Chic., 1963.
512. WHIPPLE, F. L. The origin of comets. *In*, Chebotarev, G. A., E. I. Kazimirchak-Polonskaya, and B. G. Marsden, Eds. *The Motion, Evolution of Orbits, and Origin of Comets*, pp. 401–408. Dordrecht, Holland, D. Reidel, 1972.
513. WHITAKER, E., and R. GREENBERG. Eccentricity and inclination of Miranda's orbit. *Comm. Lunar Planet. Lab.* 10:70–80, 1973.
514. WHITEOAK, J. B., F. F. GARDNER, and D. MORRIS. Jovian linear polarization at 6 cm wavelength. *Astrophys. Lett.* 3:81–84, 1969.

515. WILDEY, R. L. Hot shadows of Jupiter. *Science* 147:1035–1036, 1935.

516. WILDEY, R. L., B. C. MURRAY, and J. A. WESTPHAL. Thermal infrared emission of the Jovian disk. *J. Geophys. Res.* 70:3711–3719, 1965.

517. WILKINS, G. A., and A. T. SINCLAIR. The dynamics of the planets and their satellites. *Proc. Roy. Soc. London A* 336:85–104, 1974.

518. WILLIAMS, J. G. Proper elements, families, and belt boundaries, *In*, Gehrels, T., Ed. *Physical Studies of Minor Planets*, pp. 177–181. Washington, D.C., NASA, 1971. (NASA SP–267)

519. WILLIAMS, J. G. Meteorites from the asteroid belt? EθS (*Trans. Am. Geophys. Union*) 54:233, 1973.

520. WILLIAMS, J. G., and G. S. BENSON. Resonances in the Neptune-Pluto system. *Astron. J.* 76:167–177, 1971.

521. WITKOWSKI, J. M. On the origin of comets. *Solar Syst. Res.* 5:66–71, 1971.

522. WITKOWSKI, J. M. On the problem of the origin of comets. *In*, Chebotarev, G. A., E. I. Kazimirchak-Polonskaya, and B. G. Marsden, Eds., *The Motion, Evolution of Orbits, and Origin of Comets*, pp. 419–425. Dordrecht, Holland, D. Reidel, 1972.

523. WOELLER, F., and C. PONNAMPERUMA. Organic synthesis in a simulated Jovian atmosphere. *Icarus* 10:386–392, 1969.

524. WRIXON, G. T., and W. J. WELCH. The millimeter wave spectrum of Saturn. *Icarus* 13:163–172, 1970.

525. WRIXON, G. T., W. J. WELCH, and D. D. THORNTON. The spectrum of Jupiter at millimeter wavelengths. *Astrophys. J.* 169:171–183, 1971.

526. WURM, K. The substructure in the heads of comets with type I and type II tails. *Astrophys. Space Sci.* 27:211–216, 1974.

527. YABUSHITA, S. Stability analysis of Saturn's rings with differential rotation. *Mon. Not. Roy. Astron. Soc.* 133: 247–263, 1966.

528. YERBURY, M. J., J. J. CONDON, and D. L. JAUNCEY, Observations of Saturn at a wavelength of 49.5 cm. *Icarus* 15:459–465, 1971.

529. YOUNG, A. T., and W. M. IRVINE. Multicolor photoelectric photometry of the brighter planets. I. Program and procedure. *Astron. J.* 72:945–950, 1967.

530. YOUNKIN, R. L. *Spectrophotometry of the Moon, Mars, and Uranus*. Los Angeles, Calif., Univ. Calif., 1970. (Doct. diss.)

531. YOUNKIN, R. L. The albedo of Titan. *Icarus* 21:219–229, 1974.

532. YOUNKIN, R. L., and G. MÜNCH. Spectrophotometry of Uranus from 3300 to 11 000 Å. *Astron. J.* 72:328–329, 1967.

533. ZABRISKIE, F. R., W. A. SOLOMON, and J. P. HAGAN, Jr. Low-frequency observations of Jupiter. *Astron. J.* 70:151, 1965.

534. ZAPOLSKY, H. S., and E. E. SALPETER. The mass-radius relation for cold spheres of low mass. *Astrophys. J.* 158:809–813, 1969.

535. ZELLNER, B. On the nature of Iapetus. *Astrophys. J.* 174:L107–L109, 1972.

536. ZELLNER, B. The polarization of Titan. *Icarus* 18:661–664, 1973.

537. ZHARKOV, V. N., and V. P. TRUBITSYN. Adiabatic temperatures in Uranus and Neptune. *Phys. Solid Earth* (Izv.) (7):496–500, 1972.

538. ZIMMERMAN, P. D., and G. W. WETHERILL. Asteroidal source of meteorites. *Science* 182:51–53, 1973.